Report of Investigations No. 122

FRIO FORMATION OF THE TEXAS GULF COAST BASIN – Depositional Systems, Structural Framework, and Hydrocarbon Origin, Migration, Distribution, and Exploration Potential

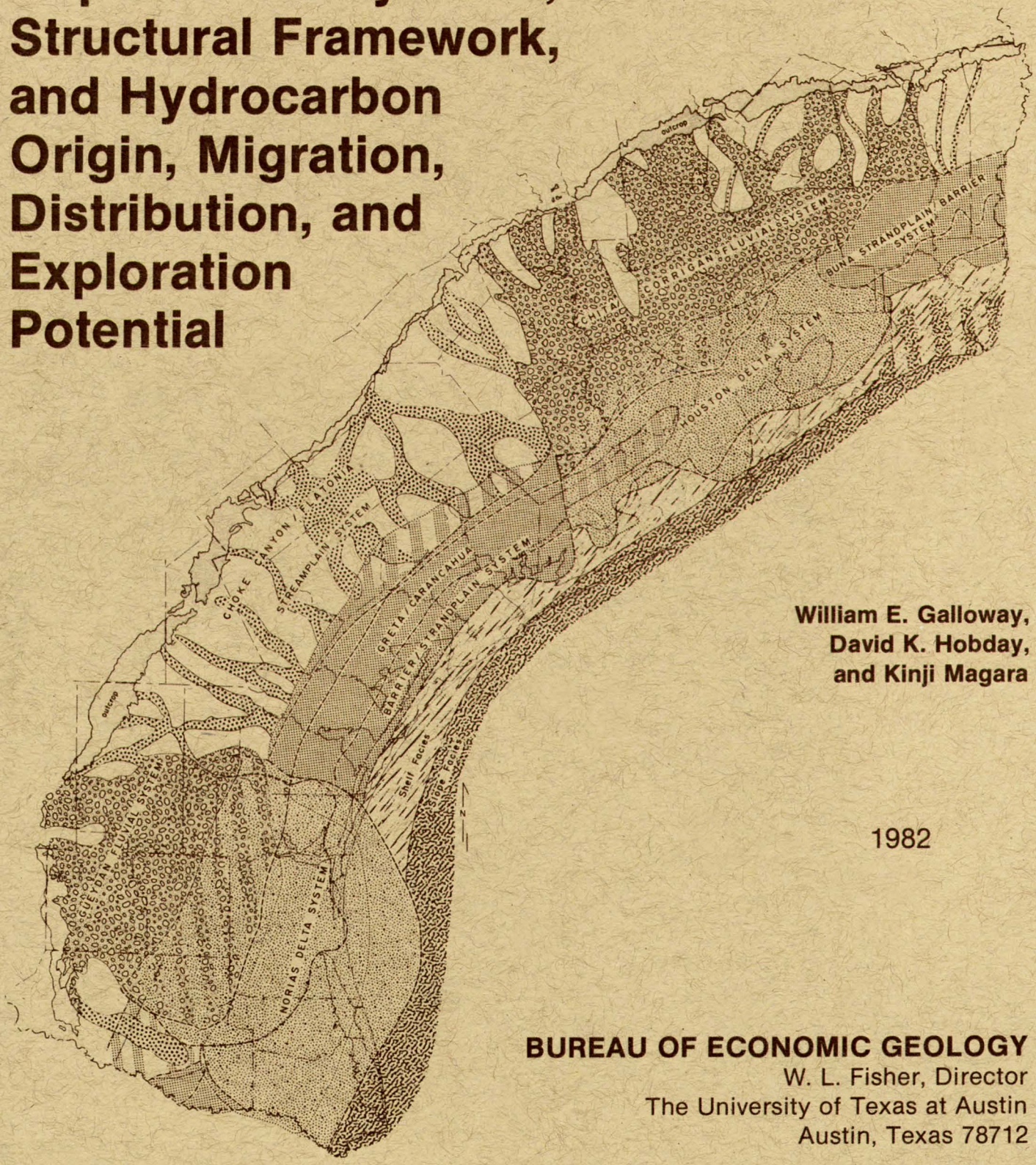

William E. Galloway,
David K. Hobday,
and Kinji Magara

1982

BUREAU OF ECONOMIC GEOLOGY
W. L. Fisher, Director
The University of Texas at Austin
Austin, Texas 78712

Report of Investigations No. 122

FRIO FORMATION OF THE TEXAS GULF COAST BASIN – Depositional Systems, Structural Framework, and Hydrocarbon Origin, Migration, Distribution, and Exploration Potential

By
William E. Galloway,
David K. Hobday,[1]
and Kinji Magara[2]

Partially funded by the
U.S. Geological Survey,
U.S. Department of the Interior,
under Grant No. 14-08-0001-G-640.

Assisted by
Diana Morton,
Mark Helper,
Victor Gavenda,
and Nathan Smith

1982

BUREAU OF ECONOMIC GEOLOGY
W. L. Fisher, Director
The University of Texas at Austin
Austin, Texas 78712

[1]The University of Sydney, Sydney, New South Wales 2006, Australia; formerly with the Bureau of Economic Geology.
[2]Petroleum consultant; formerly with the Bureau of Economic Geology.

CONTENTS

FIGURES

TABLES

PLATES (in pocket)

ABSTRACT

The Frio Formation is one of the major Tertiary progradational wedges of the Texas Gulf Coast Basin and has yielded nearly 6 billion bbl of oil and 60 trillion ft^3 of gas. The Frio and its updip equivalent, the Catahoula Formation, consist of deposits of two large fluvial and associated deltaic systems centered in the Houston and Rio Grande Embayments. Structures in the Houston Embayment are dominated by syndepositional deformation of underlying Jurassic salt. Mobilization of thick, undercompacted prodelta and slope muds characterized the tectonic evolution of the deltaic sequence in the Rio Grande Embayment. These two major deltaic depocenters are separated by a vertically stacked, strike-parallel barrier and strandplain system. Underlying, interbedded, and transgressive shelf, prodelta, and continental slope mudstone sequences provide principal source and sealing facies. Sparse organic geochemical data and regional thermal and compaction-history analyses show that large volumes of hydrocarbons have probably been generated within, and effectively expulsed upward and landward from, normally to moderately undercompacted sequences of these mudstone facies.

All Frio depositional systems contain economically significant, geologically defined hydrocarbon-producing plays. Volume, production style, and type of hydrocarbon within each of 10 recognized plays reflect source-rock quality and type, differing compaction and pore-fluid-migration history, and reservoir and trap configurations characteristic of each depositional system. Analysis of volumetric, historical, and geological relationships for production and discovery within each play provides a basis for estimating the undiscovered hydrocarbon resource potential as well as for assigning that potential to specific geographic and stratigraphic subdivisions of the depositional basin.

INTRODUCTION

The Frio Formation, of Oligocene-Miocene age, is one of the principal progradational wedges of the Texas Gulf Coast Basin (fig. 1). Aggradation of the ancient coastal plain by as much as several hundred feet was accompanied by progradation of a continental platform that is more than 15,000 ft (4,500 m) thick and up to 50 mi (80 km) wide. The Frio wedge, which consists of interfingering marine and nonmarine sands and shales, has produced more than 16 billion boe of hydrocarbons, making it one of the most important petroleum reservoirs in the Gulf Coast Basin. (Throughout this report, natural gas is converted to barrel-of-oil [boe] equivalents on an approximate Btu basis of 1 bbl = 6 Mcf.)

More than 50 years of intensive, and increasingly deeper, exploration and development make the Frio wedge a major stratigraphic unit (MSU) that may well have yielded most of its contained and recoverable hydrocarbon reserves. Even a small remaining fraction of undiscovered petroleum, however, would constitute a major target for continued exploration and an energy resource of regional significance.

OBJECTIVES

The objectives of this report are (1) to provide the geologic data base necessary for a thorough assessment of the undiscovered oil and gas within the Frio MSU and (2) to present a methodology integrating the geologic framework facies, historical indices of finding rate, and geochemical material-balance calculations as a basis for definition and comparative resource evaluation of Frio hydrocarbon plays. The play, which is the working subdivision of production in this analysis, is a geologically homogeneous subdivision of the MSU that is characterized by its production style or suite of styles

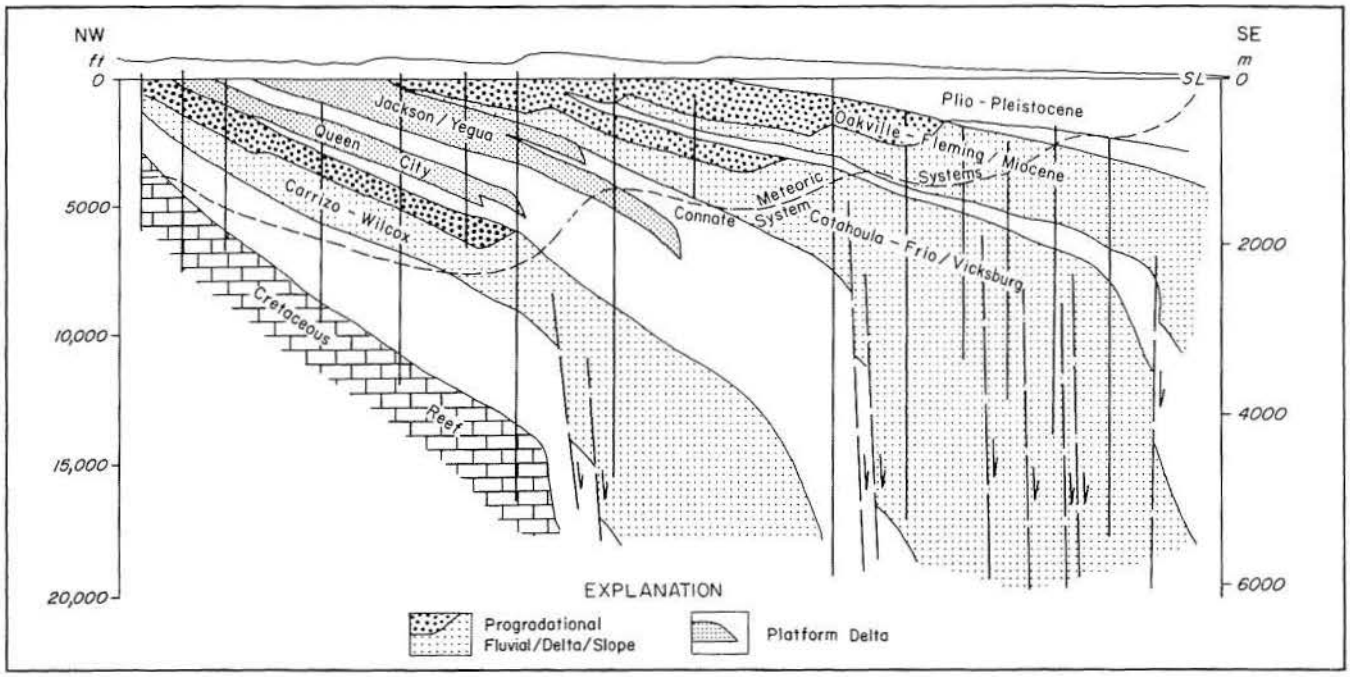

Figure 1. Schematic dip cross section illustrating the offlapping Tertiary stratigraphic sequence of the Texas Gulf Coastal Plain. Major progradational wedges include the Carrizo-Wilcox, Catahoula-Frio, and Oakville-Fleming cycles.

(White, 1980). Plays as delineated in the Gulf Coast Basin are typically more heterogeneous than those described by Ryan (1973); consequently, the history of hydrocarbon discovery in the Frio is characterized by multiple peaks or surges recording the discovery of successive fairways.

METHODOLOGY

The study incorporated five component steps: (1) regional delineation of the MSU; (2) compilation of a systematic inventory of known hydrocarbon distribution; (3) compilation and interpretation of the Frio geologic framework; (4) delineation and quantitative description of plays; and (5) determination, using various assessment techniques, of the probable volumes of remaining undiscovered hydrocarbons.

Regional delineation of the Frio MSU was based on a grid of strike- and dip-oriented cross sections (pl. 1) modified from regional sections of Dodge and Posey (1981). Conventional subsurface nomenclature was correlated with the physical stratigraphic framework to relate local terminology in the regional context of the Frio MSU.

The *hydrocarbon inventory* required manual collation of data from public sources, including the International Oil Scouts Association's "Texas Yearbook" (1978), the annual report of the Railroad Commission of Texas (1978), published field papers, and tabulated calculations of field reserves compiled by the Office of Applied Analysis, Energy Information Administration, U.S. Department of Energy. The resultant inventory provides systematic information on reservoirs in all Frio fields that have produced more than 1 million bbl of liquid-equivalent hydrocarbons and includes year of discovery; number of producing wells; depth, thickness, and hydrocarbon gravity of producing zones; cumulative production of oil, condensate, casinghead gas, and nonassociated gas; and calculated reserves of gas and oil.

Geologic framework studies included regional mapping of thickness, structure, and sand distribution, as well as delineation of principal depositional systems and component facies, discrimination of controls on reservoir quality, determination of the volume, quality, and distribution of potential source-bed facies, and evaluation of thermal and fluid-flow histories and concomitant hydrocarbon expulsion and migration efficiency.

Play delineation integrated the geologic and production studies to outline geographically, and to describe key aspects of, the major hydrocarbon plays that characterize the Frio MSU.

Resource assessment was attempted on a play-by-play basis. For each play, limiting factors and key variables, such as drilling density, depth range, temperature, reservoir quality, and source-rock potential, were defined. Historical finding rates and volumetric extrapolations were used to calculate ranges of possible undiscovered

hydrocarbons. Results were modified, where appropriate, on the basis of geologic and material-balance estimations, and probable and possible ranges of undiscovered hydrocarbons were estimated.

Although none of the methods applied are new or unique (Mallory, 1975; White and others, 1975; White and Gehman, 1979), the careful delineation of geologically defined plays, and consequent data synthesis and projection within relatively homogeneous populations, should provide not only the best basis for improved resource estimation, but also should produce a comparative index of exploratory potential for different segments of a major hydrocarbon-producing stratigraphic unit. Significantly, different plays within the Frio MSU may have more in common, geologically, with plays in other formations or basins than with each other. For example, some Frio plays may be more analogous to certain Wilcox plays than to sister plays in the Frio itself.

GEOLOGIC FRAMEWORK

The Frio MSU was deposited along the northern margin of the Gulf Coast Tertiary basin, an extracratonic basin characterized by rapid subsidence in areas of sediment loading. The Tertiary infill accumulated to great thicknesses where the continental platform was built gulfward beyond the underlying Mesozoic shelf margin (fig. 1) and onto transitional to oceanic crust (McGookey, 1975). Major progradational wedges such as the Frio MSU consist of an updip and relatively shallow section of interbedded terrestrial and marginal marine sand and mudstone underlain by several thousand feet of undercompacted slope and basinal mudstone. Instability caused by rapid loading of plastic, water-saturated sediment at the crest of a gently inclined subaqueous slope resulted in large-scale, syndepositional down-to-the-coast faulting and intrastratal deformation.

Three major structural provinces are defined by their syndepositional structural style and by the nature of the diapiric material incorporated in the deformational process (pl. 2). The broadly defined Houston Embayment of East Texas was characterized by salt diapirism and associated faulting and large salt-withdrawal subbasins (Gulf Coast Association of Geological Societies, 1972; Bebout and others, 1978). Across the San Marcos Platform and southward toward the Rio Grande Embayment, underlying salt is thin or absent; long, linear belts of growth faults and associated shale ridges, massifs, and diapirs dominate the structural style (Bishop, 1978; Bruce, 1973). In the Rio Grande Embayment, large but more discontinuous belts of growth faults and deep-seated shale ridges and massifs occur. In addition to the strike-parallel fault trends, subsidiary, oblique trends of deep, low-relief anticlinal structures are particularly prominent along the northern boundary of this province (pl. 2).

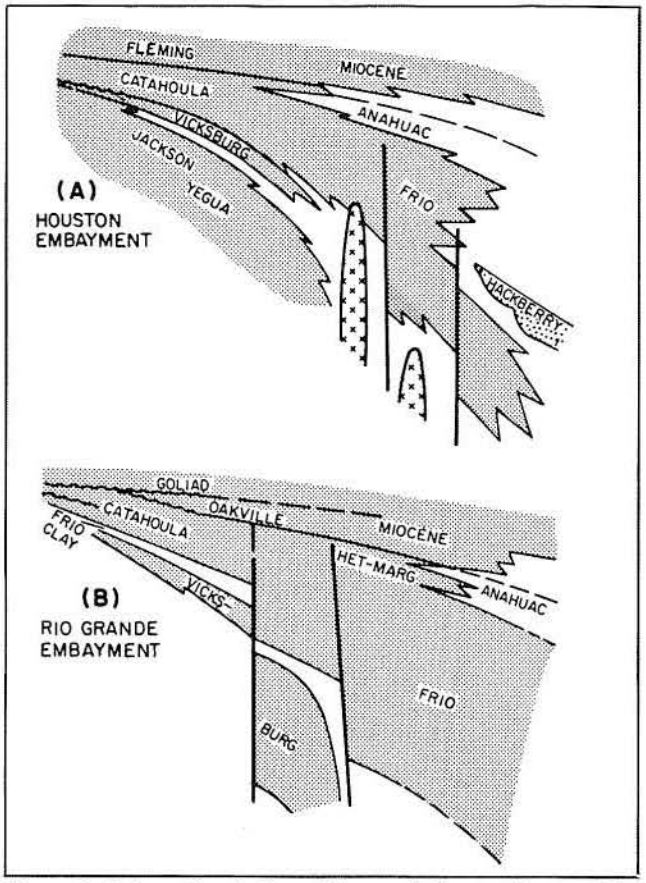

Figure 2. Schematic stratigraphic correlation sections of the Frio MSU for the (A) Houston and (B) Rio Grande Embayments, Texas Gulf Coastal Plain, showing commonly applied nomenclature and principal bounding units.

Structural dislocation decreases upsection within the major wedges. Consequently, updip parts of the Frio dip gently and uniformly basinward (pl. 2) and were little affected by faulting that displaced the underlying Eocene section. Gulfward, the Frio section thickens; major fault and diapiric displacements extend up into and through the unit, structures become increasingly complex, and the strata become highly segmented (pl. 2). The Vicksburg Flexure, a uniquely continuous, narrow fault zone characterized by extreme vertical displacement of the older, deeply buried section, forms the updip limit of significant structural deformation of the Frio (Loucks, 1978).

STRATIGRAPHIC CORRELATION AND RELATIONSHIPS

Lateral and vertical stratigraphic relationships of the Frio Formation that are defined in this report are illustrated in figure 2. In both the Houston and Rio Grande

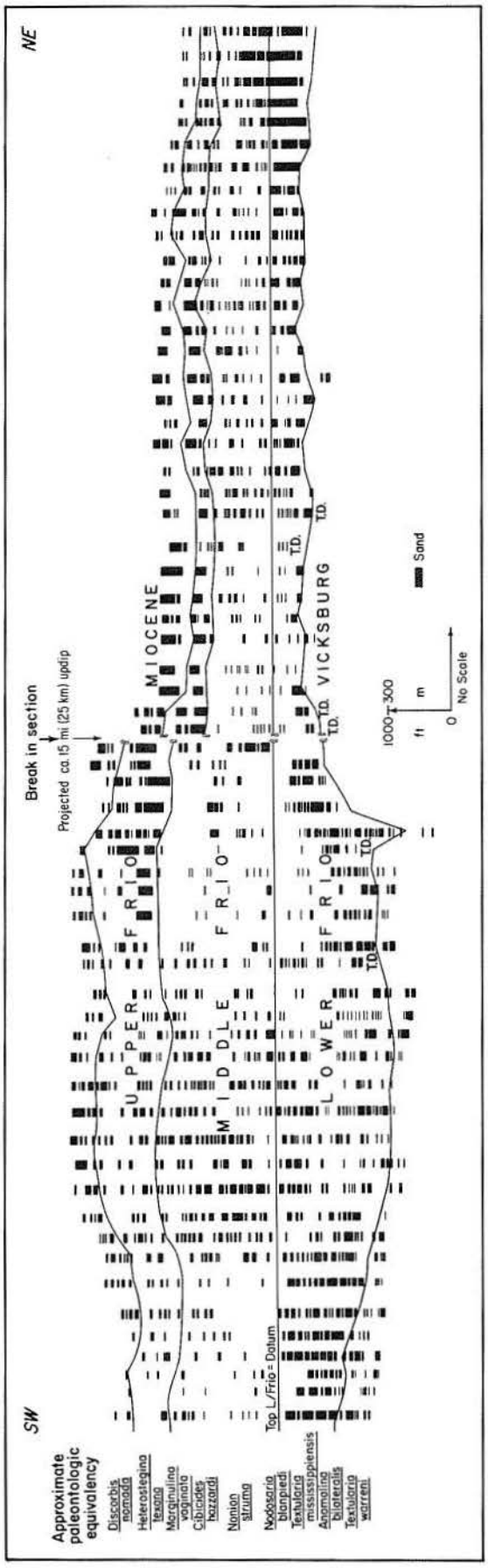

Figure 3. Regional composite strike section β displays the lithostratigraphic basis for subdivision of the total Frio section into three operational units for facies mapping. Downdip correlation of the operational units defines their relationship to the conventional micropaleontologic zones of the marine section. For location see plate 1.

Embayments, the outcrop and shallow subsurface equivalent of the Frio is the Catahoula Formation. The Frio is underlain by the Oligocene Vicksburg Formation, which is thickest and best developed within the Rio Grande Embayment. Also, a thin, mud-rich unit, called the Frio Clay, is mapped at outcrop in South Texas (fig. 2). Contrary to older published cross sections, this thin unit is now correlated in part both to the Vicksburg and to the lowest Catahoula and Frio Formations of the deep subsurface (Galloway and Kaiser, 1980; Baker, 1978). The confusion of names is a relic of repeated redefinition of type sections in the early 1900's. Downdip, the Frio Formation is regionally overlain by an onlapping, transgressive marine shale wedge, the Anahuac Formation. In the Rio Grande Embayment, updip extent of the trangression was limited by continued active influx of coarse sediment, commonly called the *Heterostegina* and *Marginulina* sands. Renewed progradation of the Miocene Oakville Formation (South Texas) and equivalent Fleming Formation (East Texas) terminated the Anahuac transgression. The westernmost edge of the Hackberry facies of Louisiana extends into the Houston Embayment and lies within middle Frio marine facies (fig. 2).

Within the global framework of sea-level cycles defined by Vail and others (1977), progradation of the Frio wedge was initiated at or slightly before a major fall. Deposition then continued through a period of slowly rising sea level, punctuated by sharp temporary rises, in early Miocene time. If commonly accepted dating of the subsequent Miocene cycle is followed, renewed progradation and seaward advance of the shoreline following the Anahuac transgression predated the middle Miocene highstand by several million years.

Careful projection to outcrop and into regional depositional sequences, such as the Anahuac Shale, and paleontologic zonation of key wells allowed correlation of a grid of stratigraphic cross sections, providing an internally consistent framework for further subdivision and mapping of the Frio. Analysis of intermediate-depth strike section β suggested a regionally correlative lithostratigraphic subdivision of the MSU into upper, middle, and lower operational units of subequal thickness (fig. 3). Downdip projection of these broadly defined operational units established their relation to commonly used paleontologic markers (fig. 3).

A regional Frio isopach map was constructed by using wells on the cross-section network (pl. 3). The map shows a gradual coastward thickening of the updip Catahoula/Frio interval that is accentuated across the Vicksburg Flexure and increases markedly at the next downdip belt of faults, which is commonly called the Frio Flexure. Documented thickness exceeds 10,000 ft (3,000 m) in the Houston Embayment and 12,000 ft (3,600 m) in the Rio Grande Embayment. Correlation of the three operational units further defines the nature of the basinward expansion of the Frio. In the central and

southern Coastal Plain, three fault-defined depositional subbasins are recognized (pl. 1). The updip subbasin (I) is characterized primarily by moderate thickening of the lower Frio operational unit across the underlying Vicksburg Flexure. Subbasin II lies downdip of the well-integrated series of major growth faults that constitute the Frio Flexure. The lower Frio expands tremendously and then abruptly loses sand content farther downdip. The middle Frio also displays significant expansion in thickness. Subbasin III is well developed only within the Rio Grande Embayment and lies downdip of a somewhat diffuse, irregular zone of growth faults. Within this subbasin, the middle Frio operational unit expands greatly, and the lower Frio is rarely penetrated by drilling. Regional strike sections were intentionally aligned within each of the major fault-defined subbasins (pl. 1). The subbasins do not extend as recognizable entities into the salt dome province of the Houston Embayment.

PRIMARY FACIES MAPPING

Several hundred wells were projected into the cross-section framework, correlated, and used to prepare a suite of primary facies maps that are the basis of further interpretive mapping, geologic reconstruction, and volumetric calculations. Comparison of the maps supports the general validity of the three-fold subdivision of the total Frio section.

Primary facies maps include net-sand isolith maps (pls. 4 through 6), sand-percentage maps (pls. 7 through 9), and electric log facies maps (pls. 10 through 12). Preparation of isolith and percentage maps was based on summation of total sand thickness, which was interpreted from either spontaneous potential (SP) or resistivity curves within each of the operational units. Log facies maps were generated by establishing a suite of type log sequences representative of patterns typically encountered in the Frio (fig. 4), followed by visual interpretation of all logs in the cross-section grid using the type log sequences for comparison. Log facies were grouped as aggradational (sharp-based, blocky, or upward-decreasing deflections), progradational (thin to thick, transitional lower boundaries on sand bodies), or mixed suites (fig. 4). In general, coastal regression produces "funnel-shaped" log patterns, whereas transgression results in a "bell-shaped" pattern (Conybeare, 1976), although there may be significant departures from this rule (Kraft and John, 1979). For example, complexities may be introduced by inlet migration (producing an upward-fining pattern) during regression. The most common log facies for each operational unit was transposed to the map, providing an overview of geographic and vertical distributions. Distribution and relationships of progradational and aggradational sequences are important criteria for interpreting depositional environment and history (Frazier, 1974).

Examination of the primary facies maps for each operational unit revealed several important features:

1. All maps show generally parallel contour trends.
2. Total sand content, as expected, is sensitive to major changes in gross thickness associated with expansion into fault-defined or salt-withdrawal subbasins.
3. Sand-percentage contours best reflect primary reservoir trends, particularly where abrupt interval changes result from syndepositional structural movement.
4. Although similar facies of lower and middle Frio intervals show a generally basinward offset, especially in South Texas, upper Frio facies trends are displaced inland.
5. Three different patterns characterize each map. In both the Rio Grande and Houston Embayments, dip-oriented trends expand downdip into irregular, lobate patterns. Between the embayments and extending across the San Marcos Arch, log facies boundaries and contours are strongly strike oriented, particularly near the present coast.

DEPOSITIONAL SYSTEMS

Division of the Frio MSU into a number of distinct but spatially related depositional systems was accomplished primarily on the basis of sand isolith maps of the upper, middle, and lower Frio operational units (pls. 4 through 9) and on the basis of facies maps (pls. 10 through 12) constructed from SP and resistivity log patterns. Fundamental procedures in the recognition and delineation of these genetic units followed the approach of Fisher and McGowen (1967), but utilized a greater density of well control.

Major progradational complexes, designated the Houston and Norias delta systems, are centered in the Houston and Rio Grande Embayments, respectively (fig. 1; pl. 13). The Houston delta system is characterized by numerous small, laterally dispersed lobes, in contrast to the more clearly defined, vertically stacked lobes of the considerably larger Norias delta system. These delta systems in East and South Texas were supplied by fluvial systems of different character. The East Texas Chita/Corrigan fluvial system consisted of several rivers and carried a mixed load of sand, silt, and clay, whereas the Gueydan system, to the south, was a single, considerably coarser grained river system (Galloway, 1977).

Separating these two major, structurally controlled fluvial-deltaic facies tracts was an area in Central Texas

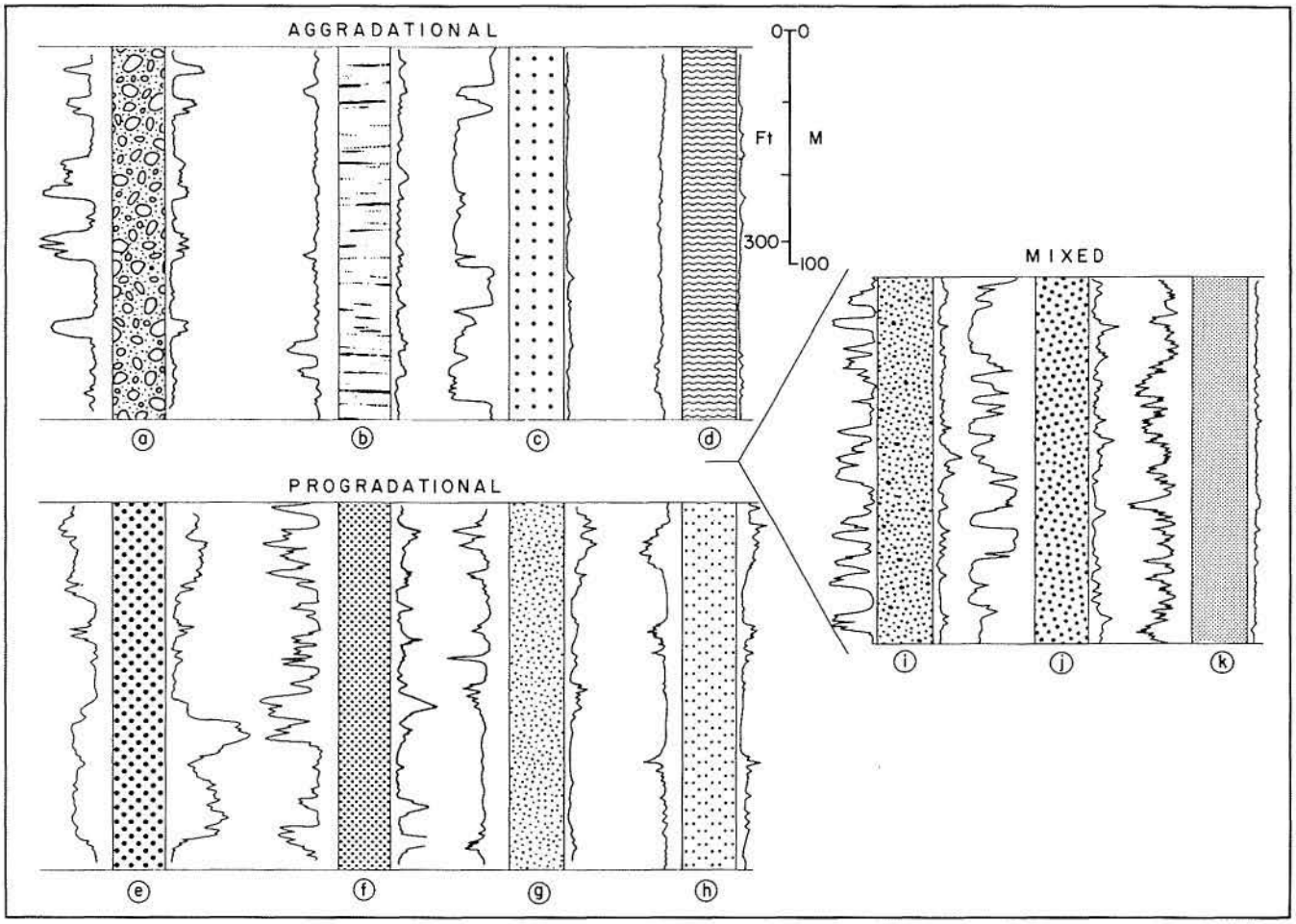

Figure 4. Electric log facies used to prepare log facies maps of the Frio MSU (pls. 10-12). Aggradational facies include (a) multiple blocky sand bodies within a sand-rich sequence, (b) thin, upward-fining to blocky sands within a sand-poor sequence, (c) thick, blocky sand bodies within a sand-rich sequence, and (d) massive mudstone. Progradational sequences are characterized by upward-coarsening bases of sand bodies and include (e) thick sand bodies within a sand-rich sequence, (f) multiple thin to medium, erratically upward-coarsening sand units, (g) multiple thin sand units, and (h) thick, well-developed, upward-coarsening units within a mud-rich section. Mixed log facies types include (i) composite sequences of upward-coarsening and upward-fining, thin to medium sand bodies, (j) blocky, thick sand bodies within sand-dominated sections, and (k) thinly interbedded sand and mud forming thick facies sequences that display both transitional and abrupt unit boundaries.

spanning the San Marcos Arch and traversed by relatively minor coastal plain streams. Deposition of the Choke Canyon/Flatonia coastal lake/streamplain system in this lower coastal plain area was dominated by silt and mud accumulation; widely spaced, minor belts of coarser grained stream deposits are best developed in the western half. Shore-zone sediments of Central Texas were derived in part along strike from adjacent deltaic depocenters, building up the substantial system of Frio coastal barriers and beach ridges first documented by Boyd and Dyer (1964). This trend is termed the Greta/Carancahua barrier/strandplain system (pl. 13) in this study. The similar but smaller Buna strandplain system developed on the eastern flank of the Houston delta system and thickens toward the Louisiana border. Updip from this zone of accreting beach ridges was an extension of the Chita/Corrigan fluvial system, which was progressively less active eastward, where it graded into muddy coastal lake and streamplain deposits (pl. 13).

Basinward, Frio elements include a shelf platform created by Jackson and Vicksburg deposition and a broad, unstable progradational slope, which locally in East Texas was deeply incised and embayed. The extensive, deep-water Hackberry Embayment of Louisiana continues into Orange and Jefferson Counties, and it is possibly represented by other smaller submarine slope-gorge and embayment fills along the Texas coast (Stuckey, 1964). Although the 2,000-ft (600-m) thickness of the Hackberry section in Jefferson County is less than its maximum in Louisiana, both the lower Hackberry Sand

and upper Hackberry Shale are recognized. Together, these correspond approximately to the middle Frio operational unit of this study.

Erratic, upward-coarsening log patterns and elongate, basinward-diverging sandstones emerging from a southeast-trending canyon led Halbouty and Barber (1961) to interpret a progradational deltaic origin for the lower Hackberry sandstones of Port Acres field, Jefferson County. Subsequent studies by Paine (1971) of equivalent strata in Louisiana established a deep-water origin (Brown and Fisher, 1977); this has recently been reaffirmed by Berg and Powers (1980) for East Texas. In Louisiana, elongate, slope-channel sandstones, characterized by the typical internal sequence recording waning flow conditions, merge basinward into blanketlike fan deposits that are thickest in bathymetric and structural depressions on the pre-Hackberry unconformity; these sandstones grade upward into shales containing a deep-water fauna. In East Texas, submarine slope channel-fill deposits are characterized by stacked, massive sandstones. Interbedded sandstone and shale along the channel margins grade into interchannel overbank shales containing thin turbidite sandstones (Berg and Powers, 1980). In some cases, the coeval, deeper water fan deposits are absent in the drilled succession but are anticipated downdip. Other canyons may have filled with an onlapping succession of turbidite-bearing channel sandstones overlain by distal fan deposits.

Smaller, strike-aligned intraslope basins elsewhere along the Texas coast were a product of growth faulting. These intraslope basins trapped large quantities of sediment transported by slumping and density flow.

GUEYDAN FLUVIAL SYSTEM

The Gueydan fluvial system records the entry of a major extrabasinal river into the Gulf Basin along the axis of the Rio Grande Embayment (Galloway, 1977). The system is characterized by coarse-grained, bed-load channel fills and commonly ranges from 15-percent to more than 40-percent sand.

Location and Boundaries

Mapped extent of the main drainage axes of the system averages 75 mi (120 km) in width and trends 50 to 70 mi (80 to 110 km) downdip, where it grades into the Norias delta system. In the middle and upper Frio sequence, fluvial facies extend across the Vicksburg Flexure. The system is bounded along strike by sand-poor streamplain facies.

Facies Description

Principal component facies of the Gueydan fluvial system include bed- and mixed-load channel-fill sand and conglomeratic sand, as well as laterally associated crevasse-splay sand and floodplain mud and siltstone (Galloway, 1977). Channel-fill sequences are 10 to 30 ft (3 to 9 m) thick and are commonly stacked, producing sand bodies 50 to 100 ft (15 to 30 m) thick (pl. 18). Channel-sand units also amalgamate laterally, forming sand-rich belts up to several miles wide. Log patterns are typically blocky and display sharp bases and abrupt to gradational tops (aggradational log facies *a*, fig. 4).

Overbank splay and floodplain sequences consist of massive mudstone with thin, discontinuous sand beds and lenses. Aggradational log facies *b* typifies such deposits.

Structural Style

Fluvial sequences dip gently basinward. Low-relief, broad domes and anticlines, as well as some minor fault displacement, occur, particularly where the system overlies deep-seated Eocene or Oligocene growth-fault trends. Structural modification is greatest where the Gueydan system crosses the Vicksburg Flexure.

Reservoir and Trap Configurations

Hydrocarbons are produced where fluvial and splay sands encased in the more mud-rich floodplain sequences cross anticlinal structures. Production from such large, low-relief features typically is complicated by faulting and by stratigraphic changes. Some stratigraphic entrapment also occurs.

NORIAS DELTA SYSTEM

The Norias delta system constitutes the main Frio depocenter in the South Texas Coastal Plain. Typical sand content ranges from 25 to 40 percent for a total Frio section that is more than 12,000 ft (370 m) thick. Deposition of the system resulted in progradation of the continental margin more than 60 mi (95 km) basinward, primarily during deposition of the lower and middle Frio sections. This major offlapping episode was terminated by the Anahuac transgression, but rate of sediment supply to the Norias system was sufficient to severely limit updip incursion of transgressive marine shelf facies (pl. 10). The upper Frio *Heterostegina-Marginulina* deltaic complexes continued to prograde locally across the Frio platform in the face of regional onlap (Agagu, 1975).

Location and Boundaries

Unlike the Houston delta system, the Norias system is the product of shifting drainage axes of a single large fluvial system. Consequently, lateral boundaries of the system remained fairly fixed through time (pl. 13). Maximum width of the system exceeds 125 mi (200 km), and seismically derived velocity mapping (Domenico, 1980) indicates that sand-rich deltaic facies extend up to 10 or more miles offshore from Kenedy County. Downdip and at great depth, deltaic facies, including genetically associated prodelta and upper slope deposits, grade into deep-water slope deposits of the offlapping continental platform. Northward along strike, the system grades into the Greta/Carancahua barrier/strandplain system. Rapid and extensive progradation of the Norias delta at the south end of the barrier/strandplain system is probably responsible for development of a relatively sediment-starved delta-margin embayment, which was barred by strike-reworked delta-flank sands, producing a barrier/lagoon complex. The comparatively slower and less extensive progradation of the Houston delta system produced a marginal strandplain that lacks lagoonal mudstones, separating laterally reworked strandline sands from well-developed inland coastal plain deposits. An analogous barrier/strandplain complex appears to flank the Norias delta system to the south and extends beyond present mapping, which terminates at the Rio Grande.

Facies Description

Regional sand-distribution patterns, as well as local sand-body configurations (Weise and others, 1981), indicate that the Norias delta system is a mosaic of wave-modified, lobate to wave-dominated, cuspate deltas (terminology of Galloway, 1975). Component facies assemblages include delta-plain, delta-front, and delta-flank sandstones and mudstones, and underlying prodelta and upper slope mudstones (pl. 18).

Delta-plain and closely associated reworked delta- and splay-margin sandstones include deposits of distributary channel and crevasse splay, and destructional-bar and beach-ridge environments. Distributary and larger splay-channel fills are blocky to upward-fining, bifurcating sand bodies 20 to 60 ft (6 to 20 m) thick (Nanz, 1954). Several such units commonly stack, forming thick belts 1 to 3 mi (1.5 to 5 km) wide that also contain interbedded splay and destructional sands. Larger splays form laterally discontinuous, upward-coarsening sequences interbedded with delta-plain and interdistributary-bay mud. Mixed progradational and aggradational patterns represented by log facies *i* (fig. 4) typify the facies assemblage. Bedded organic debris is notably absent in the Norias delta-plain facies, probably a reflection of the dry, subarid middle to late Tertiary paleoclimate of South Texas (Galloway, 1977). Sands and shales do, however, contain abundant detrital carbonaceous debris.

Delta-front facies include dominantly progradational sequences of channel-mouth-bar sandstone, laterally equivalent wave-reworked delta-margin sandstone, and subaqueous delta-front splay deposits, all of which are interbedded with and cap prodelta mud and siltstone. In updip or shallower parts of the main body of the Norias system, delta-front sand bodies are commonly less than 50 ft (15 m) thick and stack to produce repetitive cycles (log facies *f*, fig. 4). In deeper or more distal settings where the deltas prograded directly onto the continental slope or into rapidly subsiding growth-fault subbasins, the overall vertical sequence increases to as much as several hundred feet, and cyclic progradation of successive delta lobes across the most active growth faults produced composite sequences several thousand feet thick (pl. 18). Large-scale slumping, faulting, and soft-sediment deformation, such as observed at the modern Mississippi delta front (Coleman and Prior, 1980), dominated Norias delta-front deposition. Thickness of distal delta-front splays (initiated by sporadic slumping, debris flow, or flood discharge) increases greatly in proportion to the wave-reworked channel-mouth-bar or delta-margin sand cap. Resultant thick, upward-coarsening sequences are characterized by highly erratic or serrated log patterns (log facies *h*, fig. 4). Across some of the largest shelf-edge growth faults, where genetically equivalent sequences may thicken by an order of magnitude, slumping and density current flow may have remobilized quantities of delta-front sand, moving it down the prodeltaic upper slope into isolated, strike-elongate intraslope subbasins. Downslope damming by intraslope basins and consequent limited basinward extent of frontal-splay and slump sands (pl. 18) are inherent products of growth-fault mechanics (Crans and others, 1980; Dailly, 1976). Logs of such highly expanded delta-front and intraslope-basin sequences include both the blocky and highly serrated patterns (log facies *k*, fig. 4).

Delta-flank facies include thick (up to 100 ft or 30 m, or more), massive sandstone bodies characterized by transitional, upward-coarsening bases and located primarily along the flanks of the Norias delta system. Such sandstone bodies are dominantly strike parallel to lobate and continuous over several miles. Sand-rich progradational log facies patterns typify the assemblage, which is interpreted to consist of wave-reworked, stacked coastal barrier and thick delta-front sands deposited along the flanks of maximum progradation and fluvial influence during delta building. The facies grades laterally into massive, stacked barrier sandstones of the interdeltaic coastline.

Structural Style

Sediments of the Norias delta system are segmented by multiple belts of coastward-dipping growth faults. Fault zones are spatially related to development of deep

shale ridges and are characterized by dip-reversal (roll-over) on the downthrown side. Greatest fault activity accompanied deposition of delta-front and prodelta facies; thus, age of fault development tends to decrease basinward, reflecting the offlapping pattern of sedimentation (pl. 18).

Reservoir and Trap Configurations

Petroleum production from distributary-channel, crevasse-splay, delta-front, and delta-flank sandstones occurs throughout the delta system. Interbedded shelf or thick prodelta shales provide the necessary seal. Traps include shale-cored rollover anticlines, faulted anticlines, and, less commonly, closure against faults in the upthrown block.

CHITA/CORRIGAN FLUVIAL SYSTEM

The Chita/Corrigan mixed-load fluvial system constitutes a broad belt approximately 150 mi (225 km) wide, extending more than 50 mi (80 km) into the subsurface beneath the Upper Texas Coastal Plain (pl. 13). Maps and cross sections suggest the contemporaneous existence of at least three main drainage axes (Galloway, 1977). Component facies include meanderbelt and crevasse-splay sand bodies encased within floodplain and interchannel lacustrine mudstones, exhibiting types *a* and *b* aggradational log facies patterns (fig. 4). The regional coastward dip of the system is little affected by structure, except near a few shallow piercement salt domes.

HOUSTON DELTA SYSTEM

Several minor, laterally coalescent, vertically repetitive deltaic cycles make up the Houston delta system (pl. 13), which is the main locus of terrigenous accumulation in the Frio Formation of the East Texas Coastal Plain. The system was supplied by streams probably comparable in size to the modern Trinity, Brazos, and Colorado Rivers; but unlike these modern analogs, the deltas periodically extended beyond the main strandline into the open gulf and thus were subject to the brunt of deep-water wave attack. Marine processes redistributed deltaic sand along strike, supplying downdrift strandplain systems. There also was constant switching of the delta lobes, accompanied by destructional marine reworking and inundation of the abandoned site. Consequently, the rate of coastal progradation was slow and, in contrast to the comparatively abrupt northern margin of the Norias delta system, resulted in a transition boundary with the Greta/Carancahua barrier/strandplain system that is very broad (pl. 13). A further consequence of the limited fluvial influx was the almost complete marine domination and retreat of the Houston delta system during the Anahuac transgression (pls. 10 and 15). Thickness of the total Frio interval corresponding to the Houston delta system ranges between 1,800 and 7,500 ft (550 and 2,300 m), and sand content decreases distally from a local maximum of 60 percent to 10 percent (pls. 7 through 9).

Location and Boundaries

The Houston delta system (pl. 13) of East Texas extends 130 mi (200 km) along strike and 30 to 45 mi (50 to 70 km) downdip. It underlies parts of nine counties, but its most typical and consistent development is centered in southern Harris County. Whereas the boundaries with the adjacent barrier and strandplain systems fluctuated substantially, the updip and downdip boundaries of the delta system were relatively constant, shifting within narrow limits in response to both local and regional patterns of transgression and regression. The resulting superposition of successive progradational sequences within a coast-parallel tract contrasts with the broadly prograding Norias deltaic headland.

Facies Description

Log patterns and the areal distribution of sandstone bodies reflect their deposition by multiple, frequently shifting delta lobes. Updip deltas probably exhibited wave-dominated, arcuate geometries described by Galloway (1975), whereas a lobate configuration characterized deltas deposited either during episodes of maximum progradation or in areas of accelerated subsidence associated with salt withdrawal (Bebout and others, 1978). Facies of the Houston delta system include delta plain and backbarrier, strandplain and destructional bar, and delta front and prodelta/upper slope (pl. 15).

Delta-plain and backbarrier facies are closely associated and are distinguished from one another only on the basis of their position relative to equivalent seaward facies and, to a lesser extent, on the basis of the great strike continuity of certain backbarrier units. Environments represented include distributary channel and splay channel (blocky or upward-fining sandstones with little lateral continuity along strike), splay subdelta (thin, upward-coarsening units with moderate strike continuity, which are commonly stacked in multiples totaling several hundred feet thick), and destructional-barrier washover fan and flood-tidal delta (thin sandstones that normally exhibit gradational bases and strike elongation and that grade landward into lagoonal shales). Together, these units, characterized by log

facies *i* (fig. 4), constitute a predominantly aggradational succession that gradationally overlies a progradational delta sequence. In contrast to the older Tertiary delta systems, such as that of the Wilcox (Fisher and McGowen, 1967), bedded lignite is absent.

Strandplain and destructional-bar facies comprise blocky, strike-oriented sandstones of log facies *c* (fig. 4) between 50 and 1,000 ft (15 and 300 m) thick that lie above or updip of delta-front facies. They resemble sandstones of the broad interdeltaic tracts but are an integral part of the Houston delta system. This facies is notably absent in the most regressive deltaic units. The origin of the strandplain and destructional-bar facies was related to pronounced marine modification of deltaic deposits, probably in part contemporaneous with progradation of arcuate deltas (Galloway, 1975). The considerable thickness of several of these blocky sandstones is too great to be accounted for by progradation alone. It is more likely that transgressive reworking resulted in aggradation of the destructive-bar sands and the development of stacked strandplain sands along strike.

Delta-front and prodelta/slope facies are represented by upward-coarsening sequences or partial sequences. Two variants are distinguished on the basis of sequence thickness, position relative to major growth faults, and sandstone geometry; one originated on the shallow shelf and the other in the deeper, unstable shelf edge.

Updip, progradational cycles of the stable shelf are thin (50 to 150 ft or 15 to 45 m thick) and vertically repetitive. Log facies *g* (fig. 4) represents purely progradational units, whereas log facies *f* represents a combination of delta-front progradation and delta-plain, strandplain, and destructional-bar aggradation. Some of the sandstone units are broadly lobate, but most appear strike oriented as a result of effective alongshore redistribution of sand by marine processes acting on arcuate delta fronts.

Thick, growth-faulted sequences of the unstable shelf edge attain a maximum thickness of 1,000 ft (300 m), and on the downthrown side of major growth faults they are superimposed to a thickness of 3,000 ft (900 m) or more (pl. 15). The greater part of these sequences consists of shale; however, they show an upward increase in the proportion of erratic, thin sandstone units, probably representing storm-generated or gravity-resedimented deposits of the upper prodelta and distal mouth bar. Massive delta-front and mouth-bar sandstones of these shelf-edge deltas are relatively thin, averaging between 40 and 100 ft (15 and 30 m), and tend to be lobate or elongate perpendicular to the paleoshoreline (Bebout and others, 1978).

Structural Style

A very complex structural framework includes deep salt anticlines, shallower salt diapirs and associated radial faults, salt-withdrawal basins, and regional growth faults. Once initiated, growth faulting continued to displace successively higher strata, even though additional loading may have been insignificant because of the inherent instability of the buoyant salt at depth. Continued fault displacement and ready initiation of new faults produced a close pattern of strike-parallel, broadly arcuate fractures. This pattern is quite distinct from the more widely spaced, clearly defined regional fault systems of South Texas. Isolated, circular to ovoid areas of anomalously thick sand accumulation may represent salt-withdrawal basins or sites of major growth faulting.

Reservoir and Trap Configurations

Delta-front and delta-plain sands coalesce along strike to form moderately continuous reservoirs. Reservoir continuity in the dip direction is severely limited by facies changes, which for the most part are related to growth faulting. Locally abrupt changes in sandstone geometry and thickness are associated with salt diapirs.

Most producing traps are related either to faulted anticlines above deep salt ridges or to growth-fault traps, where they are sealed against either the upthrown or downthrown block. Stratigraphic factors contribute to trapping in areas of abrupt facies change; but in all cases, facies stratigraphy is subordinate to structure in determining the configuration of the major traps.

BUNA STRANDPLAIN/BARRIER SYSTEM

Location and Boundaries

The Buna strandplain/barrier system is restricted to parts of Liberty, Jefferson, Hardin, Jasper, Newton, and Orange Counties and continues eastward into Louisiana. Limited shore-zone progradation persisted throughout Frio deposition, even during upper Frio deposition, when elsewhere there was a tendency toward shoreline retreat. More importantly, however, coastal aggradation produced thick sequences of stacked shore-zone sands.

Facies Description

Strike-oriented sands containing a relatively small proportion of finer sediments are the distinguishing feature of the Buna strandplain/barrier system. Blocky log patterns are common, as are irregular, upward-coarsening, sandy successions up to 500 ft (150 m) thick, some of which include subordinate upward-fining packages.

The dominant sandy facies are shoreface and beach, which together produce thick aggradational sequences.

Abundant sand carried along strike from the Houston delta system, and possibly from other comparable delta systems in Louisiana, provided a lateral gradation from shallow-water, arcuate deltas through a strandplain to a barrier/lagoon shoreline. The latter is distinguished by moderate updip development of shore-parallel, back-barrier shales and sporadic sand beds introduced from the seaward side. The strandplain immediately east of the Houston delta system received some sediment directly from major, but relatively short-lived, fluvial axes.

Subordinate finer grained facies, which vertically separate thick packages of strandplain and barrier sands, accumulated during episodes of regression in marsh, slough, and lagoonal environments and during episodes of minor transgression in lower shoreface and shelf environments. The blocky shore-zone sands are multistoried and imply prolonged aggradation (Winker, 1980; Fisher and others, 1969). Additional variations between upward-coarsening (log facies *d*, fig. 4) and upward-fining packages (pl. 14, for example) are attributed to minor shifts of the strandline position occasioned by variable rates of sediment input, local subsidence, or, possibly, eustatic sea-level change.

Finer grained lagoonal facies show complex interfingering along the landward margin of the barrier trend (pl. 14, log 9). Sandy beds within the predominantly shale succession probably represent flood-tidal-delta and washover deposits.

Structural Style

The dominant structures are a combination of growth faults, low-amplitude anticlines underlain by salt, and shallow salt diapirs. There is not the major disruption of facies patterns characteristic of the adjacent salt-withdrawal basins.

Reservoir and Trap Configurations

The strandplain and barrier reservoir sandstones are thick, exhibit great lateral continuity along strike, and have high porosity and permeability; however, they lack seals. Traps are therefore largely confined to major growth faults and salt domes, along with some deep anticlinal traps.

CHOKE CANYON/FLATONIA COASTAL LAKE/STREAMPLAIN SYSTEM

The middle of the Texas Frio coastal plain consists of a broad, sand-poor apron containing many thin, narrow, dip-oriented, mixed-load to bed-load fluvial channel-fill and meanderbelt sandstone bodies, which are encased in silt and mudstone sequences deposited in floodbasin, open-shallow-lake, and tributary settings (Galloway, 1977). The section dips gently basinward. Minor local faults and low-relief anticlinal structures are associated with deep-seated Eocene growth-fault zones. Numerous shallow fields produce from such low-relief structures and from stratigraphic traps. The system is characterized by aggradational log facies *b* (fig. 4).

GRETA/CARANCAHUA BARRIER/STRANDPLAIN SYSTEM

Location and Boundaries

The Greta/Carancahua barrier/strandplain system was first documented by Boyd and Dyer (1964). It comprises a linear sandstone belt separating marine from brackish-water shales and extends from Nueces County in the west, where it is gradational with the Norias delta system, to the Houston delta system in the east. The barrier system thus coincides with the updip sand-poor streamplain and coastal lake system. The locus of sand accumulation shifted 10 to 20 mi (15 to 30 km) basinward during lower to middle Frio deposition before undergoing a transgressive reversal in the upper Frio. As in the Buna strandplain/barrier system, however, vertical upbuilding of sands was the main depositional pattern.

Facies Description

Massive, blocky, stacked barrier and strandplain sandstones dominate intervals of as much as 4,000 ft (2,500 m); thin, irregular, shaly interbeds are more abundant near the base and top. In cross section (pls. 16 and 17), the sands pinch out abruptly seaward into shaly shelf facies containing neritic foraminiferal faunal assemblages (Martin, 1969). Landward, the gradation into backbarrier-lagoon, bay, or lower coastal plain fluvial-deltaic mudstone extends over a broader area, particularly in the upper parts most affected by marine transgression.

Shoreline conditions remained remarkably uniform during lower and middle Frio deposition. To the south, a wave-dominated barrier coast, probably resembling the Padre/Mustang/Matagorda complex of modern Texas islands, underwent significant aggradation. Northward, many small streams supplied sediment directly into the gulf, where sands were combined with strike-reworked sediment to form a complex assemblage of strandplain and delta-destructional facies. Large proportions of these barrier sands were preserved during ensuing transgressions because of continued subsidence. Analogous multistoried sands of the Ingleside (Pleistocene)

strandline trend are as much as 5 mi (8 km) wide and 80 ft (25 m) thick (Winker, 1979). Frio deposition was characterized by a comparably stable shoreline position during a much longer interval of geologic time. The modern Texas coast is aggrading (Morton, 1977), but little vertical growth of stable barriers has occurred during the limited timespan of a few thousand years. The lenticular and tongue-shaped sands along the landward margin of the Frio barrier trend are probably stacked washover-fan and flood-tidal-delta deposits. As in the other coastal facies of the Frio Formation, extensive sheet sands occur near the top. In the southern part of the Greta/Carancahua system, irregular aprons of sand and silt were deposited on the lower shoreface and inner shelf by storm-generated waves and wind-set or storm-surge currents. Barrier-front and interbedded shelf facies sequences may exceed 1,000 ft (300 m) in thickness in rapidly subsiding, fault-bounded subbasins (pls. 16 and 17).

Boyd and Dyer (1964) suggested that the barrier and strandplain sands were derived from the Norias delta system. It is equally possible that, like the modern Padre Island coast, Frio longshore drift systems converged from the southwest and northeast (Morton, 1977), supplying sand from the Houston delta system as well. Littoral convergence would have ensured an adequate supply of sand over the considerable distance represented and would account for the relatively uniform development of shoreline sands between the two delta systems. Sand mineralogy (Bebout and others, 1978) supports such convergence and indicates that little sand from the Norias delta system was transported northward beyond San Patricio County.

Structural Style

The dominant structural control was growth faulting. This accentuated the strongly strike-parallel facies orientation. The greatest vertical stacking of sandstone occurs between the Vicksburg and Frio Flexures; however, the mapped axis of the system crosses to the downdropped side of the Frio Flexure as it approaches the Norias deltaic headland during deposition of the middle and upper Frio (pls. 8 and 9). Parallel structural and depositional trends suggest a strong interaction between fault growth and localization of specific depositional environments.

Reservoir and Trap Configurations

The rarity of hydrocarbon seals has severely limited oil and gas accumulation in the thickest axis of multistoried barrier/strandplain sandstone. Landward of the sandstone depocenter, numerous stratigraphic and combination traps are present. Structure plays a key role, however, and trapping is most commonly related to simple and faulted anticlines and rarely to fault seals.

ANAHUAC SHALE WEDGE

The Anahuac Shale wedge constitutes a regional marine unit. In part it was deposited contemporaneous with, and is indistinguishable from, upper Frio prodelta muds. In the Rio Grande Embayment, continued active deltaic deposition and progradation in the face of basinwide submergence resulted in a dominance of prodelta facies that are interbedded with deltaic sands, producing an ill-defined updip margin of the wedge. The shale is thick, well developed, and easily correlated beneath most of the Middle Texas Coastal Plain, where it is likely the product of open-shelf, suspension sedimentation. A mix of shelf and prodeltaic mudstone characterizes the Anahuac wedge of the Houston Embayment. In thicker, basinward parts of the wedge, prodeltaic and lower shoreface muds and muddy silts of the subsequent Miocene Fleming progradation were deposited upon the transgressed continental platform.

FRIO DEPOSITIONAL HISTORY

Geometry of the Frio progradational wedge developed in response to pronounced subsidence of the extensive, inherently unstable platform margin. Updip, the time-equivalent Catahoula Formation is as much as 1,000 ft (300 m) thick and accumulated on the progradational continental platform inherited from Yegua, Jackson, and Vicksburg deposition. The large, integrated Gueydan fluvial system that originated in the desert Southwest flowed down the axis of the Rio Grande Embayment. In contrast, at least two separate river networks constitute the Chita/Corrigan fluvial system in the Houston Embayment; however, net-sand isopachs show that the positions of the fluvial axes changed substantially with time (Galloway, 1977).

A semiarid climate prevailed in the south. Widespread destruction of vegetation by ash emanating from the volcanic terrane of northwestern Mexico and attendant flash floods, along with the dry climate, favored evolution of low-sinuosity, bed-load channels flanked by broad, ash-laden crevasse splays (Galloway, 1977). Paralleling the modern climatic zonation, relatively humid conditions existed in East Texas. Sinuous, mixed-load channels draining a diverse sedimentary hinterland were separated by large lacustrine basins and floodplains (Galloway, 1977). Small, localized streams flowing across the San Marcos Arch drained a basin margin where Cretaceous carbonates and marls were exposed.

A downdip succession of fluvial, deltaic, barrier, and strandplain deposits occurred below a present-day burial depth of approximately 2,000 ft (600 m). Patterns of coastal progradation varied according to local structural controls. In East Texas, continued regional subsidence was accentuated by salt withdrawal and by foundering of the platform edge. Infilling of the Rio Grande Embayment proceeded across successive fault-bounded subbasins, each of which underwent slope offlap capped by progradation of deltaic complexes over the thick, muddy platform sequence.

Main processes contributing to deep-water deposition were the accumulation of pelagic clays and terrigenous muds and the gravity resedimentation of shallow-water deposits. Mass movement of delta-front deposits was probably responsible for irregularly interbedded slope sandstones marginal to both the Norias and Houston delta systems. Delta-front mudflows (Roberts, 1980) and slumps (Coleman and Prior, 1980) were undoubtedly important mechanisms for downslope transport, particularly in the most regressive deltaic units containing a relatively large component of fine-grained sediment. According to Roberts (1980), the high water content (up to 80 percent), together with the gas liberated by the abundant organic matter in fine-grained deltaic sediments, produces excess pore-water pressures that lead to slope failure. Strike-parallel intraslope basins related to growth faults and mud or salt ridges may have trapped large quantities of delta-front sediment transported by slumping, mass flow, and turbidity currents.

Mass-flow processes comparable to those operating on the modern Mississippi delta slope may have been responsible for initiating erosion of the large submarine canyons in the outer neritic to deep-water Hackberry Embayment, a prominent feature during middle Frio deposition. Bathyal depths of accumulation are established by the foraminiferal assemblage in the Hackberry sequence (Garrett, 1938). The major part of the embayment was located in Louisiana, but extended through much of Orange and Jefferson Counties, Texas, where canyons in the outer shelf and slope were at least 600 ft (180 m) deep and 3.5 mi (5.6 km) wide (Berg and Powers, 1980). Erosionally carved canyons were filled by onlapping turbidity channel and overbank deposits, suggesting that major submarine fan sand deposits might occur at greater depth (Paine, 1971; Brown and Fisher, 1977; Berg and Powers, 1980). Headward retreat of gully systems by slumping updip of the major canyons would have tapped large volumes of shelf and possibly even shoreface sand. This would account for the stacking of numerous turbidite beds, which average about 10 ft (3 m) thick, to produce channel-fill sand bodies up to 200 ft (60 m) thick (Berg and Powers, 1980). Canyon-fill shales are distinguished from adjacent shallow marine shales on the basis of microfaunal content.

Additional deep-water embayments probably existed along the Texas coast during Frio deposition. Stuckey (1964) identified a broad, mudstone-filled reentrant extending through coastal Brazoria and Matagorda Counties, corresponding in position to the outer shelf and slope fronting the Houston delta system.

The Norias delta system constituted the most actively prograding coastal sector. Deposition of the lower Frio operational unit (pl. 12) was characterized by shoal-water, arcuate deltas and wave-modified, lobate deltas that produced a massive, sandy facies sequence extending basinward to the approximate position of the Frio fault zone. Beyond this were deposited highly expanded, shelf-edge delta sequences. These deltas probably assumed a more fluvially dominated, lobate plan-view geometry because of rapid subsidence and reduced marine redistribution of sand. This was followed by middle Frio progradation (pl. 11) of the deltaic platform by as much as 40 mi (65 km). By upper Frio deposition (pl. 10), the shelf edge had built gulfward to eastern Cameron County and locally beyond the modern coastline.

Regional Anahuac marine transgression and onlap caused the Norias delta shoreline to retreat by only 25 mi (40 km), and delta progradation persisted locally during this regionally transgressive interlude, spreading muds across the foundered platform. Marine redistribution of sediment was accentuated, and arcuate delta geometries were likely (Curtis, 1970; Galloway, 1975). Interspersed destructional-bar and strandplain facies were abundant, and graded into a barrier/lagoon facies in the delta-margin embayment to the north.

The delta-margin embayment of South Texas merged across the San Marcos Arch with a broad strandplain flanking the Houston delta system. This Greta/Carancahua barrier/strandplain system constituted a prominent zone of strike-parallel aggradation brought about by a combination of structural and depositional factors. Growth faults accentuated a consistent coast-parallel trend, defining narrow, linear zones of subsidence. Convergent littoral drift provided large volumes of sand from the deltaic headlands on either side. Shoreline conditions along the Greta/Carancahua trend remained remarkably uniform during lower and middle Frio deposition, resulting in the development of an exceptionally thick but narrow, vertically homogeneous, sandy succession. Minor progradation occurred during lower and middle Frio deposition, accompanied by landward retreat of the progressively less well defined shore-zone sand belt during upper Frio deposition.

The Houston delta system of East Texas, like the Norias delta system, was characterized by elongate to lobate deltas during the most regressive phases and by more arcuate deltas during episodes of general transgression and shoreline retreat. Because of the greater structural complexity of the salt-floored Houston Embayment, the systematic patterns of delta-front pro-

gradation observed in deposits of the Norias delta system were not developed in the Houston delta system. Furthermore, because of the more dispersed, multiple-drainage network in the eastern Coastal Plain, which supplied sediment at several points along the coast, and because of the constant switching of delta depocenters, imbricate stacking of facies tended to occur along a regional strike-parallel belt. Thus, vertically repetitive, upward-coarsening sequences and partial sequences characterize the Houston delta system. Maximum thickness of individual prodelta/delta-front sequences approaches 1,000 ft (300 m) in shelf-edge progradational deposits of the lower Frio; thinner platform-delta sequences 50 to 300 ft (30 to 185 m) thick typify the middle and upper Frio operational units. Capping many of the individual or stacked progradational sequences are lithologically complex, aggradational delta-plain deposits. These include blocky distributary sandstones and thin, upward-coarsening bayfill and crevasse-splay subdelta packages. Much thicker (250 to 1,000 ft or 75 to 300 m) blocky sandstones, which are interspersed within and marginal to the delta-plain deposits, record the development of multistoried, wave-reworked sands of recurrent delta-destructional phases.

During deposition of the lower Frio, the shelf edge was approximately coincident with the eastern extension of the Vicksburg fault zone, although the fault is poorly defined in East Texas. Localized shelf-edge deltas of frequently changing position built seaward over muddy, aggrading slope environments that were subject to sporadic influx of resedimented delta-front sands. The greatest volumes of delta-front and mouth-bar sand were preserved coincident with the seaward terminations of major fluvial axes; the trend through Wharton and central Matagorda Counties is one example.

By middle Frio deposition, the shelf edge had been extended seaward and the main locus of coarse-grained deposition had shifted to the east, where sandy, marine-modified deltas were supplied by large fluvial channel systems flowing through Fort Bend, Harris, and Liberty Counties. The middle Frio expands westward and contains a greater proportion of mud. Small, lobate, shoal-water deltas built rapidly to the shelf edge but were largely reworked into coast-parallel bars after abandonment.

Depositional style of the upper Frio Houston delta system was strongly influenced by the Anahuac marine transgression. Successive transgressions extended farther landward, but were separated by episodes of delta progradation. The deltas became smaller as successive lobes shifted landward, and wave reworking along the encroaching shoreline produced thick, time-transgressive blanket sands, such as the Greta sand, near the top of the Frio Formation.

The Buna strandplain/barrier system marginal to the Houston delta system on the east resembles the Greta/Carancahua system, but shows evidence of frequent, though minor, coastal regressions and retreats punctuating the sequence of blocky, strike-parallel sandstones. These oscillations probably stemmed from variations in alongshore sediment supply resulting from changing positions of the delta lobes and from a fluctuating local supply of sediment from coastal plain streams.

This easternmost segment of the Frio shoreline was subject to lower rates of subsidence than elsewhere along the Texas coast, a situation that favored prolonged reworking by waves. Wave-dominated, arcuate deltas, in which marine reworking was contemporaneous with progradation, developed locally during lower Frio deposition, but were volumetrically less important than strike-fed strandplain systems. Water depths decreased following these initial episodes of delta progradation, and remaining Frio deposition was characterized by slower accumulation of sand in a stable shore zone. Areas of backbarrier mud accumulation were subject to sporadic influx of washover and flood-tidal-delta sands.

Sands were spread greater distances landward by minor marine transgressions during deposition of the uppermost part of the Frio Formation. Log patterns in the Miocene succession above the Anahuac transgressive shale wedge indicate a continuation of the Buna strandplain/barrier style of sedimentation, but show considerable thickening of analogous facies as the Miocene depocenter migrated eastward into Louisiana.

COMPARISON OF FRIO AND LATE PLEISTOCENE PALEOGEOGRAPHY

The geographic distribution of reconstructed Frio systems (fig. 5) bears striking resemblance to those of the late Pleistocene (Winker, 1979, 1980; McGowen and others, 1976; Brown and others, 1976; Fisher and others, 1973) and modern coastal plain and shelf (McGowen and others, 1977; Morton and McGowen, 1980). Oligocene tectonic framework, climatic zonation, drainage pattern, and coastal and nearshore hydrologic regime were comparable to those of the present. A primary difference is that early- to mid-Tertiary sea levels were not subject to the short-term glacio-eustatic oscillations characteristic of the Quaternary. These glacio-eustatic base-level changes exceeded regional subsidence rates (Winker, 1979), except near the shelf edge. In contrast, intrabasinal factors were more important than the slower tectonic-eustatic changes during Frio deposition. The same depositional phases—progradational, aggradational, and transgressive (Winker, 1979)—are nevertheless represented in the Frio and Quaternary successions, marking a similar response to shifting shorelines and depocenters, albeit on a different time scale. This time factor has

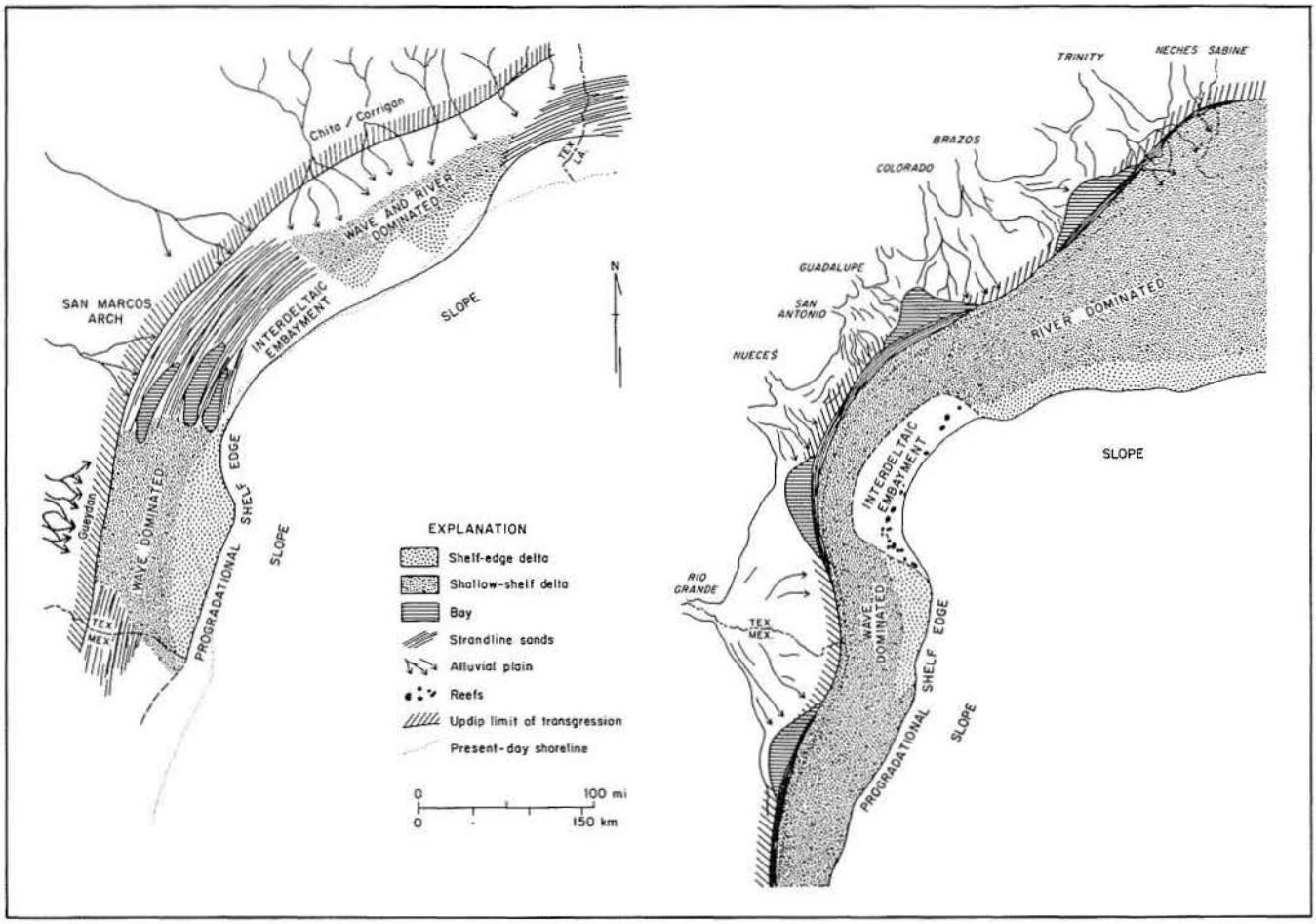

Figure 5. Comparative Frio Formation and late Pleistocene (Winker, 1979 and 1980) paleogeography of the Texas coastal plain and shelf. Pleistocene deltaic deposition dominated the upper and lower coastal plain and shelf, particularly during low-sea-level periods of maximum progradation. Fluvial, strandplain, and backbarrier-bay/lagoon deposition occurred primarily during the aggradational phase concurrent with maximum transgression. During Frio deposition, aggradation also occurred concurrently with progradation and local downdip transgression. During both late Pleistocene and Frio deposition, the central Texas coast formed a large, wave-reworked, interdeltaic embayment dominated by barrier and strandplain depositional systems.

resulted in major differences in the thicknesses of units occupying the same paleogeographic zone.

The modern Texas coast, having recently recovered from a rapid post-glacial rise in sea level, has reached a stage of general stability, although minor transgression still prevails over much of its length (Morton, 1977). The aggradational phase has commenced, but has not yet proceeded significantly. A more advanced stage of development is recorded in the late Pleistocene Beaumont Formation (Winker, 1979), which was deposited under conditions practically identical to those of the present day. The greater thickness, broader lateral extent, and more fully developed range of depositional phases in the Beaumont Formation make it a useful analog to the Frio (fig. 5).

Winker's (1979, 1980) synthesis of the Beaumont Formation showed that a characteristic facies architecture typifies each of the depositional phases—progradational, aggradational, and transgressive. Winker further divided the progradational phase into shallow-shelf and shelf-edge components.

Shallow-shelf deposits of the progradational phase developed in response to the falling sea level accompanying onset of Wisconsin glaciation. Progradation was rapid, generating thin, upward-coarsening sequences that were best developed in the wave-dominated deltas of the Rio Grande Embayment. Deltas in East Texas were multilobate and river dominated. Rivers became entrenched during the progradational phase (fig. 6), resulting in limited fluvial accumulation.

Frio drainage patterns and distribution of delta types were strikingly similar to those of the late Pleistocene coastal plain (fig. 5), but slower rates of relative

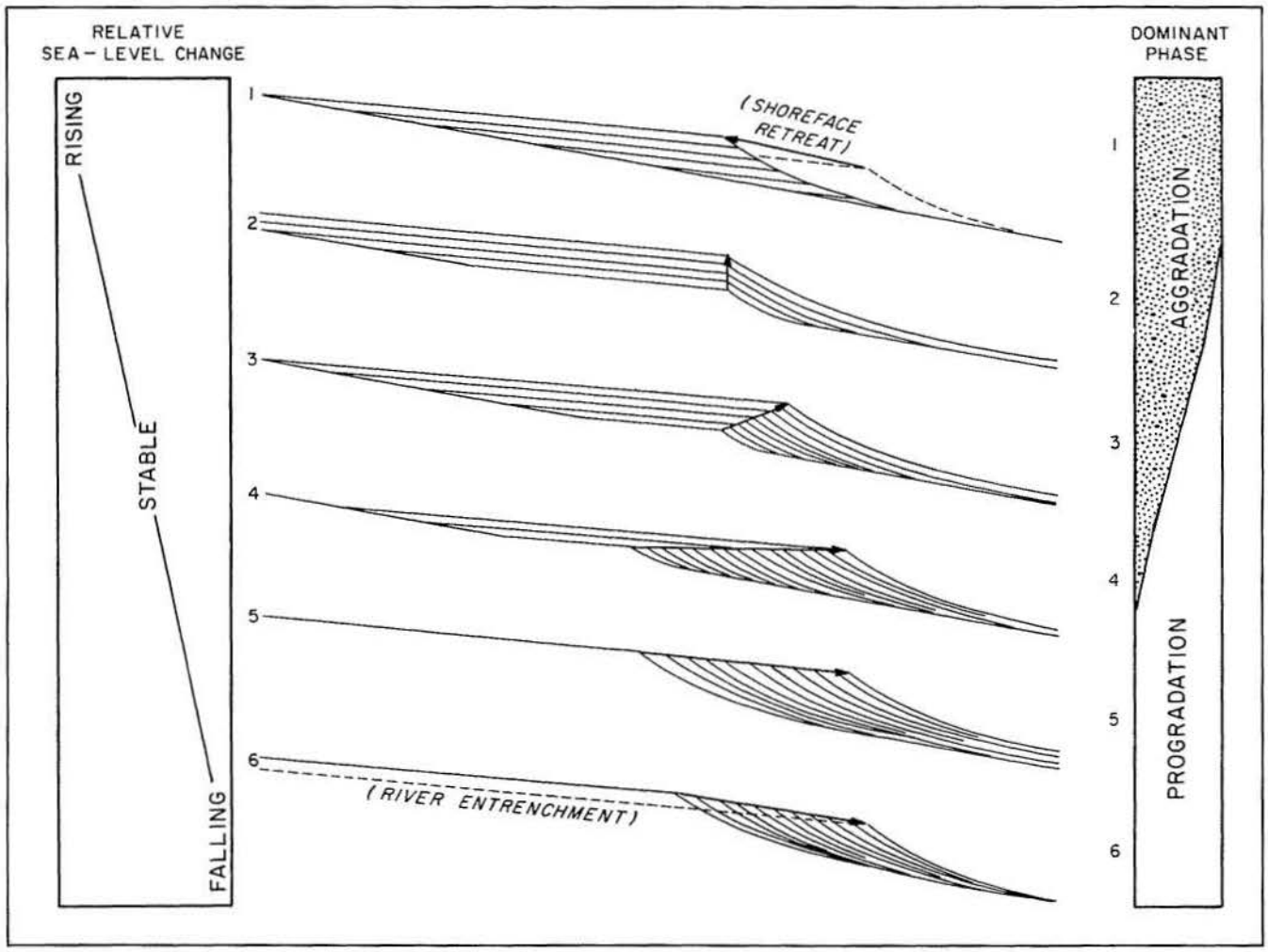

Figure 6. Relative importance of progradation and aggradation associated with rising, stable, and falling relative sea levels (after Winker, 1979 and 1980). During Frio deposition, only the Norias delta system was dominated by progradation. Elsewhere along the coast, aggradational patterns 1, 2, and 3 tended to alternate with minor progradational episodes marked by patterns 4, 5, or 6.

subsidence permitted fluvial deposits to spread laterally and to coalesce within the Rio Grande and Houston Embayments. Rates of growth faulting were slow, and delta sequences characteristically are thin but areally extensive.

Shelf-edge deposits of the progradational phase of the Beaumont Formation were characterized by rapid vertical accumulation in a narrow zone along the shelf margin (Winker, 1979), a pattern closely duplicating that of Frio deposition. The same three factors contributed to rapid subsidence in both cases: growth faulting, salt and mud withdrawal, and isostatic loading.

The *aggradational phase* (fig. 6) of the Beaumont Formation followed Sangamon transgression (Winker, 1979). Major sand bodies deposited during this phase are barrier, strandplain, and fluvial deposits. Strandplains developed along the flanks of deltaic headlands, and barriers formed in marginal embayments. The same patterns prevailed during Frio deposition, except that the aggradational phase was not so clearly defined, because significant aggradation also occurred contemporaneous with downdip progradation and transgression. Thick, multistoried Frio barrier/strandplain successions record reworking during numerous local transgressive events produced by shifting deltaic depocenters and rapid subsidence.

The *transgressive phase* of the late Pleistocene and Holocene was characterized by slow sediment influx and sediment reworking. Many of the thin, laterally extensive shale units within the Frio Formation reflect analogous phases, contain a neritic fauna, and pinch out updip. The considerably thicker Anahuac Shale wedge marks the regional incursion of a comparatively sediment-starved shelf that punctuated early Miocene deposition.

STATISTICAL CHARACTERIZATION OF FACIES ASSEMBLAGES

In an attempt to quantify the lithologic characterization of the interpreted Frio depositional systems, statistical data on sandstone and shale units of the Frio MSU were compiled, using five genetic facies assemblages characteristic of one or more systems: streamplain, fluvial, delta, barrier, and shelf. The first four assemblages define major depositional systems. The shelf assemblage represents sand-poor sections that lie beneath or downdip of the deltaic or strandline facies; it is thus a component facies of each of the coastal systems defined in this report. Statistical data compiled from electric logs of 860 wells included bed thickness, sandstone percentage, and frequency of interbedding of sandstone and shale units. The dominant facies assemblage represented by each well was interpreted from facies maps.

Quantitative description of lithofacies characteristics is potentially useful for (1) statistical estimation of average reservoir thickness and variability, (2) determination of contact area between reservoir and source units, which in turn influences hydrocarbon expulsion efficiency, and (3) demonstration of significant differences in fundamental bedding relationships within the depositional systems that might affect their hydrocarbon productivity capacity.

Thicknesses of Sandstone and Shale Units

Distributions of sandstone-unit thickness for each of the five Frio depositional facies assemblages are shown in figure 7. The X axis of each graph in this figure has a logarithmic scale, and the plots suggest log-normal distributions.

To test log-normality of the thickness distribution of sandstones, cumulative percentage was plotted against sandstone thickness on a log-probability scale (fig. 8). The distribution of sandstone thickness for each of the five facies assemblages can be approximated by a straight line, confirming that a log-normal distribution represents the samples. Except for the shelf assemblage, all the environments display relatively parallel distribution trends variously shifted to the left or right along the horizontal axis. The distribution pattern for the shelf assemblage shows a more inclined trend, indicating that sandstone-body thickness is more variable in this assemblage. This is reasonable, as sandstone bodies within the shelf assemblage include a mix of scattered, growth-faulted delta- and barrier-front, as well as slope, sand units.

Using cumulative-percentage plots such as those shown in figure 8, one can graphically determine the median and the standard deviation. Median sandstone thickness can be estimated directly from the plot by reading the thickness at the 50-percentile point for each environment. The approximate standard deviation is the difference between the median sandstone thickness and the thickness at either 16- or 84-percentile points on the Y axis.

Table 1. Statistics (in feet) of sandstone-unit and shale-unit thickness.

	← one standard deviation		one standard deviation →	
	Minimum	**Median**	**Maximum**	**Average**
Sandstone				
Streamplain	8	17	35	29
Fluvial	10	18	33	28
Delta	14	25	42	36
Barrier	19	37	72	55
Shelf	7	18	47	33
Shale				
Streamplain	46	84	150	118
Fluvial	32	56	98	77
Delta	26	47	87	66
Barrier	17	37	78	59
Shelf	70	50	320	300

Values estimated from figure 8 are shown in table 1, along with the average sandstone thickness. Because of its log-normal distribution, the median sandstone-body thickness is significantly less than the average thickness. The thicknesses of sandstones corresponding to the maximum (84-percentile point) and the minimum (16-percentile point) values may be considered the upper and lower limits to be used in assessing reservoir thickness by statistical methods, such as Monte Carlo random sampling. Interestingly, median sand-body thicknesses for Frio fluvial, deltaic, and barrier facies suites closely approximate those of their Quaternary counterparts.

The fact that the sandstones of the Frio MSU are distributed log-normally may also be important in evaluating how most sandstones pinch out. It suggests that the pinch-out would occur logarithmically rather than arithmetically. In other words, when sandstone-thickness contours are drawn around a pinch-out area, equal spacing of the contours, which implies a uniform or arithmetic change of sandstone thickness, is unlikely. Changes from a certain thickness to zero thickness must be more abrupt (logarithmic change). The statistical data discussed above, therefore, can be used to guide sandstone isopach mapping style.

Similar plots (figs. 9 and 10) show that the distribution for shale thickness is also approximately log-normal. Trend lines of the streamplain, fluvial, and deltaic facies suites are nearly parallel, but shifted relative to the

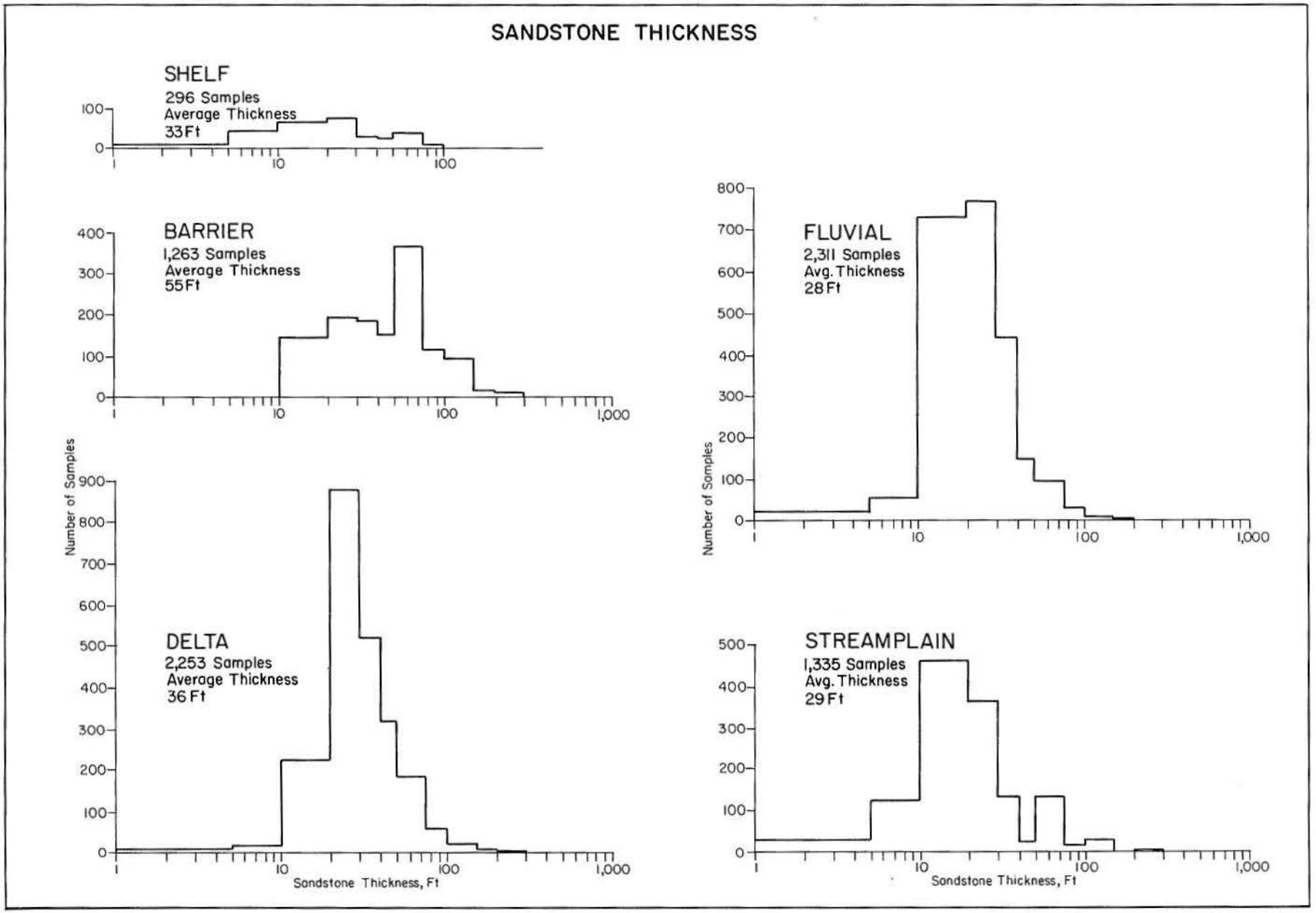

Figure 7. Distribution of sandstone-body thickness for the five facies assemblages of the Frio Formation. Scale on the X axis is logarithmic.

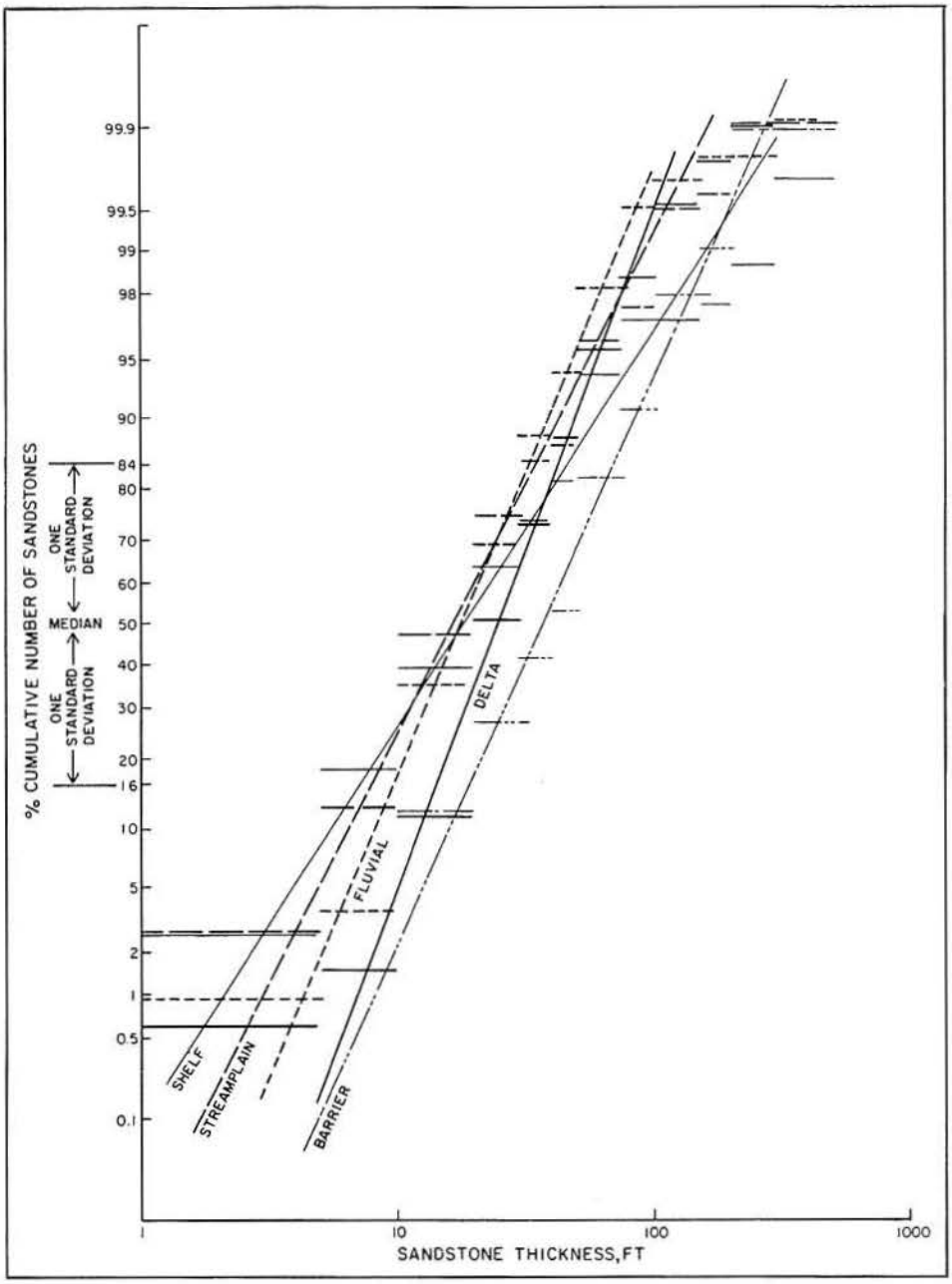

Figure 8. Cumulative-percentage plots of sandstone-unit thickness on a log probability scale. Each of the five facies assemblages approximates a log-normal distribution pattern, which is shown by a straight line on the plot.

horizontal axis. The lines representing both the barrier and shelf environments are flatter than those of the other environments, suggesting that the populations are more widely distributed. The standard deviations for the barrier and shelf, both of which reflect greater marine influence than the others, are thus greater (table 1).

Number of Sandstone and Shale Units

To expedite data gathering, the number of shale units was assumed to equal the number of sandstone units counted. The numbers are normalized on 1,000-ft (300-m) intervals. Figure 11 depicts frequency distributions for the number of sandstones (or shales) per 1,000 ft (300 m) within each of the five facies assemblages. A normal graph scale was used on the assumption that the distribution pattern of the sandstone-shale interbedding should be normal rather than log-normal. This assumption appears justified because the plots can be approximated by a straight line (fig. 12). Toward the upper end of each plot, however, trends flatten, suggesting that a normal distribution does not persist where the number of sandstones (or shales) is relatively large. The statistical parameters estimated from figure 12 are summarized in table 2. Here, the median values are relatively close to the

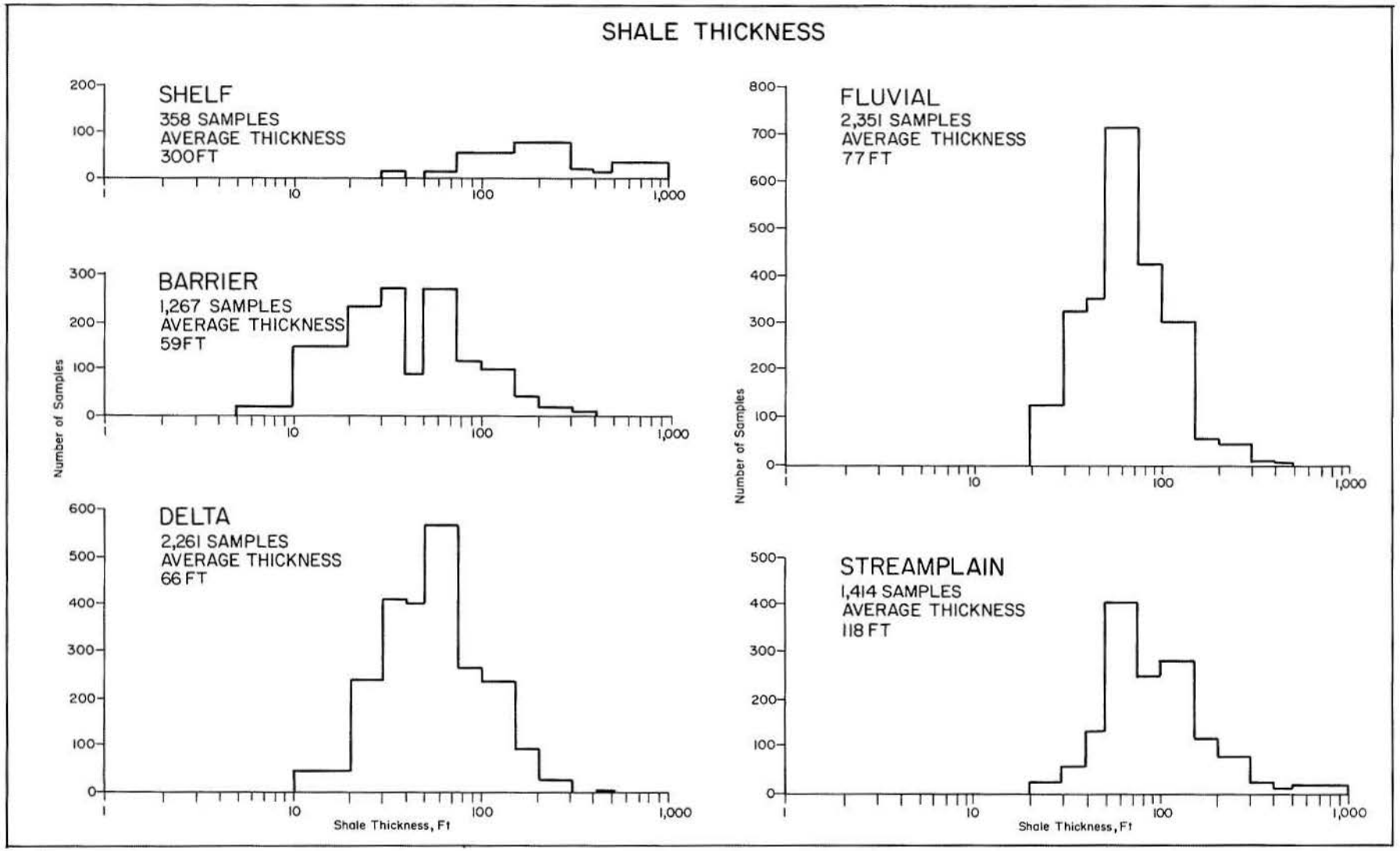

Figure 9. Distribution of shale-unit thickness for the five facies assemblages of the Frio Formation. Scale on the X axis is logarithmic.

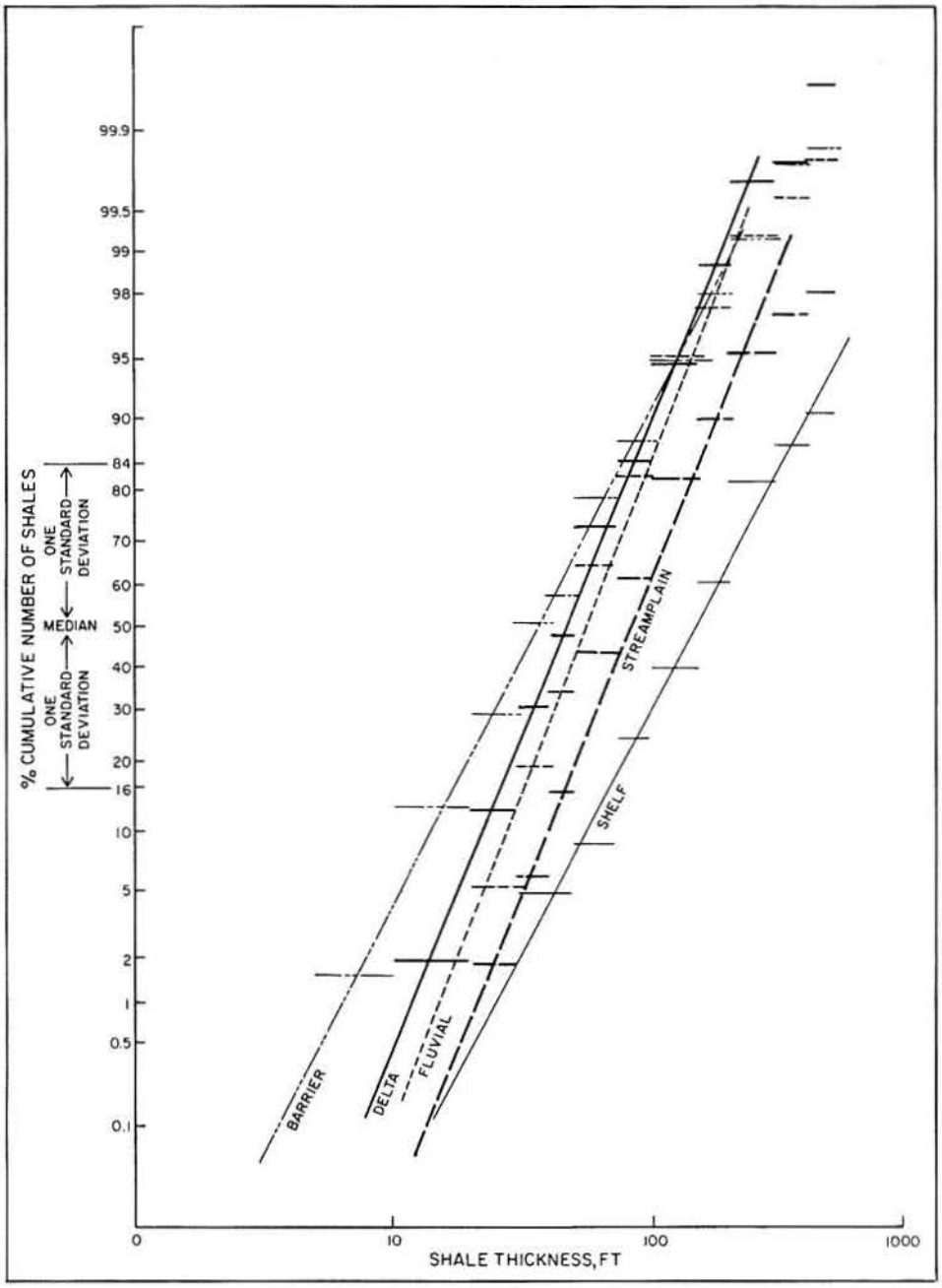

Figure 10. Cumulative-percentage plots of shale-unit thickness on a log probability scale. Each of the five facies assemblages approximates a log-normal distribution pattern, which is shown by a straight line on the plot.

average values because the distribution patterns are approximately normal.

Sandstone Percentage

Sandstone percentage in a geologic unit is a function of the number and thickness of sandstone beds. Because the distribution of the number of sandstones is normal, whereas that of the bed thickness is log-normal, the distribution of sandstone percentage should display an intermediate pattern.

Figure 13 plots frequency distributions for sandstone percentage on normal graph paper, and figure 14 depicts the cumulative frequency on both normal and log-normal probability scales. Neither scale produces straight-line plots, confirming that the distribution patterns of sandstone percentage lie between normal and log-normal. For comparative purposes, however, sandstone-percentage statistics estimated from figure 14 are summarized in table 3.

Summary

Statistics for the five depositional facies sequences of the Frio MSU are summarized in figure 15. Although considerable overlap is evident, each of the highly

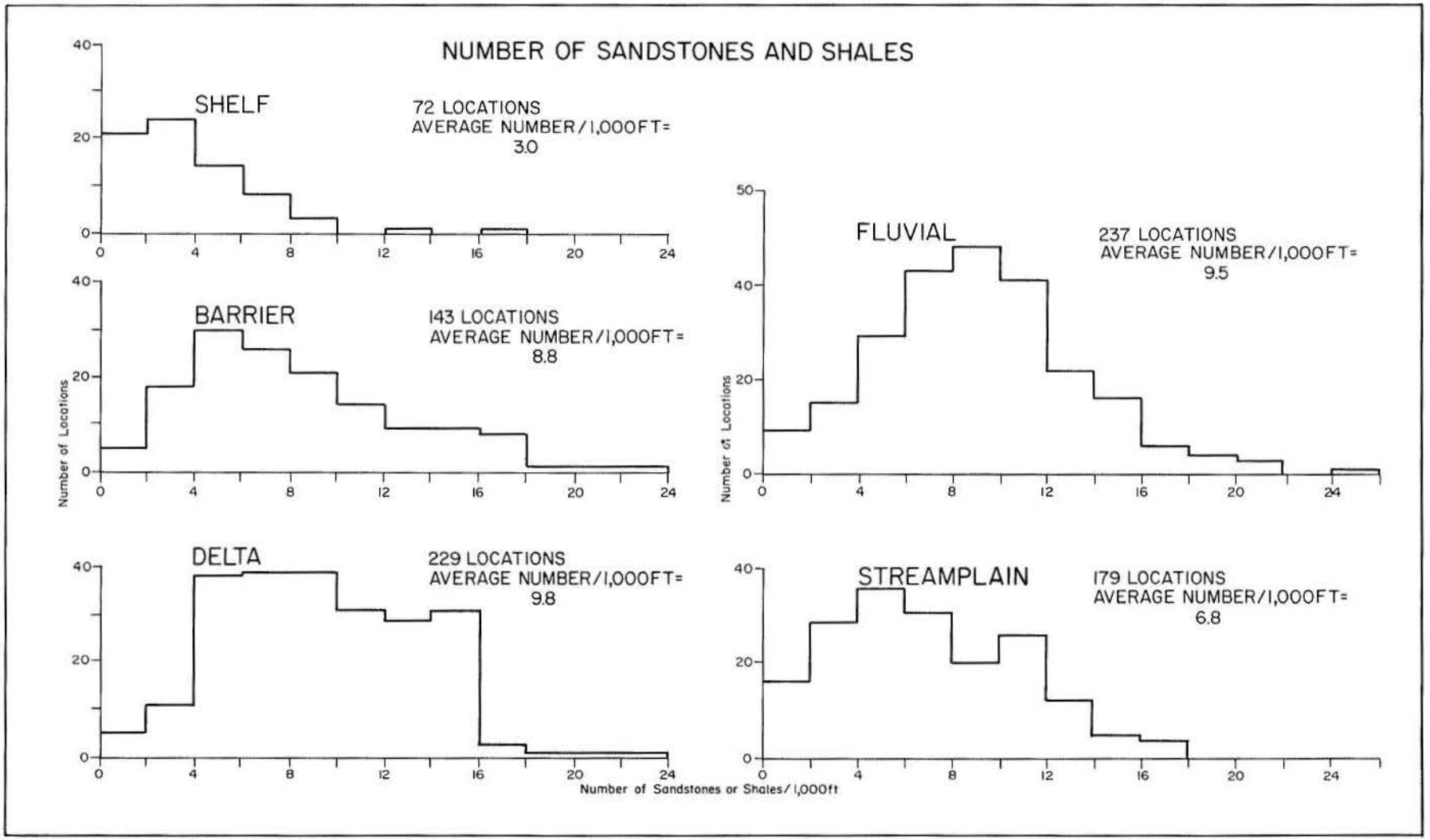

Figure 11. Frequency distributions of number of sandstones (or shales) normalized to a 1,000-ft (300-m) interval for the five facies assemblages of the Frio. A normal (arithmetic) scale is used.

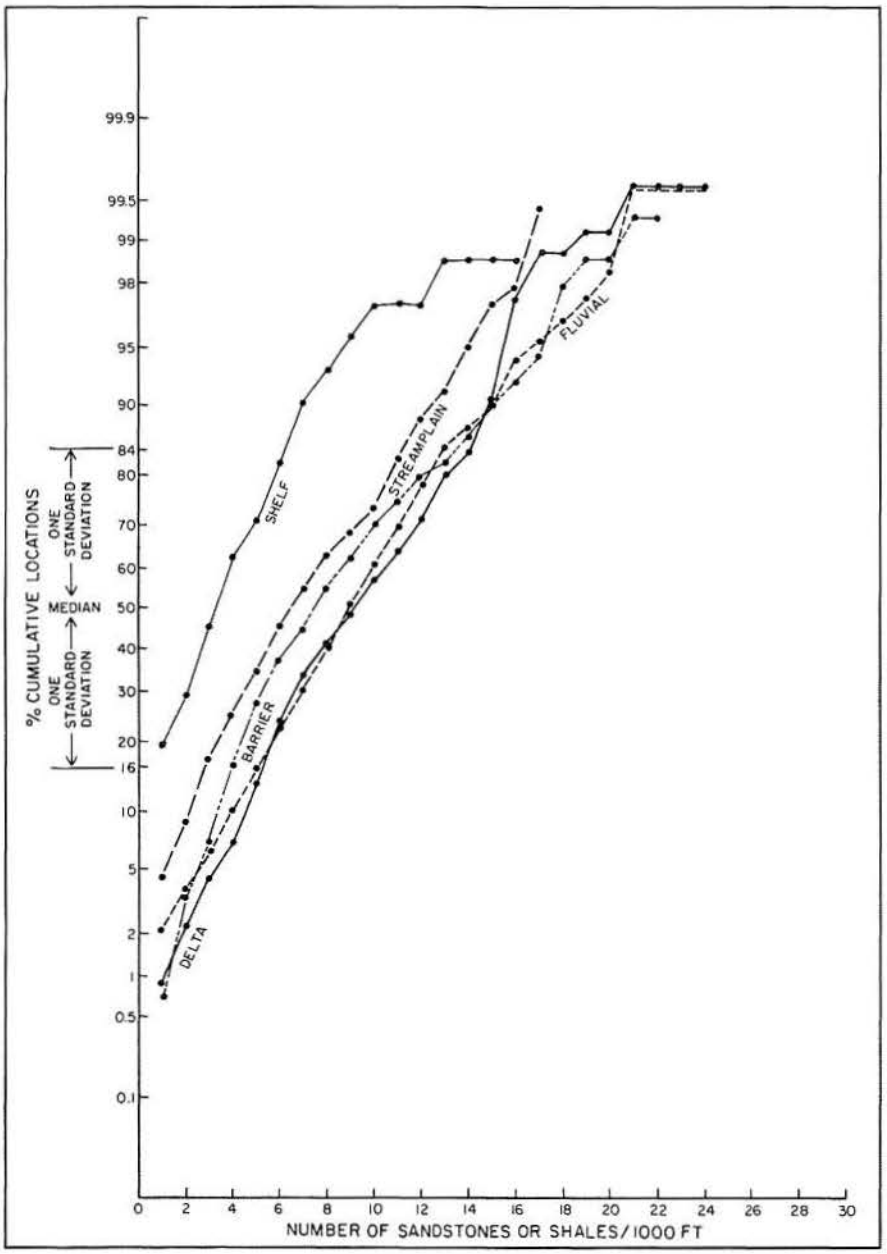

Figure 12. Cumulative-percentage plots of number of sandstones (or shales) per 1,000 ft (300 m) on normal probability scale. Each of the five facies assemblages approximates a normal distribution where number of sandstones is less than 10 per 1,000 ft (300 m) for shelf and is less than 20 per 1,000 ft (300 m) for other facies suites.

generalized facies assemblages can be characterized by variations in lithologic composition, bed thickness, and degree of sandstone-shale interbedding. Deltaic facies in particular exhibit maximum contact between abundant reservoir sandstones and potential source rocks. In contrast, the barrier facies assemblage has the greatest median thickness and percentage of sandstones of the five depositional facies, resulting in the thinnest interbedded shales. One would, therefore, anticipate good reservoir development in this facies; however, the hydrocarbon-sealing potential may be relatively poor.

The progressive decrease of both sandstone percentage and number of beds per 1,000 ft (300 m) characterizes the fluvial and streamplain facies assemblages, and shale thickness accordingly increases. Reservoir distribution and quantity could be a problem in streamplain sequences, but in general, sealing potential is excellent. The quality of organic matter and the level of petroleum maturation, however, may have been limiting factors in creating significant oil and gas accumulations, unless large-scale vertical or lateral migration of petroleum from zones of better organic facies and maturation occurred.

The differing depositional systems, which consist of different proportions and combinations of these five basic facies sequences, are statistically different in terms of spatial relationships among potential reservoir, source, and seal lithologies.

Table 2. Number of sandstone (or shale) units normalized for 1,000-ft (300-m) intervals.

	← one standard deviation		one standard deviation →	
	Minimum	Median	Maximum	Average
Sandstone				
Streamplain	2.8	6.5	11.2	6.8
Fluvial	5.0	9.0	13.0	9.5
Delta	5.3	9.2	14.0	9.8
Barrier	4.0	7.5	13.6	8.8
Shelf	0.5	3.3	6.2	3.0

HYDROCARBON SOURCE, MATURATION, MIGRATION, AND ENTRAPMENT

To assist in the evaluation of the overall potential for hydrocarbon generation in the Frio MSU, available organic geochemical data were collected. Several factors were considered: (1) concentration of organic matter (or organic carbon) in sediments, (2) type of organic matter, (3) maturity level, (4) expulsion history, and (5) migration conditions.

The Gulf Coast Tertiary basin has been regarded as a region of relatively lean and immature source rocks, particularly if only those shales stratigraphically equivalent to the reservoir facies are considered. Indeed, it is difficult to explain the mechanisms responsible for the large oil and gas accumulations found in the Frio Formation on the basis of conventional concepts developed in other major oil-producing regions.

As a possible solution to this problem, Price (1976) offered a model of hydrocarbon migration in aqueous solution along fault planes from mature source rocks as deep as 40,000 ft (12,000 m). Price's migration model was based on extensive laboratory studies of solubilities of petroleum hydrocarbons in water at elevated temperatures as high as 356° F (180° C), where aqueous solubility of petroleum is relatively high. This model, however, has several potential limitations:

1. McAuliffe (1978) stated that

> the water solubilities of hydrocarbons vary significantly with hydrocarbon class (alkanes, cycloalkanes, and aromatics, etc.) and decrease markedly with increasing molecular weight within a class. The relative composition of crude petroleum with respect to the relative water solubilities of petroleum hydrocarbons suggests that solution is not a reasonable migration mechanism.

McAuliffe argues against the possibility of significant hydrocarbon migration in aqueous solution on the basis of the vast difference between the composition of dissolved hydrocarbons and the composition of crude oil accumulated in reservoirs.

2. As compaction water moves upward along the fault planes, the temperature of the water would continue to decline. With temperature decline, hydrocarbons would continuously be separated from solution, possibly forming small globules. Movement of the globules would be slowed by the capillary restrictions inherent in fine-grained rocks. There has been no reported evidence of such continuously increasing amounts of the separate phase hydrocarbons upward along fault planes.

3. Before hot petroliferous compaction water moves to fault zones, it must traverse the pore spaces of the undercompacted shales. This would not seem to be a major process, given the poor drainage evidenced by the high degree of overpressure in these deeply buried shales.

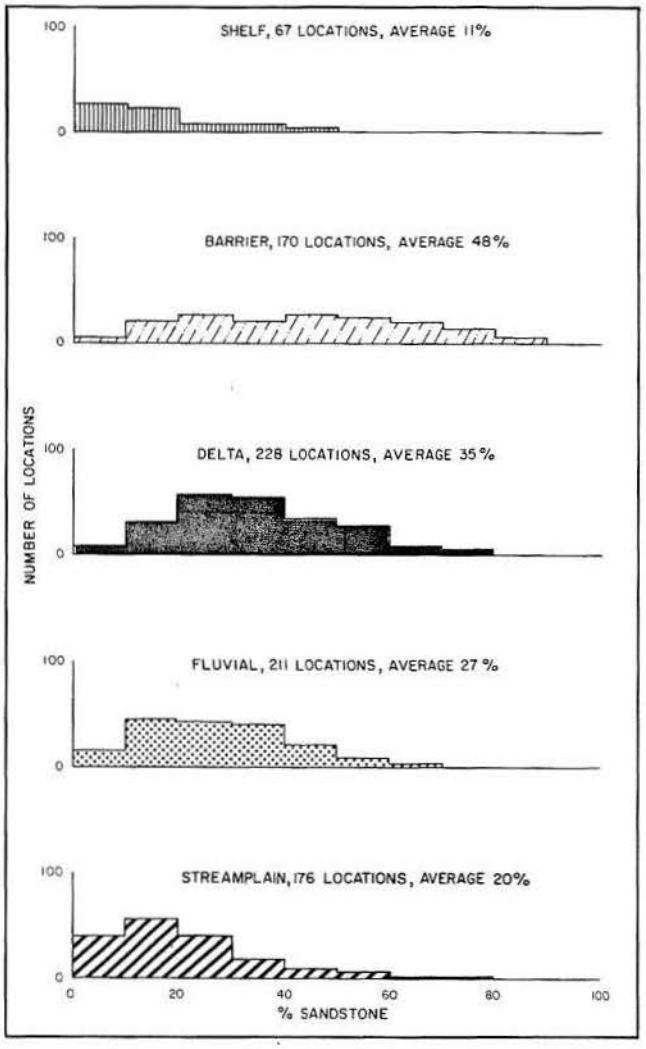

Figure 13. Frequency distributions of sandstone percentage for the five facies assemblages of the Frio. A normal (arithmetic) scale is used.

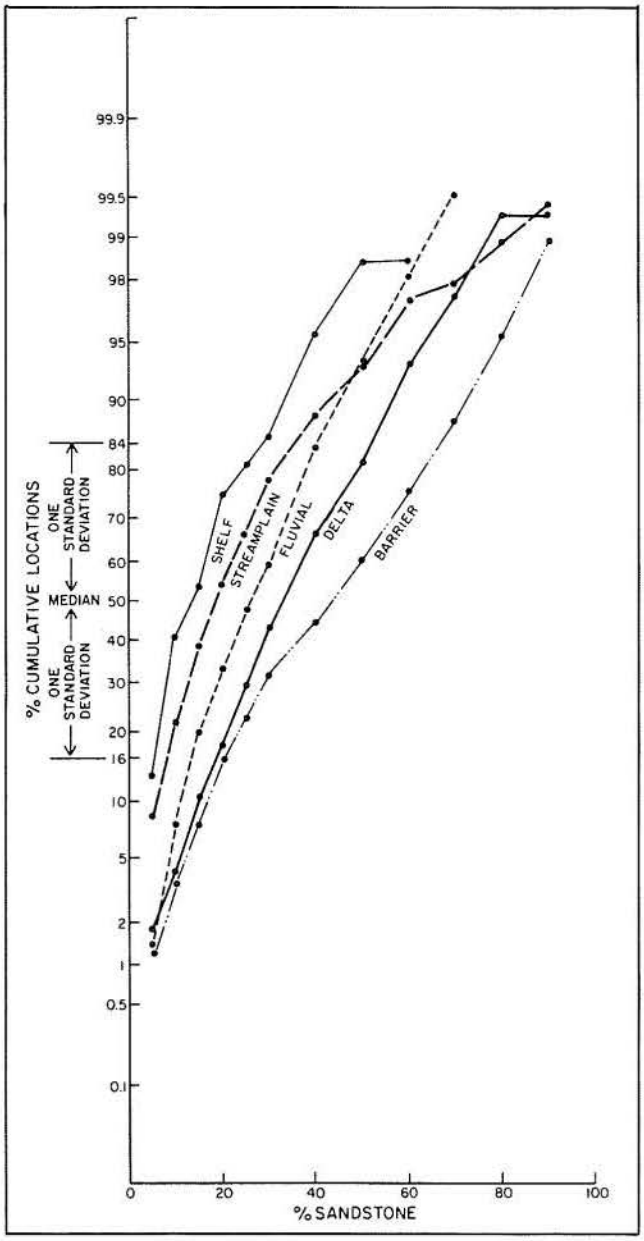

Figure 14. Cumulative-frequency plots of sandstone percentage on normal and log probability scales. Neither scale produces a straight-line trend, showing that sandstone-percentage values have a distribution that is between normal and log-normal.

4. A fault can be an avenue for fluid movement within a hydrostatically pressured interval in an extensional basin. A fault cutting the hot, undercompacted, and abnormally pressured section, however, may not provide a good conduit, as it can be effectively closed by the ductile shales.

On the basis of the measured and estimated vitrinite reflectance (R_o), which is commonly used for assessing the level of petroleum maturation, Dow (1978) found a possible oil-generating interval (0.6 to 1.35 percent R_o) in the Louisiana Gulf Coast (fig. 16). For Cretaceous- to Miocene-age sedimentary sequences, oil-producing intervals are located above the oil-generating interval of 0.6 to 1.35 percent R_o. This suggests that although the accumulated oils were not derived from shales interbedded with the reservoirs, the source rocks do not lie far below the reservoirs. The distance of vertical oil migration required would range from a few to several thousand feet. Petroleum migration may also have followed bedding planes from the hotter and more mature source rocks in the downdip synclinal areas into the shallower traps.

Table 3. Sandstone-percentage statistics.

	← one standard deviation		one standard deviation →	
	Minimum	**Median**	**Maximum**	**Average**
Sandstone				
Streamplain	8	19	36	20
Fluvial	14	26	41	27
Delta	19	33	52	35
Barrier	20	43	67	48
Shelf	6	14	29	11

CONCENTRATION OF ORGANIC CARBON IN SHALES

There are seven requirements for petroleum accumulation: source, maturation, primary and secondary migration, trap, seal, and reservoir. Source ranks first in importance because the other attributes are useless if adequate source rocks are absent (Momper, 1978). The quality of the source rocks is in part determined by the concentration of contained organic carbon (commonly expressed as total organic carbon or TOC).

Research indicates that a certain minimal amount of TOC in source rocks is necessary to form major petroleum accumulations. On the basis of 25,742 samples from the Russian Platform, Ronov (1958) reported a significant difference in concentrations of organic carbon in petroliferous and nonpetroliferous regions. Sediments (clays, sands, and carbonate) of the petroliferous region contain 0.5 to 1.4 average weight percent organic carbon, whereas those of the nonpetroliferous region contain 0.1 to 0.4 average weight percent. Based on Ronov's data (1958) and subsequent studies, an empirical lower limit of 0.4 weight percent organic carbon (about 0.5 weight percent organic matter) has been accepted by most organic geochemists as the minimum concentration

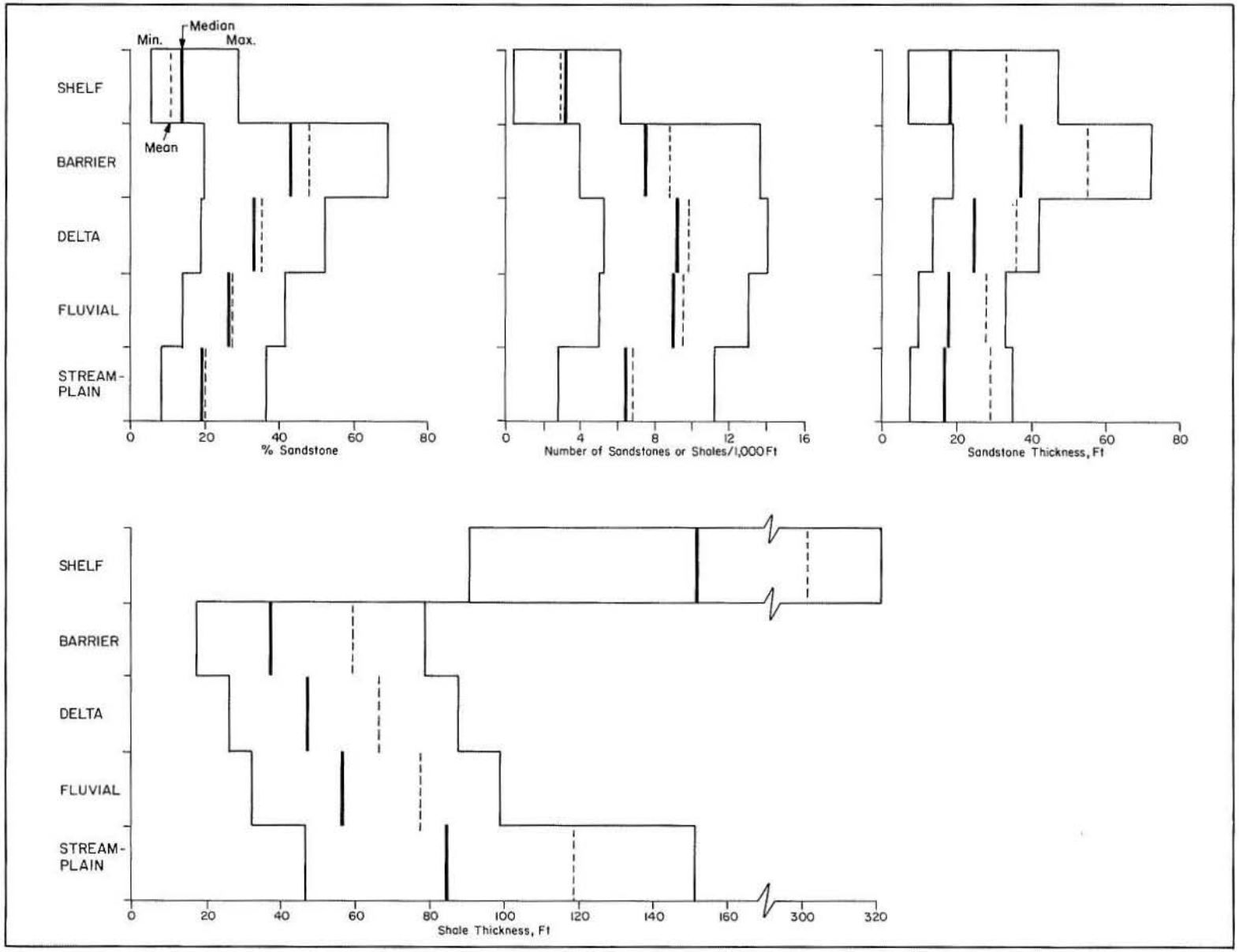

Figure 15. Statistical summary of the five facies assemblages of the Frio. Shown are sandstone percentage, number of sandstones (or shales) per 1,000 ft (300 m), sandstone thickness, and shale thickness. Blocks shown for each facies indicate graphically determined minimum and maximum values. The heavy vertical line in each block indicates the median, and the dashed line shows the mean (or average) value.

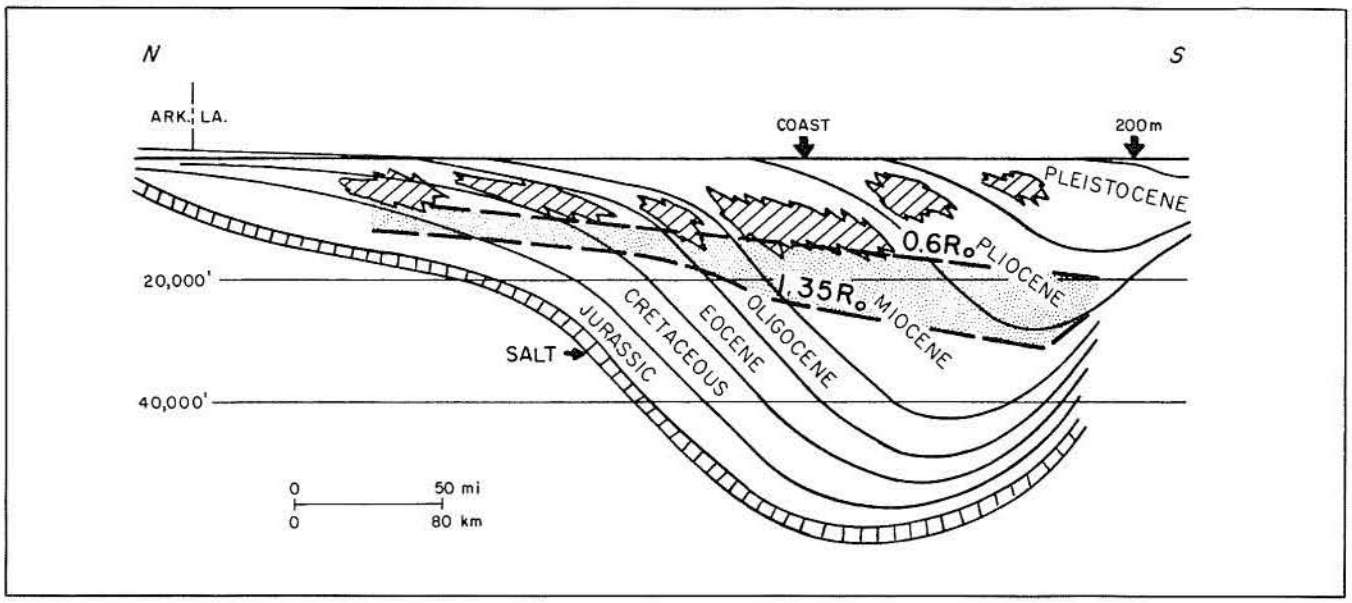

Figure 16. Cross section of the Louisiana Gulf Coast Basin showing distribution of productive intervals for oil (hachured areas) and most probable oil generation zone (measured vitrinite reflectance [R_o] between 0.6 and 1.35 percent). Modified from Dow (1978).

required for large-scale hydrocarbon generation (Dow, 1978).

Barker (1977) compared the distributions through geologic time of (1) average weight percent organic carbon, (2) relative amount of expandable clay, and (3) number of giant petroleum fields worldwide, which contain nearly 75 percent of the world's known petroleum reserves. He concluded that the organic carbon concentration predicts the volume of stratigraphically associated petroleum much better than does the amount of expandable clay minerals; consequently, the concentration of organic carbon in sedimentary rocks is a major factor controlling accumulation of petroleum.

During burial and petroleum generation, the percent of organic carbon continuously decreases because of the thermal effect. In a mature source rock, the measured concentration of organic carbon could be significantly less than the original concentration in the immature source rock. Tissot (1978) suggested that in the deeper parts of sedimentary basins, a measured residual of 0.5 weight percent organic carbon may reflect an original content of 1 percent or more. Therefore, an acceptable lower limit for subsurface rocks might be less than the accepted figure of 0.4 weight percent. Indeed, Frio source-rock quality suggests such source depletion.

Available organic-carbon-concentration data for the Frio MSU were compiled (fig. 17) from company files and published reports. Distribution of organic carbon content, expressed as weight percent organic carbon, from 140 samples of Frio mud rocks is shown in figure 18; most samples are distributed between 0.1 and 0.4 percent organic carbon, and the average figure is 0.28 percent. The Frio MSU in this region is generally lean in organic matter, with an average TOC concentration below 0.4 weight percent. Nevertheless, world-class petroleum reserves have been discovered in this formation.

Dow (1978) noted that low values for Frio shales are not surprising:

> If the supply of organic matter is constant, its concentration in sediments should be inversely related to the depositional rate of mineral particles. Therefore, areas of high sedimentation rates, such as deltas, should contain sediments with relatively low organic-carbon concentrations. If the sedimentation rate is too slow, however, much of the organic matter reaching the bottom may be consumed by heterotrophic organisms before it can be protected by burial. Intermediate sedimentation rates which minimize the effects of both dilution and consumption commonly result in the most organic-rich sediments.

This concept is illustrated schematically in figure 19. Thus, the low organic carbon concentrations in the Frio probably reflect the relatively rapid rates of Frio deposition. The average level of thermal maturation of Frio source rocks between about 9,000 and 16,400 ft (2,800 and 5,000 m) ranges only from about 0.3 to 0.9 percent R_o, indicating that further reduction of the organic carbon percent because of thermal maturation and expulsion may have been insignificant.

Because average sedimentation rate for the Frio MSU varies little in the study areas, it is impossible to establish a quantitative relationship between the concentration of organic carbon and Frio sedimentation rates. However, such relationships have been documented for other formations in other parts of the world (see, for example, data

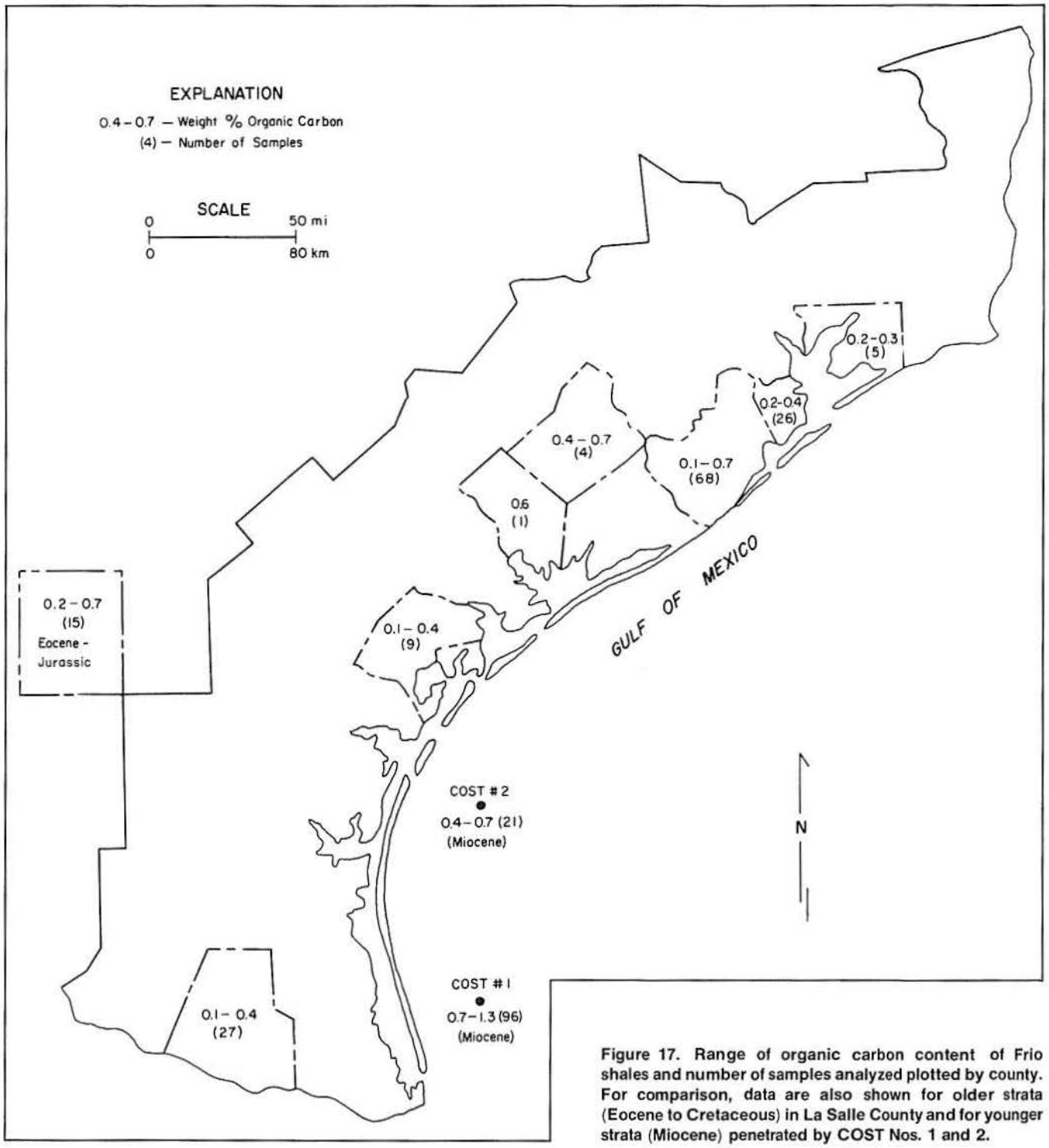

Figure 17. Range of organic carbon content of Frio shales and number of samples analyzed plotted by county. For comparison, data are also shown for older strata (Eocene to Cretaceous) in La Salle County and for younger strata (Miocene) penetrated by COST Nos. 1 and 2.

in Scholle and Arthur, 1980; Dutton, 1980; Powell, 1978; Japanese Association of Petroleum Technologists, 1973).

Dow and Pearson (1974) constructed a diagram relating water depth and percent organic carbon (fig. 20) based on the average percent organic carbon in various modern depositional facies of the Louisiana Gulf Coast. The average organic carbon content of the neritic shelf facies is relatively low, possibly because of partial oxidation. Concentration in bathyal muds is generally high, but within the lower bathyal zone there seems to be a slight dilution effect resulting from the greater depositional rate. The average organic carbon content (0.3 percent) from deep-sea regions, where the depositional rate is quite low (McIvor, 1975), is also included

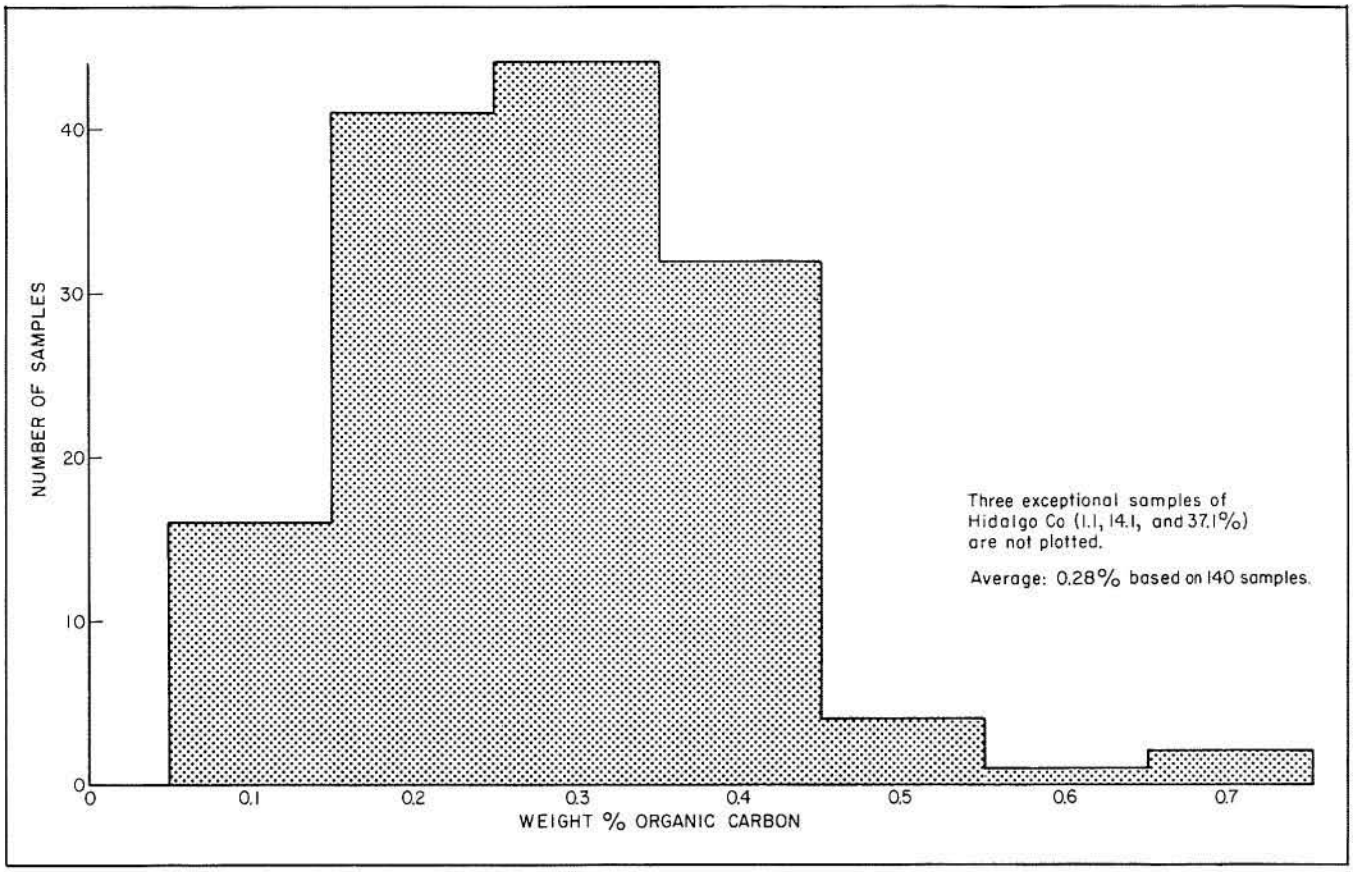

Figure 18. Frequency distribution of organic carbon content in 140 Frio samples. Most samples contain between 0.1 and 0.4 weight percent organic carbon; the average figure is 0.28 percent.

in the top diagram of figure 20. Significant oxidation of organic carbon (fig. 21) occurs in regions of deep-water upwelling (Closs and others, 1974).

The low concentration of organic carbon in the Frio MSU is primarily due to its extremely rapid rate of sedimentation, averaging as much as 1,500 ft (450 m) per million years (without compaction correction) in neritic and upper bathyal zones. However, the *total amount* of organic carbon deposited within sediments was enormous because of the tremendous volume of sediment deposited.

Ranges of organic carbon concentration for Miocene sections drilled by the Continental Offshore Stratigraphic Test (COST) No. 1 (0.7 to 1.3 percent) and the COST No. 2 (0.4 to 0.7 percent) wells are higher than that for the Frio (0.1 to 0.7 percent) (fig. 17). This probably reflects the lower depositional rates for Miocene sedimentary rocks of the South Texas shelf.

Information on organic-matter types in the Frio is scarce. Data from four regionally spaced wells, including the Department of Energy/General Crude Oil (DOE/GCO) Pleasant Bayou Nos. 1 and 2, show that gas-prone herbaceous and woody types, both considered to be prime gas sources, are predominant (Brown, 1979). Most samples contain relatively small quantities of oil-prone amorphous organic matter, but content is greatest in marine shales of the Greta/Carancahua barrier/strandplain system.

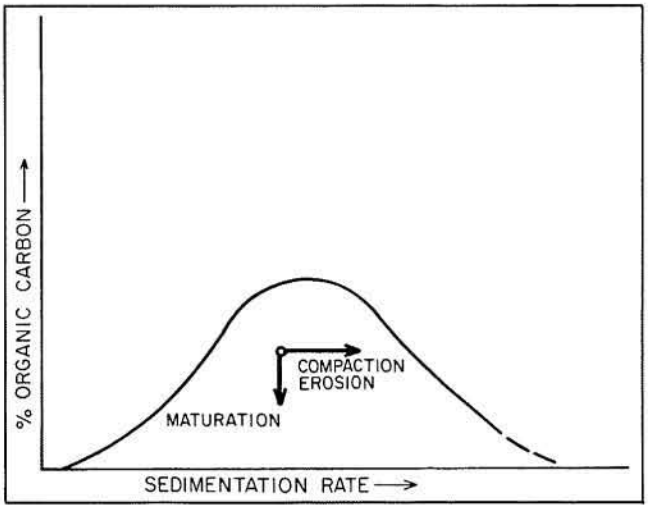

Figure 19. Schematic diagram showing relative richness of organic carbon in mudstone as a function of original sedimentation rate. Apparent effects of compaction and erosion (horizontal arrow) and of organic maturation (vertical arrow) displace the curve to the right and flatten the peak.

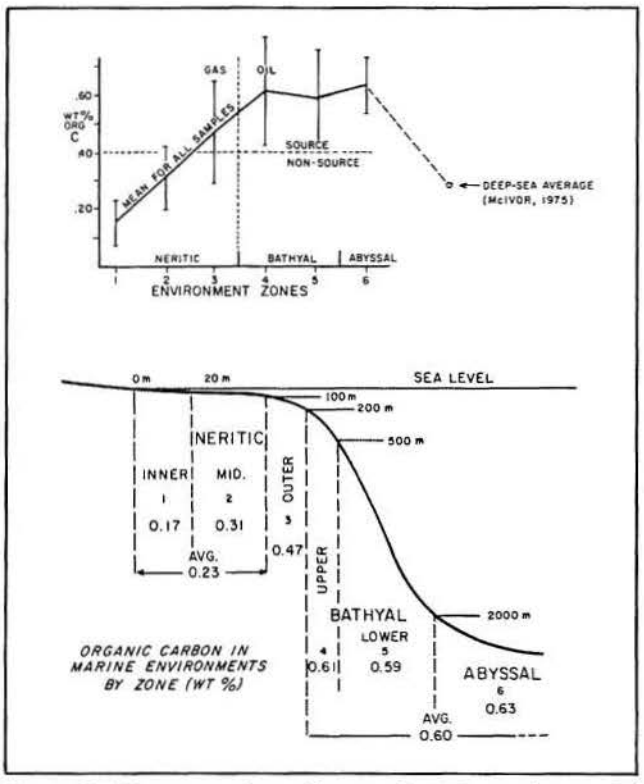

Figure 20. Mean organic carbon content by environmental depth zones in the Louisiana Gulf Coast Tertiary section. Bars in top diagram represent standard deviation of means and approximate range in values. Average organic carbon percent of deep-sea sediments (adapted from McIvor, 1975) is incorporated in top diagram. Adapted from Dow and Pearson (1974).

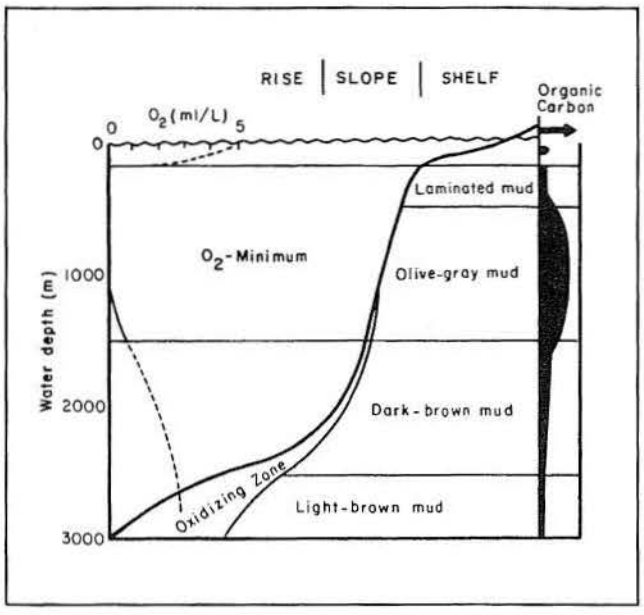

Figure 21. Schematic section of India-Pakistan continental margin showing oxygen content in seawater and qualitative content of selected components of surface sediments. Organic carbon is most abundant in upper slope oxygen-minimum zone (from Closs and others, 1974).

MATURATION AND EXPULSION OF GENERATED HYDROCARBONS

The level of petroleum generation is primarily controlled by geologic time and temperature. An effective method for evaluating the stages of petroleum generation and maturation is to construct burial history plots and to calculate the time-temperature integrals (TTI) of selected source beds, based on the known geothermal gradient of the area (Waples, 1980). Examples of the burial history plots for two shale beds of the DOE/GCO Pleasant Bayou No. 1 well are shown in figure 22. By estimating the duration of geologic time (in million years) within each temperature increment of 18° F (10° C) during burial and summing the total, the TTI value for each bed can be calculated and related to the estimated vitrinite reflectance value (fig. 22). Waples (1980) provided a detailed explanation of this method originated by Lopatin.

If, however, the rate of burial remained relatively uniform, and if there were no significant uplift and erosion involved, then the TTI and the vitrinite reflectance may be

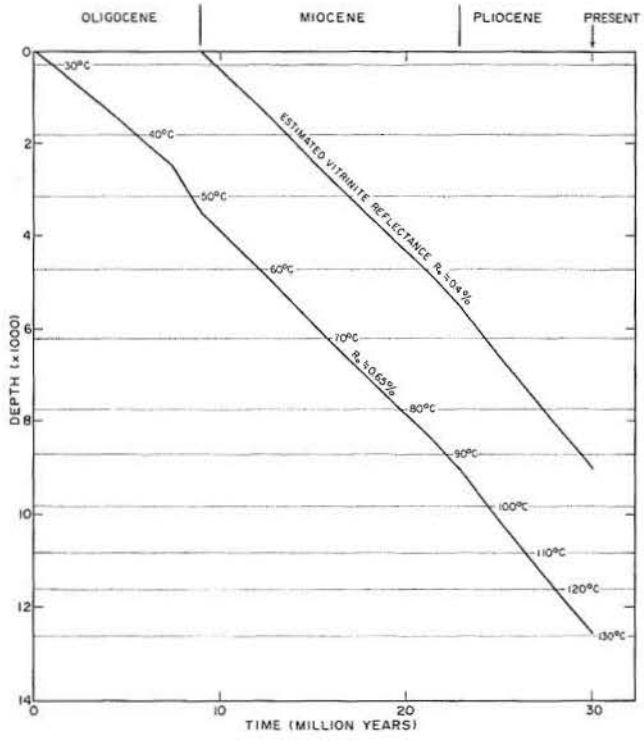

Figure 22. Examples of burial history plots for two shale beds at 9,000 and 12,500 ft (2,700 and 3,740 m) in DOE/GCO Pleasant Bayou No. 1, Brazoria County, Texas. Estimated vitrinite reflectance values (R_o) are comparable with measured values (see fig. 28).

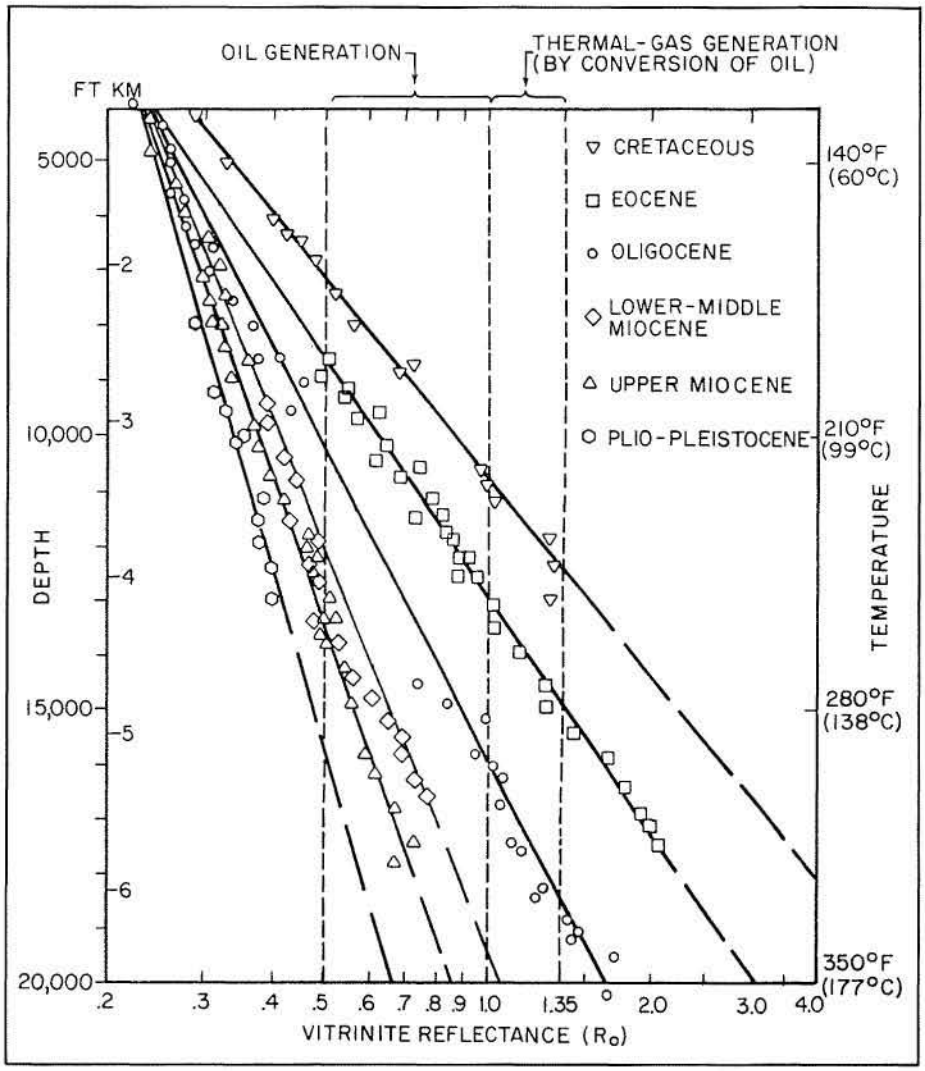

Figure 23. Composite maturation profiles of two representative wells in age-defined Gulf Coast producing trends. All wells display uniform geothermal gradients close to 1.4° F per 100 ft (2.54° C per 100 m). Note that higher temperatures are required to achieve equivalent maturities in younger rocks compared to older ones (revised from Dow, 1978).

estimated directly by plotting the present burial depth of source beds of known geologic age. The paleogeothermal gradient must, of course, be known or estimated for that region.

Dow (1978) presented composite profiles of vitrinite reflectance for Cretaceous through Pliocene-Pleistocene sediments of the Louisiana Gulf Coast (fig. 23). According to the plot for Oligocene sediments, the temperature, which corresponds to the onset of oil generation (about 0.5 percent R_o), is about 210° F (99° C). However, some oil generation can start slightly earlier (<0.5 percent R_o). The temperature corresponding to $R_o = 1.0$ percent, or the peak oil generation for Oligocene sediments, is about 300° F (148° C). Beyond the level of $R_o = 1.0$ percent, the generated oil would be converted to wet and dry gas as a result of further heating. The oil would be almost completely changed to gas at the level of 1.35 percent R_o (or at about 330° F or 166° C).

In summary, the temperature range of main oil generation, or the oil window for the Frio, is approximately bounded by the 200° and 300° F (93° and 148° C) isotherms. The range of thermal-gas generation resulting from cracking of petroleum liquids is between about 300° and 330° F (148° and 166° C).

Figures 24 and 25 are depth contour maps of 200° F (93° C) and 300° F (148° C) isotherms. An isopach map of the interval between 200° F (93° C) and 300° F (148° C) isotherms (fig. 26) shows the general tendency for coastward thickening of the oil window owing to the decreasing geothermal gradient. The total thickness of the thermally mature Frio MSU section similarly increases gulfward (fig. 27). The entire Frio section is or has been exposed to temperatures above 200° F (93° C) along its coastward margin; conversely, a large area of shallow Frio section lies entirely above the oil maturation threshold (fig. 27). Large volumes of thermally mature Frio mudrock

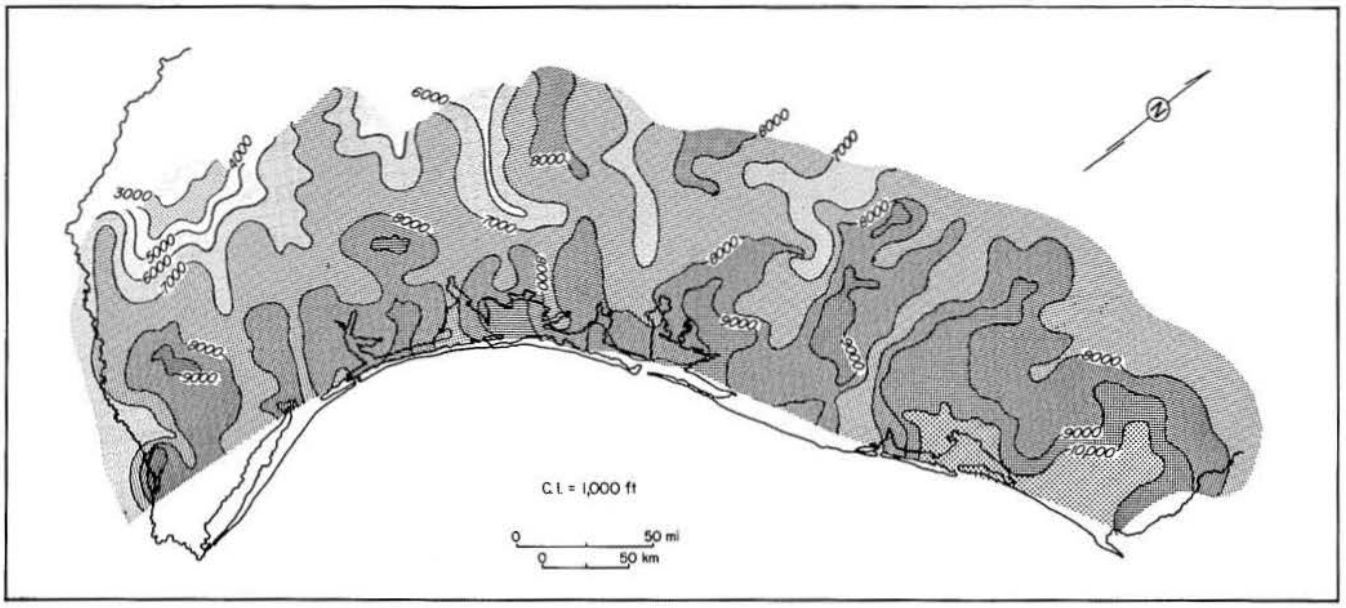

Figure 24. Depth (in feet) of the 200° F (93° C) isotherm (the approximate threshold of Frio oil generation) in the Texas Gulf Coast. Data from Gregory and others (1980).

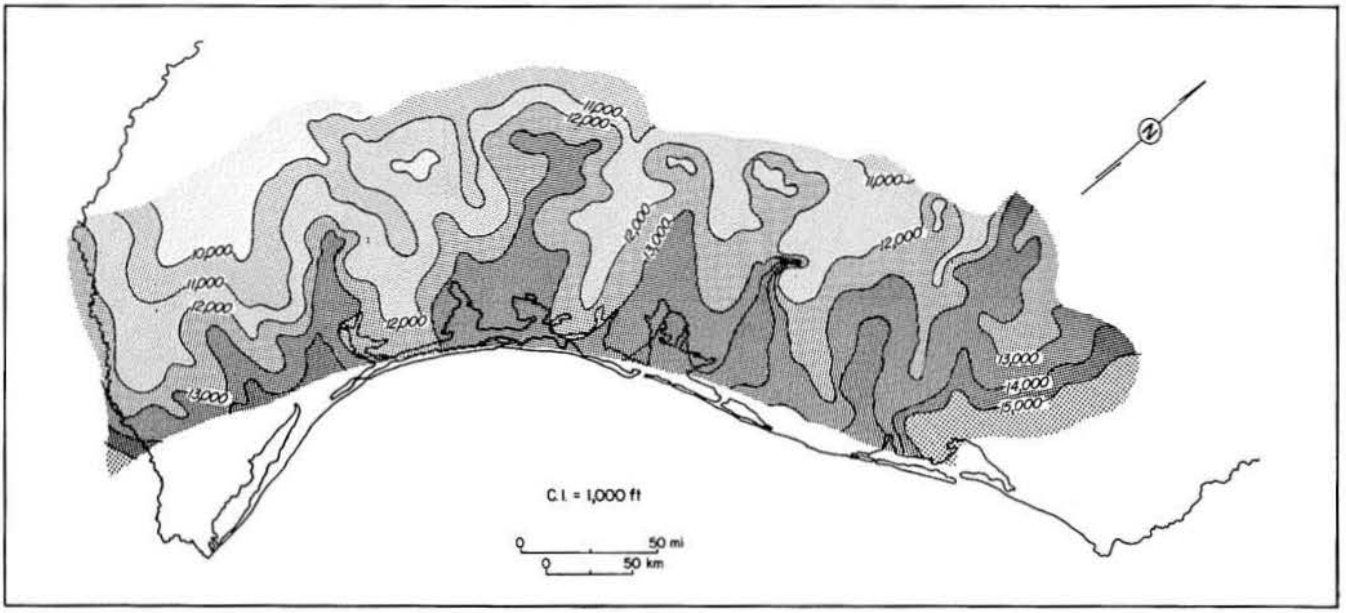

Figure 25. Depth (in feet) of the 300° F (148° C) isotherm (the approximate base of Frio oil generation) in the Texas Gulf Coast. Data from Gregory and others (1980).

included in the deltaic and barrier/strandplain systems are thought to have contributed to the accumulated hydrocarbons.

Few Frio wells have complete organic geochemical analyses. The DOE/GCO Pleasant Bayou Nos. 1 and 2 in Brazoria County are the most important sources of data. The vitrinite reflectance value for these wells ranges from an average of about 0.3 to 0.6 percent R_o at around 9,000 to 10,000 ft (2,700 to 3,000 m) near the top of Frio to an average of 0.9 percent R_o at a total depth of 16,500 ft (5,000 m) (fig. 28). In other words, the section between 9,000 and 16,500 ft (2,700 and 5,000 m) is within the oil generation zone. Corresponding temperatures are about 200° and 320° F (93° and 160° C), respectively.

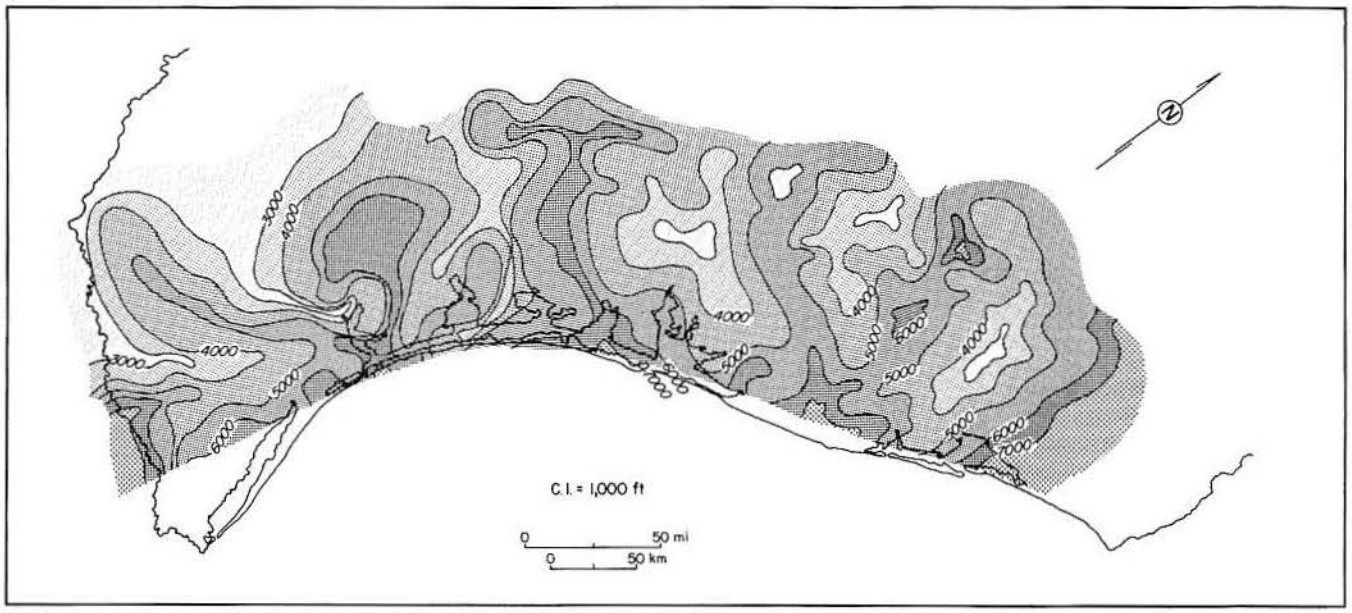

Figure 26. Isopach map of the 200° to 300° F (93° to 148° C) Frio oil window. Data from Gregory and others (1980).

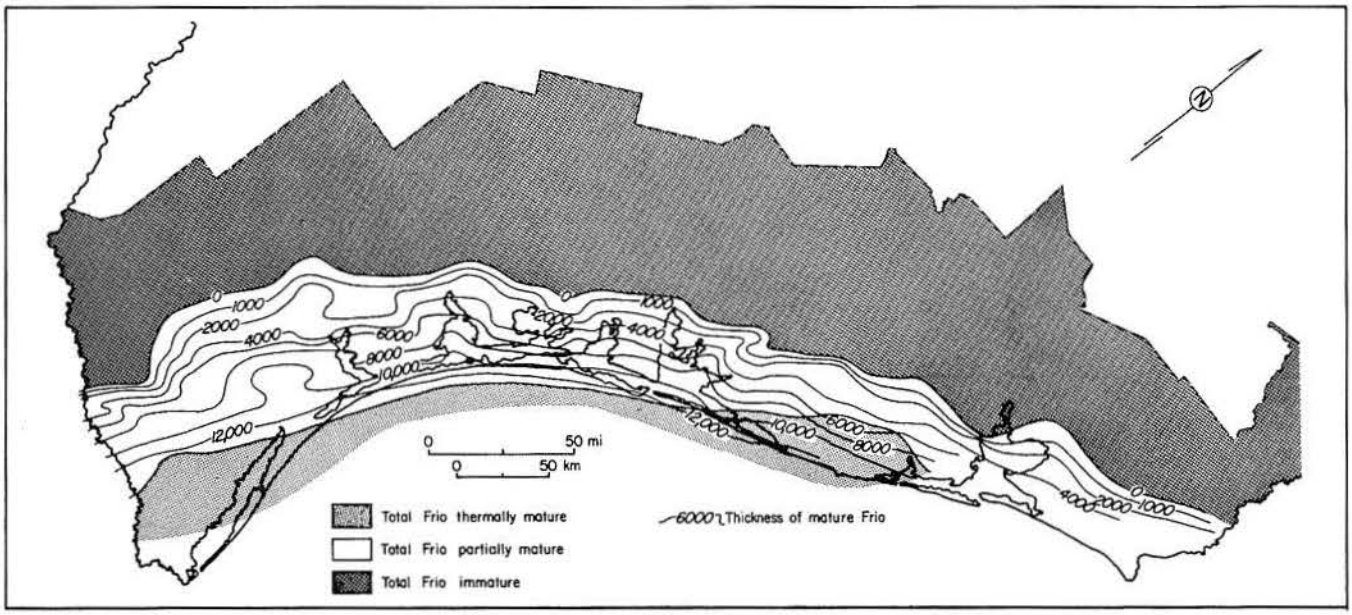

Figure 27. Isopach map of the thermally mature portion of the Frio MSU. Contours show the total thickness of Frio section that lies below the 200° F (93° C) oil generation threshold.

A summary diagram of shale compaction and organic geochemical data of the DOE/GCO wells (fig. 29) reveals three compaction zones: (1) normal compaction zone (from surface to about 7,000 ft or 2,100 m); (2) moderate undercompaction zone (from about 7,000 to 14,000 ft or 2,100 to 4,200 m), and (3) severe undercompaction zone (from about 14,000 to 16,500 ft or 4,200 to 5,000 m, or total depth). The plot of C_{15+} hydrocarbons versus depth (fig. 29B) is normalized to grams of organic carbon, which removes the effect of variation in hydrocarbons generated because of variation in the concentration of organic carbon (or matter). The plot, therefore, evaluates the

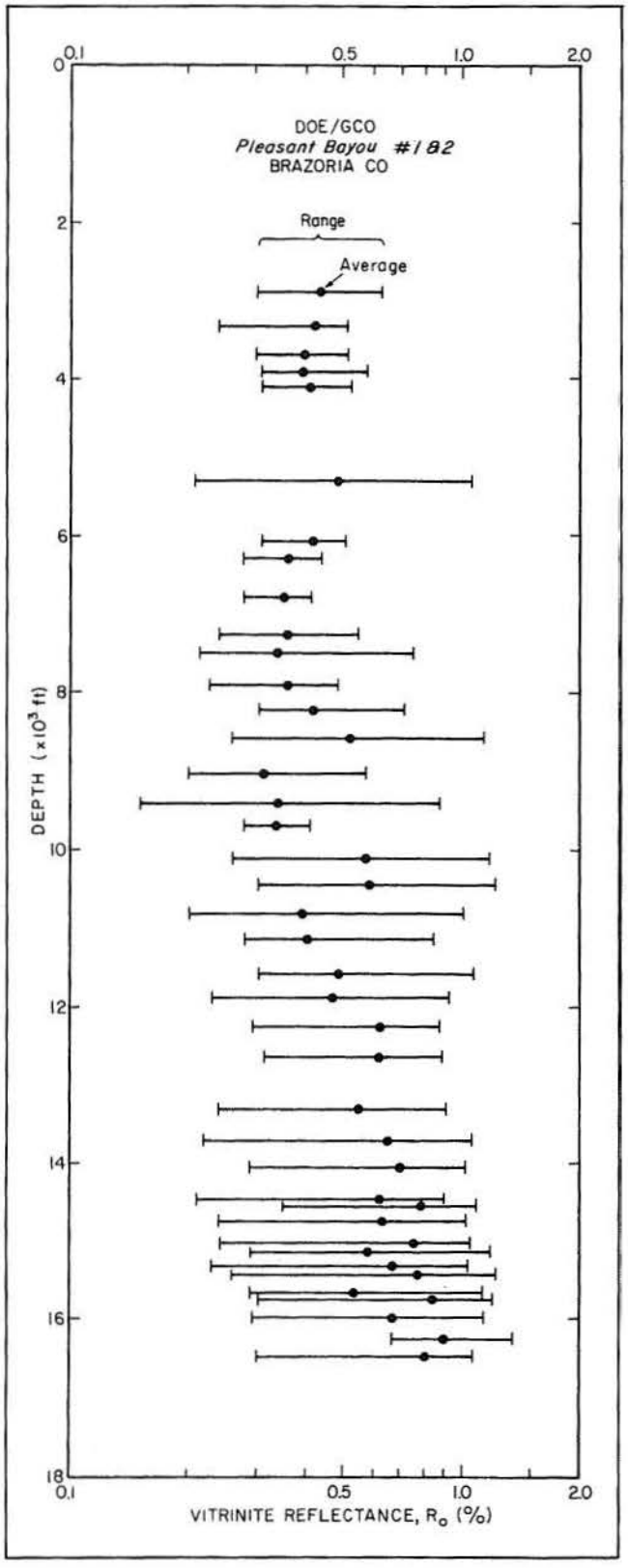

Figure 28. Ranges of average values of vitrinite reflectance (R_o) from DOE/GCO Pleasant Bayou Nos. 1 and 2, Brazoria County, Texas.

quantity of the generated hydrocarbons from a given amount of organic matter.

A line drawn through the relatively high C_{15+} values indicates the interpreted normal generation trend. The chemical kinetic function of hydrocarbon generation can be expressed by the Arrhenius equation, an exponential function (Connan, 1974), which may be shown as a nearly straight-line function on semilog paper. Several excessive hydrocarbon values from around 7,000 ft (2,100 m) are excluded from this trend on the assumption that they represent, in part, hydrocarbons that migrated from other intervals.

The possible amount of C_{15+} hydrocarbons expelled from source rocks (hachured area, fig. 29B) is relatively large in the moderately undercompacted interval, but is small in the more severely undercompacted interval below 14,000 ft (4,200 m). This observation suggests that the moderately undercompacted section (between about 8,000 and 14,000 ft or 2,400 and 4,200 m) is largely a thermally mature source interval in which proportionally more of the generated hydrocarbons were expelled. On the average, approximately 20 mg per g organic carbon of the total 30 mg per g organic carbon generated was expelled, leaving only about 10 mg per g organic carbon in shales.

It may be argued that such an effective hydrocarbon expulsion is impossible and that the relatively small quantity (10 mg per g organic carbon) of hydrocarbon remaining in the rocks is primarily owing to the poor source quality. As mentioned earlier, however, the types of organic matter in these wells are predominantly herbaceous and woody throughout the undercompacted sections, and the distribution of organic-matter types is relatively uniform. The amount of hydrocarbon measured below 14,000 ft (4,200 m) likely reflects the total hydrocarbons generated in thermally mature source rocks, because this section is severely undercompacted and hydrocarbon expulsion is greatly restricted. Shales above 13,000 ft (3,900 m) would have generated hydrocarbons on the basis of their maturity levels as shown by the normal-generation-trend line (fig. 29B), and quantities of hydrocarbons must have been expelled from the sections above 13,000 ft (3,900 m).

Below 14,000 ft (4,200 m), the amount of hydrocarbons expelled from the source rocks is relatively small because of severe undercompaction. Although the concentration of organic carbon from about 8,000 to 16,500 ft (2,400 to 5,000 m) is relatively uniform, efficiency of hydrocarbon expulsion varies greatly. There seems to be no positive correlation between concentration of organic carbon and effective hydrocarbon expulsion and migration. This fact, along with the very low organic content of Gulf Coast shales, tends to refute McAuliffe's (1978) concept that effective oil migration requires an interconnected organic network within shales.

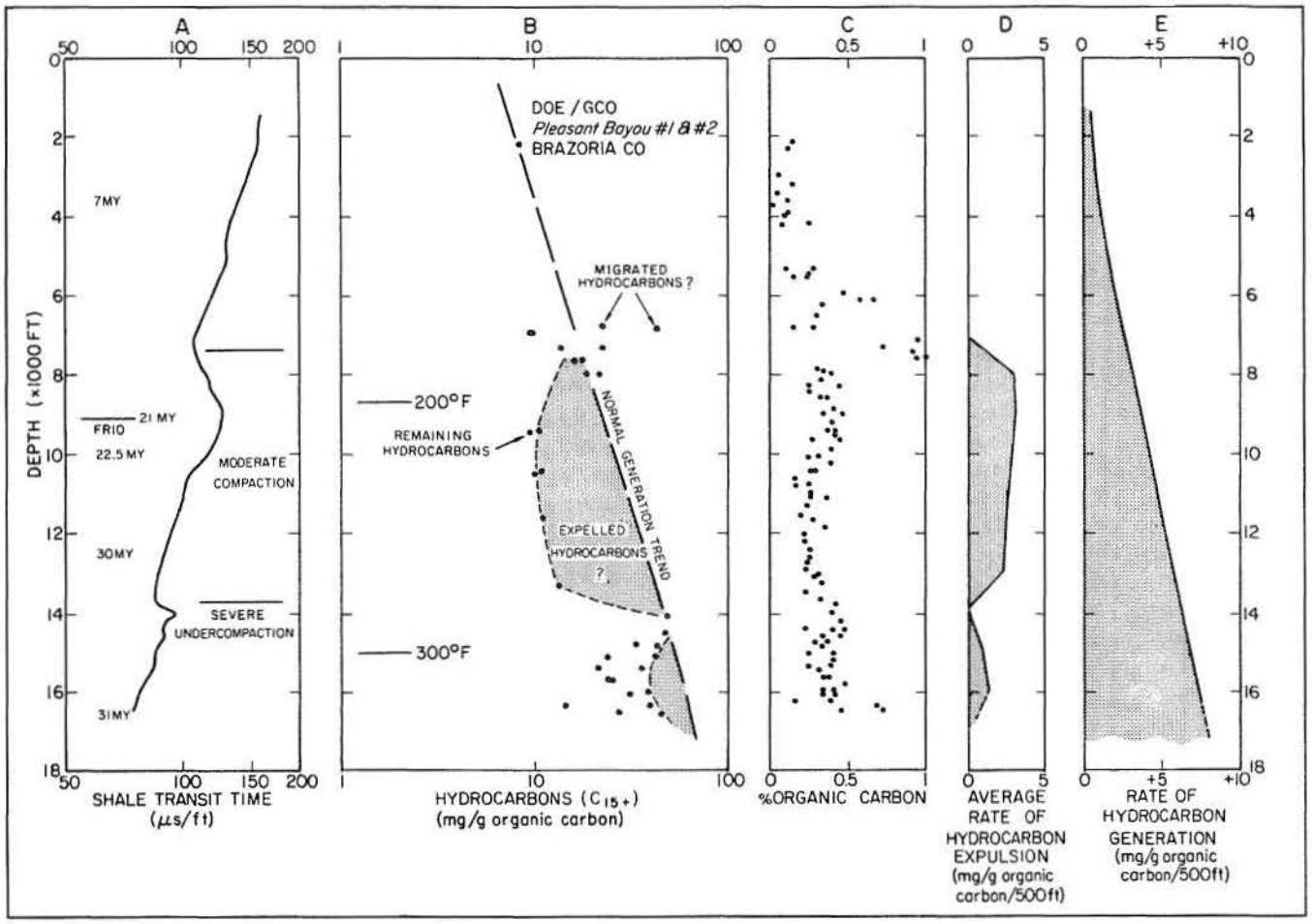

Figure 29. Summary plots of shale compaction and organic geochemical data for DOE/GCO Pleasant Bayou Nos. 1 and 2, Brazoria County, Texas. From left to right (A) shale transit time (μs per ft) versus depth, (B) C_{15+} hydrocarbons (mg per g organic carbon) versus depth, (C) weight percent organic carbon versus depth, (D) average rate of hydrocarbon expulsion versus depth, and (E) rate of hydrocarbon generation versus depth are shown.

The data indicate that hydrocarbon expulsion began at a depth of about 7,000 ft (2,100 m) (fig. 29D) and remained generally effective between 8,000 and 13,000 ft (2,400 and 3,900 m). Based on the normal generation trend (fig. 29B), a curve showing the rate of hydrocarbon generation (fig. 29E) can be constructed. Magara (1978b) gave a detailed explanation of the calculation. The rate of hydrocarbon generation increases downward, and the peak lies below the total well depth of 16,500 ft (5,000 m).

A second example of C_{15+} hydrocarbon distribution in well samples from Brazoria County is shown in figure 30 (data provided by Amoco, Tulsa, Oklahoma). Based on the normal-generation-trend line, one would predict significant hydrocarbon expulsion between 8,000 and 13,000 ft (2,400 and 3,900 m). Figure 31 is a similar plot for an Amoco well in Refugio County. It is difficult to draw a reliable normal-generation-trend line because of the few scattered data points. It is, however, possible to conclude that the points below about 7,000 ft (2,100 m) indicate hydrocarbon expulsion.

Although available organic geochemical data for the Frio MSU are limited, some data from younger (Miocene-Pliocene-Pleistocene) and older (Jurassic-Eocene) rocks of the same general basin are available and provide a useful comparison. Figure 32 shows a plot of the shale transit time and organic geochemical data for the COST No. 1 well (location given on fig. 17). Because of the continuous sedimentation of fine-grained clastics from early Miocene through Pleistocene time, most of the sequence is undercompacted (fig. 32A; data from U.S. Geological Survey). Expulsion of the generated hydrocarbons seems to have been quite ineffective, so the measured remaining C_{15+} hydrocarbons may include nearly all of the hydrocarbons generated (fig. 32B). The hachured areas (fig. 32B) show the estimated amounts of hydrocarbons expelled and the average rates of the expulsion per 500 ft (150 m) of burial (fig. 32D). There seems to be no direct relationship between such expulsion efficiency and the concentration of organic carbon (fig. 32C). Using the normal generation trend, the

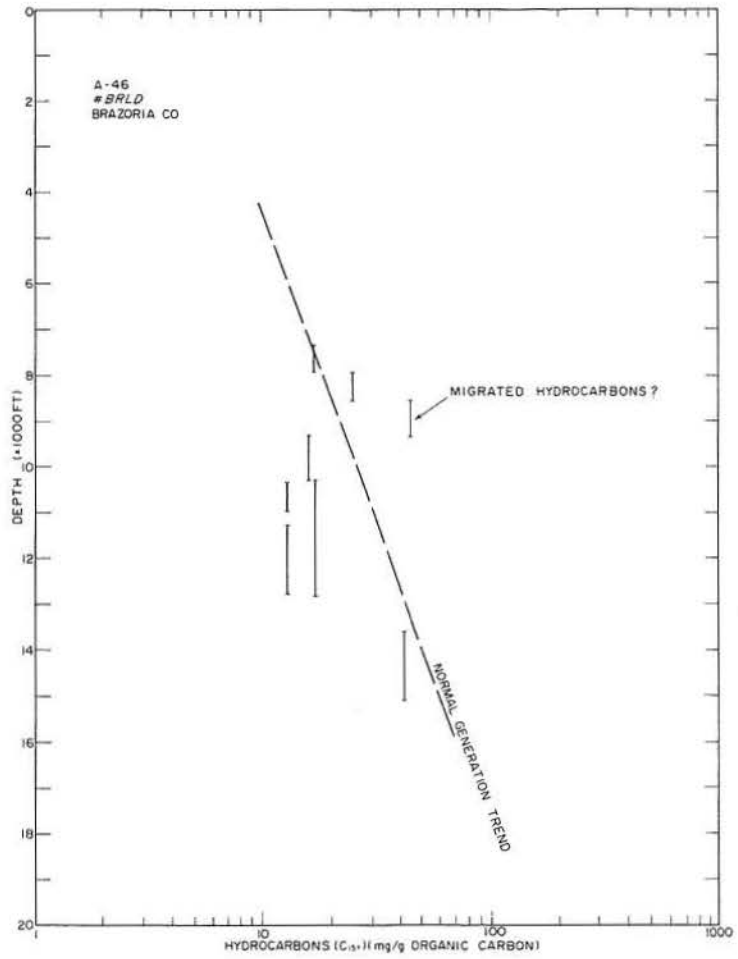

Figure 30. Plot of C_{15+} hydrocarbons (mg per g organic carbon) versus depth for a well in Brazoria County, Texas (data provided by Amoco, Tulsa, Oklahoma).

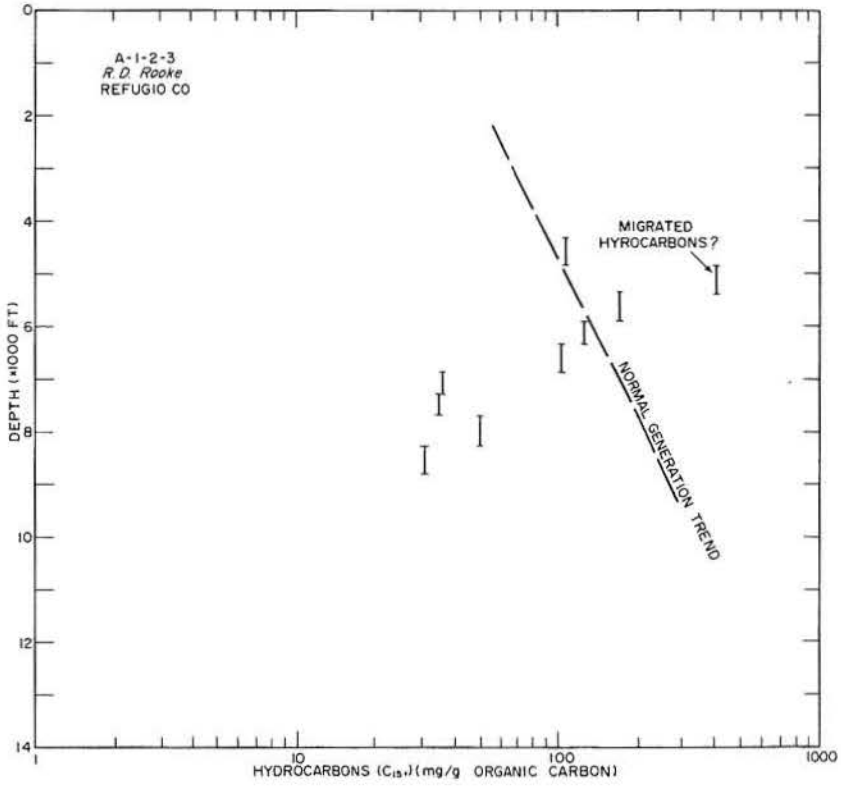

Figure 31. Plot of C_{15+} hydrocarbons (mg per g organic carbon) versus depth for a well in Refugio County, Texas (data provided by Amoco, Tulsa, Oklahoma).

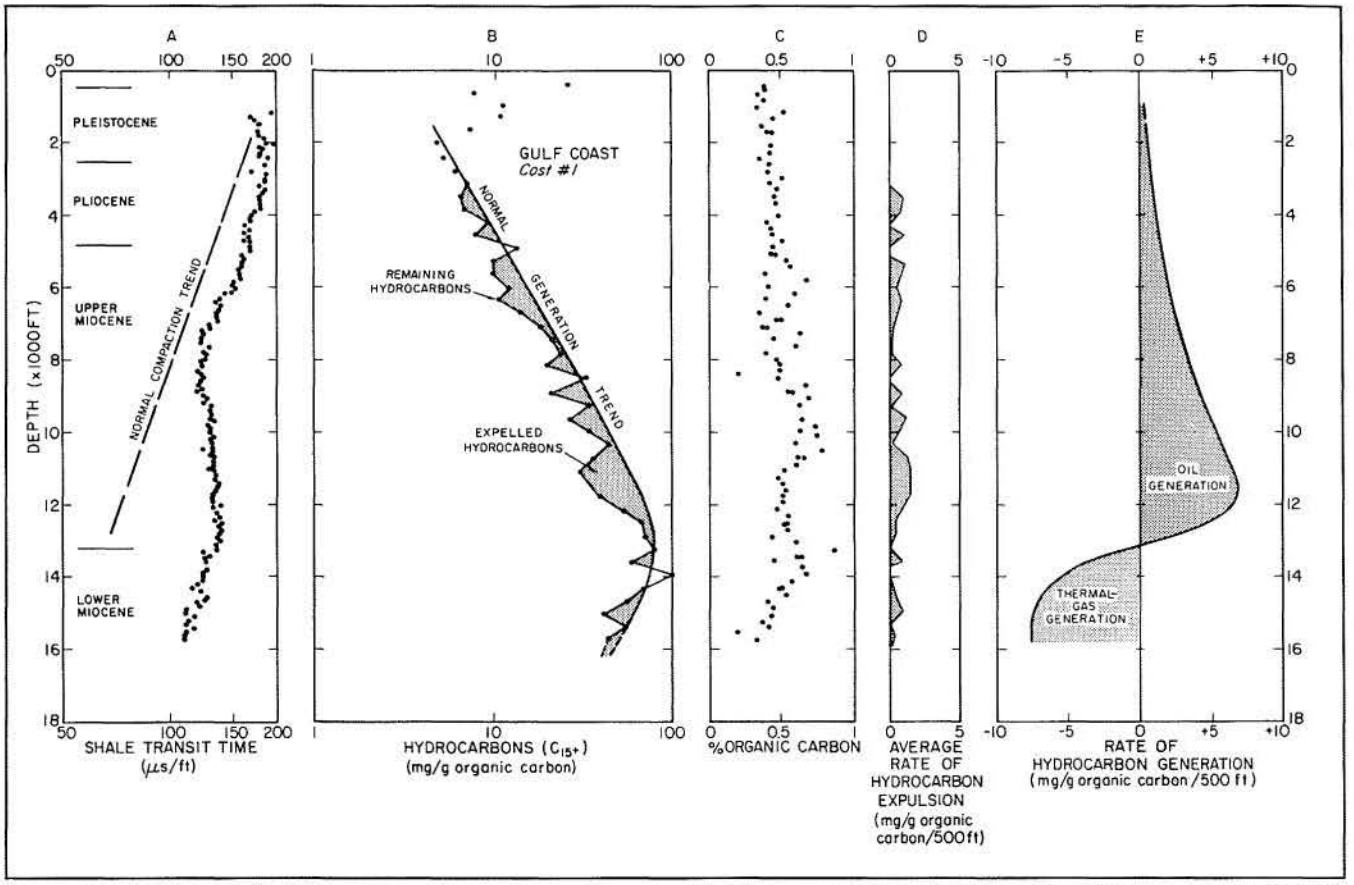

Figure 32. Summary plots of shale compaction and organic geochemical data for COST No. 1, offshore Texas (data provided by USGS; see fig. 17 for location). From left to right (A) shale transit time (μs per ft) versus depth, (B) C_{15+} hydrocarbons (mg per g organic carbon) versus depth, (C) weight percent organic carbon versus depth, (D) average rate of hydrocarbon expulsion versus depth, and (E) rate of hydrocarbon generation versus depth are shown.

rate of hydrocarbon generation was interpreted (fig. 32E); it suggests that shales have reached the main thermal-gas generation stage at total depth.

Figure 33 is a similar plot for the A. M. Foerster No. 1 well, La Salle County, Texas (county location given on fig. 17; data from USGS, Denver, Colorado). The section geochemically analyzed ranges from Jurassic to Eocene in age. The best hydrocarbon expulsion zone lies between about 10,000 and 17,000 ft (3,000 and 5,100 m) (fig. 33B and D), which corresponds to the maximum compaction zone (fig. 33A). Organic carbon content gradually decreases downward within this zone. Below this zone, the percent of organic carbon is generally higher (fig. 33C). The rate of hydrocarbon generation is negative in the deepest part of the well (fig. 33E), suggesting active thermal destruction of oil and generation of thermal gas.

In summary, thorough evaluation of geochemical data for the Frio and adjacent sections of the Gulf Coast basin fill reveals evidence not only of thermal generation of liquid hydrocarbons within the organically lean mudrocks of the deltaic, barrier/strandplain, and shelf systems, but also of significant expulsion, particularly from normally to moderately undercompacted (overpressured) sections.

Effective Hydrocarbon Expulsion From Source Rocks

Many organic geochemists maintain that a certain minimum concentration of hydrocarbons is necessary for migration to begin and that only a relatively small proportion of the total hydrocarbons generated can migrate out of source rocks. Powell (1978), for example, assumed that only 7 percent of total hydrocarbons generated was expelled in the Canadian Arctic regions. The data shown in figures 29 through 33, however, suggest that relatively low concentrations of both organic carbon and hydrocarbons are sufficient to cause significant expulsion. The proportion of the expelled hydrocarbons may, in fact, be as large as two-thirds of the total generated.

The idea that the expulsion of hydrocarbons from source rocks is ineffective seems to be in part related to methods used to evaluate such efficiency. If the oil and

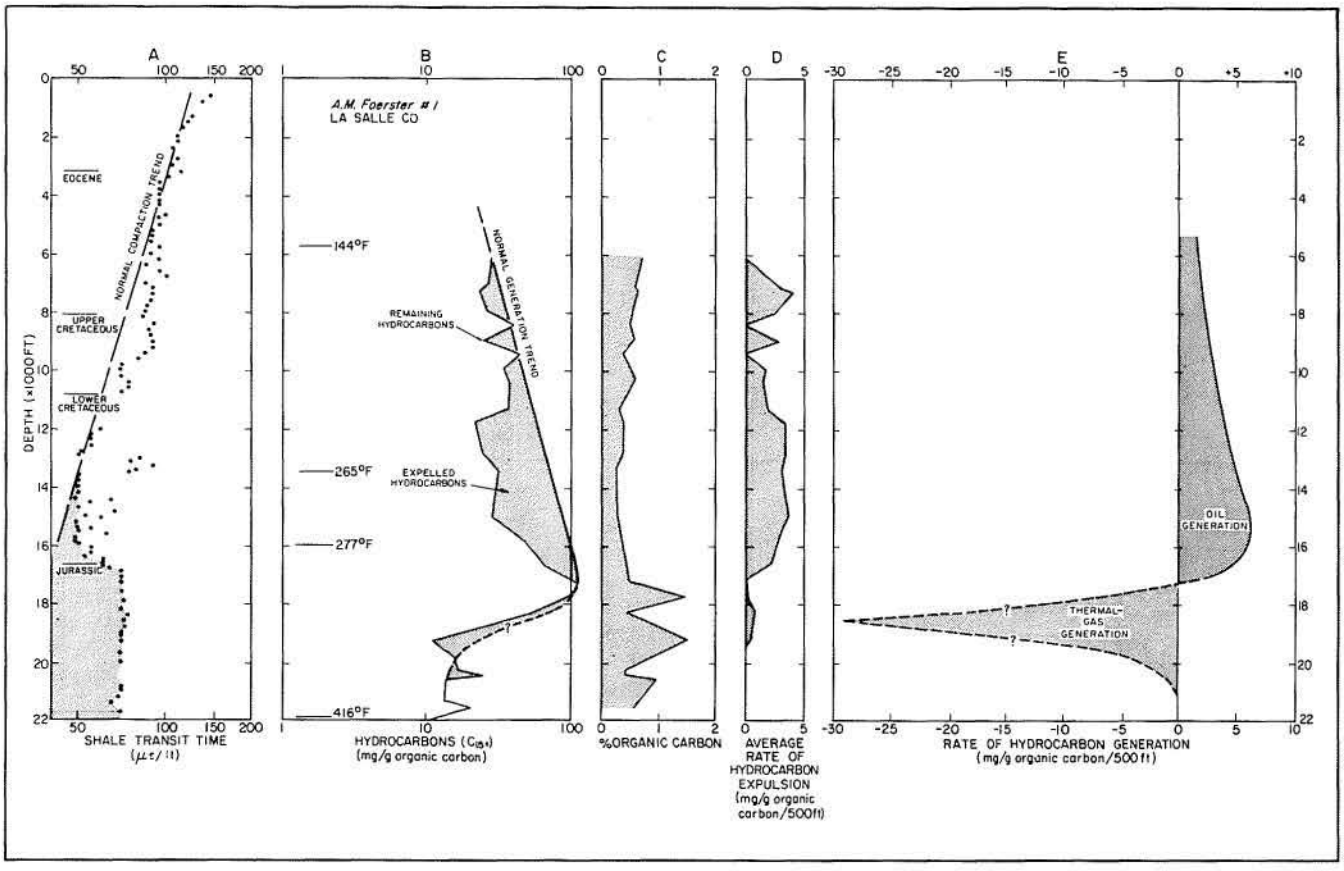

Figure 33. Summary plots of shale compaction and organic geochemical data for A. M. Foerster No. 1, La Salle County, Texas (data provided by USGS). From left to right (A) shale transit time (μs per ft) versus depth, (B) C_{15+} hydrocarbons (mg per g organic carbon) versus depth, (C) weight percent organic carbon versus depth, (D) average rate of hydrocarbon expulsion versus depth, and (E) rate of hydrocarbon generation versus depth are shown.

gas reserves in conventional reservoirs are compared with the estimated total hydrocarbons generated in a given sedimentary basin, the ratio can be quite small. This is because neither the amount dispersed in rocks other than commercial reservoirs nor the amount lost to the surface is included in such a calculation. The amount of hydrocarbons, particularly of gas, in solution in formation water can also be large. Therefore, ratios based only on reserves and total generated hydrocarbons measure primarily the efficiency of accumulating hydrocarbons in conventional commercial reservoirs, and not the efficiency of expulsion from source rocks. Expulsion efficiency as discussed in this report is the latter.

After studying several major petroleum basins, such as the Permian Basin in West Texas, the Los Angeles Basin in California, the West Siberian Basin in the U.S.S.R., and the Persian Gulf Basin in the Middle East, McDowell (1975) concluded that the oil expelled (Q_E) would be 0 to 50 percent of the total oil generated (Q), the oil lost (Q_L) between 0 and 10 percent of the oil expelled (Q_E), and the oil in reservoirs (Q_R) only 0 to 25 percent of the total generated (Q) (fig. 34). This suggests that large amounts of oil (and gas) can be dispersed both in poor-quality reservoirs and in aqueous solution.

The efficiency of oil accumulation in commercial reservoirs seems to vary greatly from basin to basin. For example, McDowell (1975) estimated that the oil contained in all reservoirs in the Permian Basin is about 75 billion bbl (12 billion m^3), whereas the oil generated is about 2.5 trillion bbl (400 billion m^3). This means that the accumulation efficiency is only about 3 percent. In the Los Angeles Basin, however, the situation is improved and the efficiency is about 30 percent.

In summary, hydrocarbon expulsion from large volumes of low-quality source rocks in the Frio MSU appears to have been quite effective. How much of the expelled hydrocarbons is trapped in conventional reservoirs is controlled by efficient juxtaposition of factors such as reservoir, trap, seal, and secondary migration. As will be shown, the proportion is small and is easily within the range of other well-studied mature basins.

Expulsion and Movement of Compaction Water and Hydrocarbons

The estimated amount of expelled hydrocarbons seems to be closely related to the degree of sediment compaction: Hydrocarbon expulsion was more effective where sediment compaction was more advanced. In order to evaluate levels of compaction, particularly in the oil-generating zone between 200° and 300° F (93° and 148° C), numerous sonic-transit-time plots were prepared (figs. 35 through 38). Each of these transit-time plots also indicates the depths corresponding to formation temperatures of 200° and 300° F (93° and 148° C).

Using the plot of the DOE/GCO Pleasant Bayou Nos. 1 and 2 wells (fig. 35) as an example, the measured level of compaction of the normal consolidation trend at the 200° F (93° C) isotherm is approximately 100 μs per ft (328 μs per m), which corresponds to a shale porosity of about 17 percent (or 0.17). The average shale transit time of the section between about 10,000 and 14,000 ft (3,000 and 4,200 m), where the expulsion of the generated hydrocarbons was relatively effective, is about 90 μs per ft (295 μs per m), corresponding to a porosity of about 13 percent (or 0.13). Using these porosity figures, one can estimate the volume of expelled compaction water (W) as follows (Magara, 1978a):

$$W = \frac{\Phi_0 - \Phi}{1 - \Phi_0} \cdot V$$

where Φ_0 = initial shale porosity (0.17 in this case);
Φ = final or post-compaction porosity (0.13); and
V = post-compaction rock volume.

Therefore, for a given unit volume of shale (1 ft^3 or 0.027 m^3), the volume of the expelled water can be calculated as follows:

$$W = \frac{0.17 - 0.13}{1 - 0.17} \times 1 = 0.05\ ft^3\ (0.0014\ m^3)$$

The volume of compaction water expelled after the onset of petroleum generation (at about 200° F or 93° C) varies geographically, depending on the degree of shale compaction at the reference subsurface temperature. Based on estimates of volumes of expelled water using about 40 wells scattered throughout the study area,

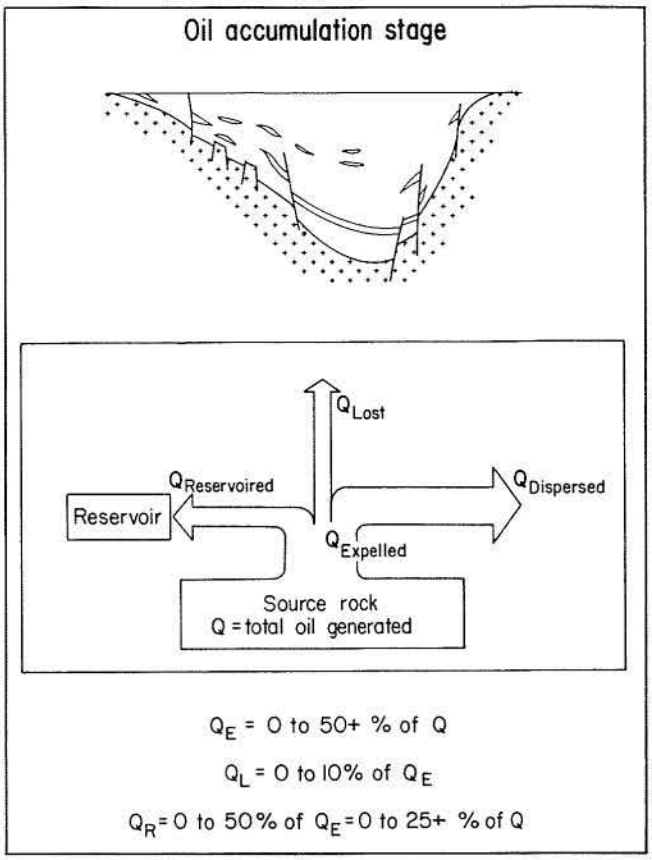

Figure 34. Schematic diagram showing the possible fates of the oil generated within a sedimentary basin (from McDowell, 1975).

0.05 ft^3 per ft^3 (0.05 m^3 per m^3) of mature shale is an average figure for the Frio. The volumetric ratio of the expelled hydrocarbons to the expelled compaction water was estimated to be approximately 1 to 30.*

The volume of mature shales in the Frio MSU is about 21,735 mi^3 or 89,000 km^3 (approximately 3,200 trillion ft^3 or 86 trillion m^3). Thus, the total volume of compaction water expelled since the onset of petroleum generation is estimated to be about 160 trillion ft^3 (about 28 trillion bbl or 4.3 trillion m^3). Using the ratio of 1 to 30 (hydrocarbons to compaction water), it can be estimated that as much as 900 billion bbl of liquid hydrocarbons have been expelled from Frio source rocks.

A contour map (fig. 39) of the average shale transit time of the thermally mature shales shows that maximum average compaction is attained in the southernmost areas

*Assuming that the average bulk density of shales is 2.3 g per cm^3 and the average organic carbon weight percent is 0.3 percent, 1 cm^3 of the rock contains about 0.07 g organic carbon. The average expelled hydrocarbon weight is 20 mg per g organic carbon, so that 1 cm^3 of the rock lost about 1.4 mg (or 0.0014 g) of hydrocarbons. If the density of the hydrocarbons is about 0.9 g per cm^3, this amount of hydrocarbons corresponds to about 0.0016 cm^3 in volume. In other words, one unit volume of mature shale lost 0.0016 volume of hydrocarbons. During the hydrocarbon expulsion, 0.05 cm^3 of compaction water was also lost. The ratio of the expelled hydrocarbons to the expelled compaction water is, therefore, about 1 to 30 (or 0.0016 to 0.05).

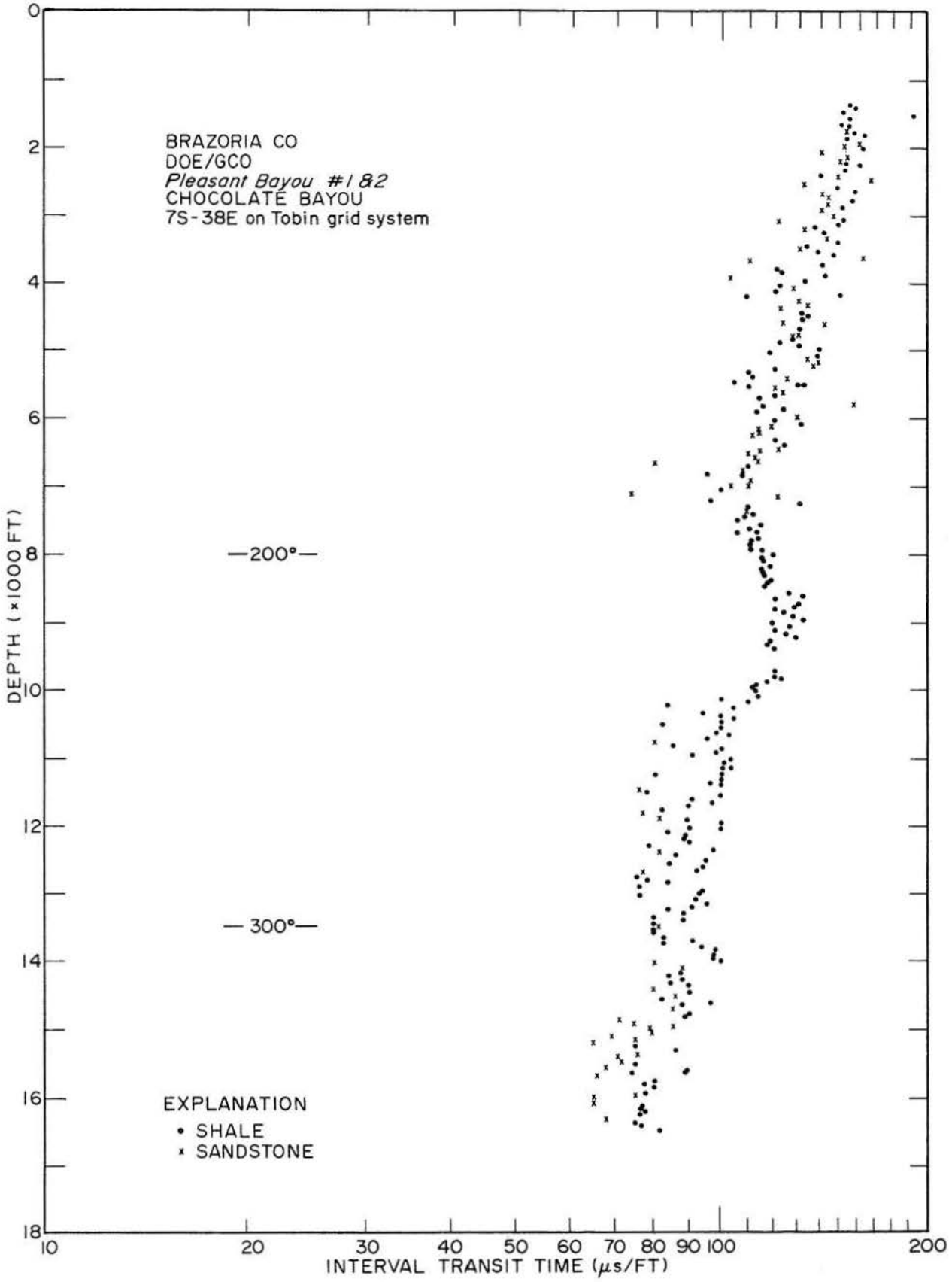

Figure 35. Example of an interval transit time versus depth plot for a well in Brazoria County, Texas.

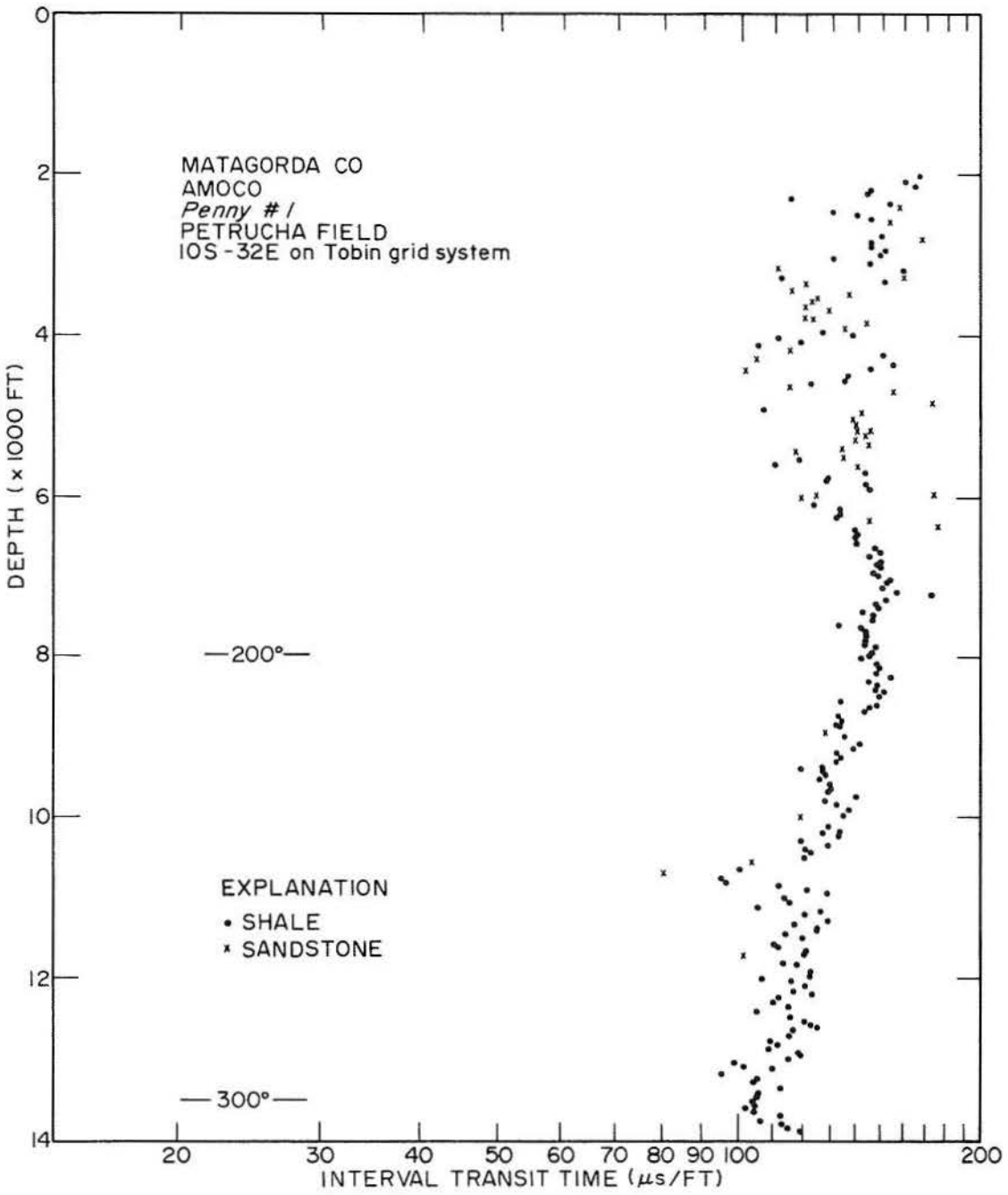

Figure 36. Example of an interval transit time versus depth plot for a well in Matagorda County, Texas.

of the region. Directions of movement of both compaction water and hydrocarbons are primarily controlled by the sediment-loading patterns and the degree of overpressuring of source rocks. Determination of such directions is a complicated matter and requires a three-dimensional analysis of the data. However, it is also obvious from the sedimentation patterns of the Frio MSU (pl. 3, isopach map) and the presence of the overpressured mature source rocks (fig. 27) that the principal migration of fluids was updip toward the basin margin.

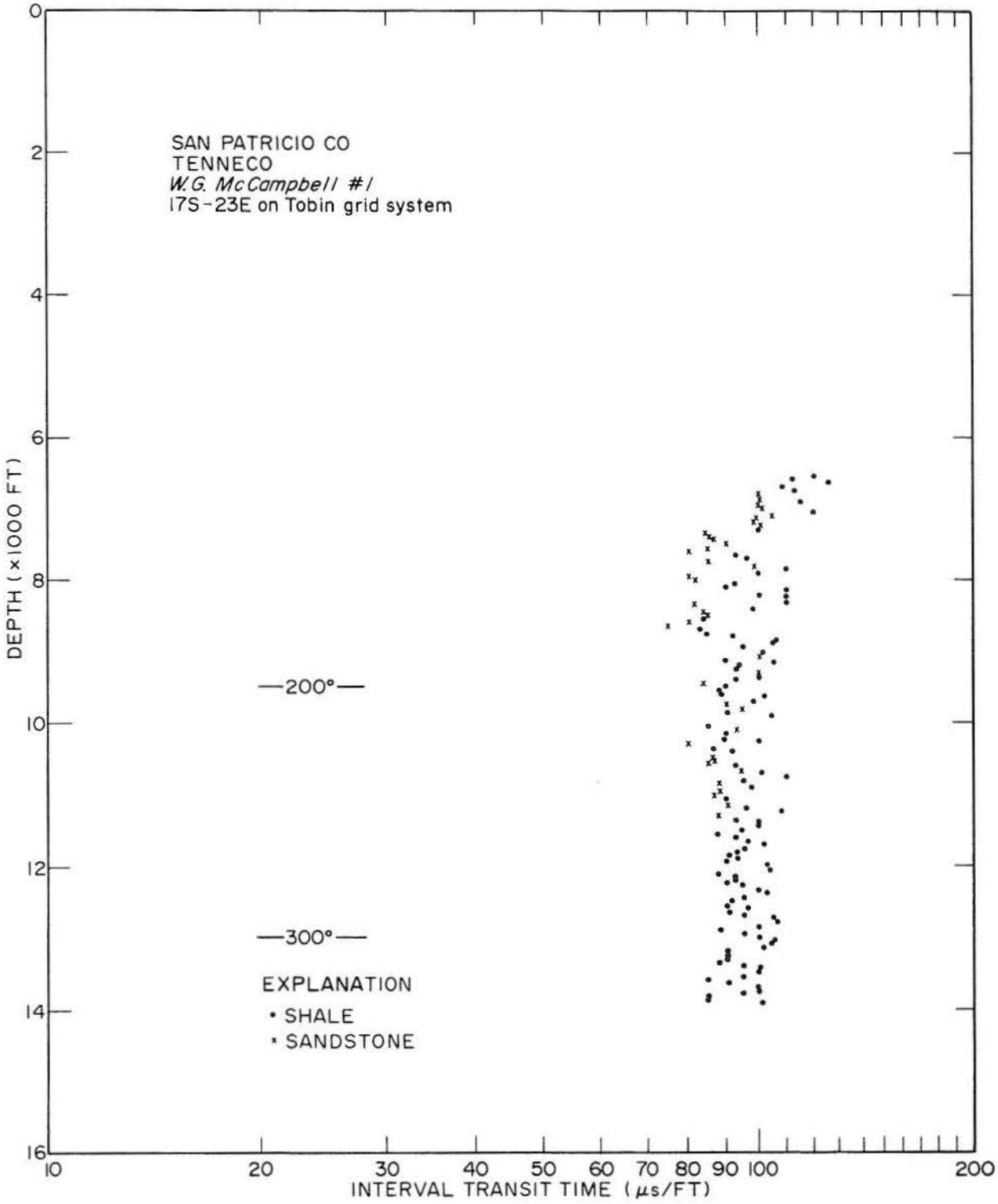

Figure 37. Example of an interval transit time versus depth plot for a well in San Patricio County, Texas.

To show the intensity of such lateral fluid flow, a loading map of the section above the top of the geopressured interval (>0.7 psi per ft or >0.16 kg per cm^2 per m) was constructed (fig. 40). This map shows the total overburden stress (in psi) of the sediments above the geopressured sections, indicating the lateral directions of fluid movement as well as its intensity. As described above, the general migration direction is from the coast to inland areas. In the Upper Texas Gulf Coast, the lateral loading pressure changes more abruptly than

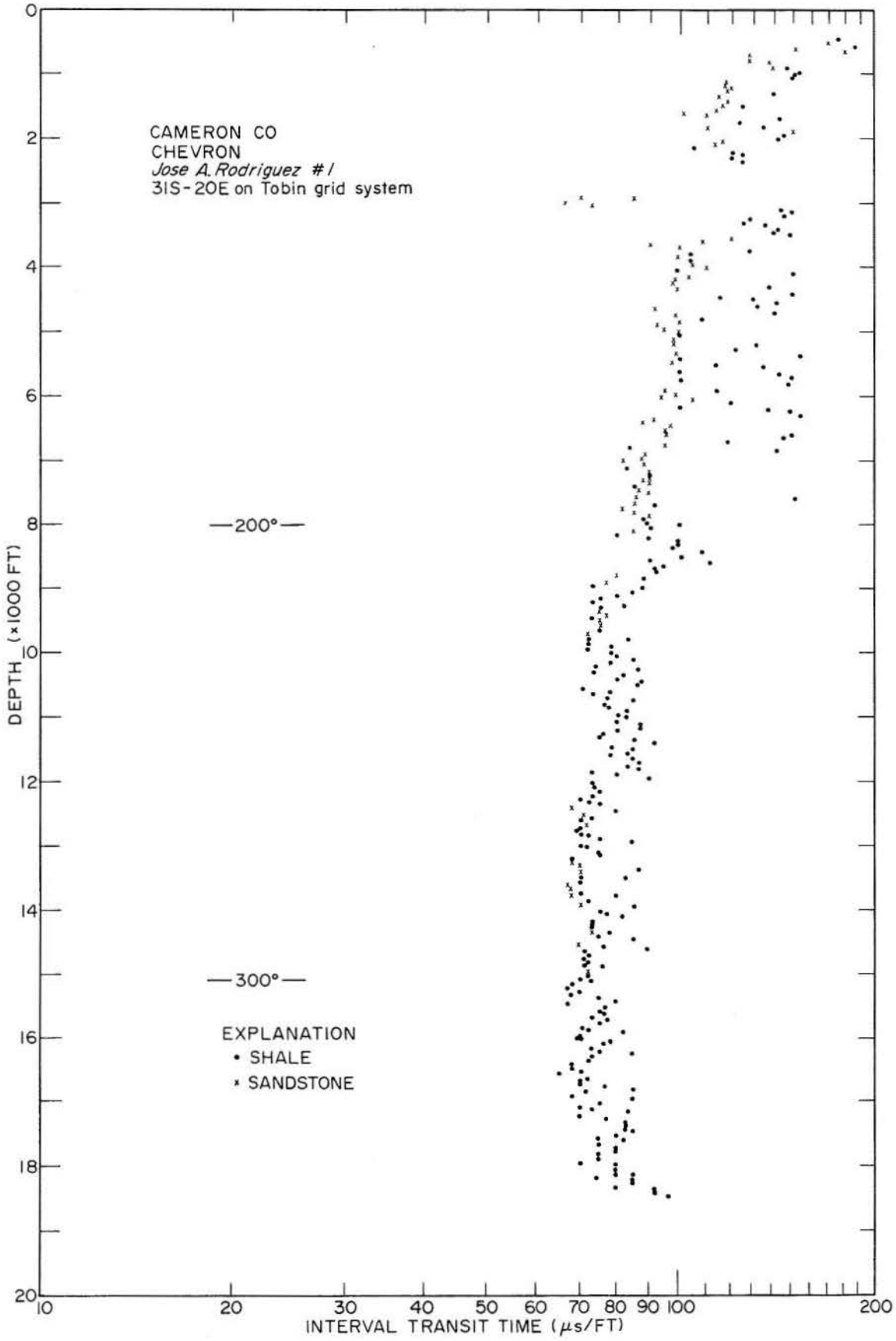

Figure 38. Example of an interval transit time versus depth plot for a well in Cameron County, Texas.

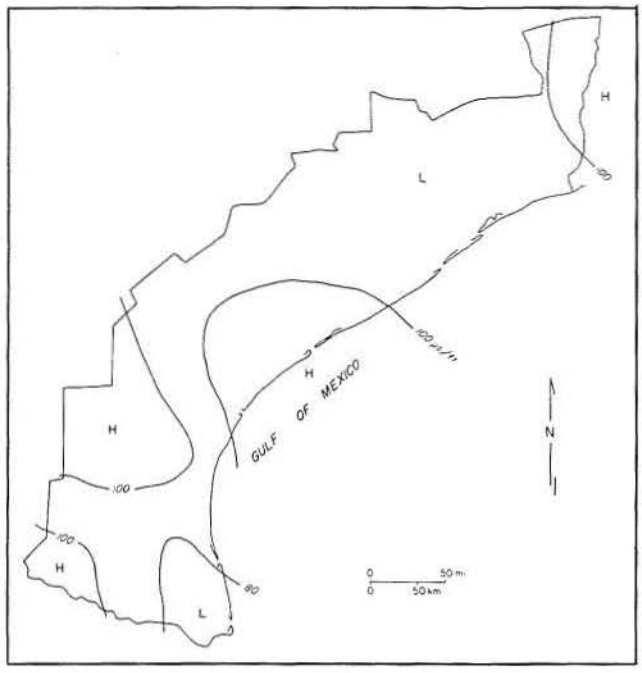

Figure 39. Average shale transit time for thermally mature Tertiary shales of the Texas Gulf Coast.

in the Lower Texas Gulf Coast. This means that stronger lateral fluid-pressure gradients existed in the Houston delta system and environs than in the Norias delta system, suggesting more effective lateral migration of hydrocarbons in the former area.

SOURCE, RESERVOIR, AND PRIMARY MIGRATION

From the observations and interpretations described above, we conclude that the prime source rocks for the Frio oil and gas reserves are the shallower parts of the undercompacted shale section that underlie or lie basinward of the reservoir facies suite. There would have been some lateral and vertical hydrocarbon migration involved in accumulating oil and gas in the reservoirs, but the distance of migration may have been relatively limited (probably several miles laterally and only a few thousand feet vertically).

If these observations and interpretations are correct, then a model of source, reservoir, and primary migration relationships can be described as follows: Assume that in a given thickness (say 1,000 ft or 300 m) of a geologic unit, a number of sandstone beds, whose thicknesses are known, are inserted. As more sandstones are inserted, the percentage of sandstones in this unit will increase (fig. 41A). As the number of sandstones increases, the average thickness of the remaining interbedded shales decreases (fig. 41B). For a smaller number of sandstones (or lower sandstone percent), the average thickness of shales is large (left side of fig. 41B). Although there are thick shales available in this case, there is likely an upper limit of drainable shale thickness (fig. 41B) and the hydrocarbon drainage may be inefficient because of the absence of interbedded permeable reservoirs (sandstones). Existence of such a limit is indicated by the poor fluid drainage and concomitant poor hydrocarbon expulsion characteristic of the sand-poor, geopressured, severely undercompacted zone.

The product of the number of the sandstones and the thickness of the shales (fig. 41C) defines the probability of finding both reservoirs and drainable source rocks. At the left margin of figure 41C, where only a few reservoirs with thick, intervening source rocks are shown, the product is small. Similarly, at the right margin, a large number of reservoirs with very thin, interbedded source rocks are shown and the product is also small. In the intermediate range of sandstone number or percentage, the product is greatest, suggesting the best combination of source and reservoir rocks. This simple model thus predicts the optimum 20- to 60-percent range of sandstone content for oil and gas accumulations observed in major petroleum provinces of the world. Even though the interbedded shales may not be a prime source of hydrocarbons, such an estimate of the product is informative. The product, in such a case, may be interpreted as an indicator of the probability of finding appropriate reservoirs and seals.

The products were calculated and mapped for the Frio MSU using the statistical data discussed previously in this report and an arbitrary upper limit of 100 ft (30 m) for the drainable shale thickness (fig. 42). This product map may be compared with the oil and gas field map (pl. 19). In area A (fig. 42) in the Lower Texas Gulf Coast, for example, the product values are generally small, mainly because of scarcity of source and seal rocks; as expected, there are only a few fields (pl. 19). In area B in the Middle Texas Gulf Coast, the product is also low because of a lack of reservoirs; here, too, there are few fields. Additionally, shales in area B are thermally immature and far removed from underlying or equivalent mature source rocks. Narrow bands (C and D strips) having relatively low product values occur along the coastline in the Middle and Upper Texas Gulf Coast. These areas coincide with an overabundance of sandstones along the axes of the Greta/Carancahua barrier/strandplain system. Hydrocarbons that have migrated from other areas may have been lost upward in these areas because of a lack of proper seals; predictably, few oil and gas fields lie in these areas (pl. 19). In area E in the Upper Texas Gulf Coast, the product values are generally high, but there are few fields (pl. 19). Interbedded mudstones here are quite immature, and potential reservoirs are far removed from the mature sources located at depth.

The average product values for the five facies assemblages discussed earlier are summarized in figure 43. The

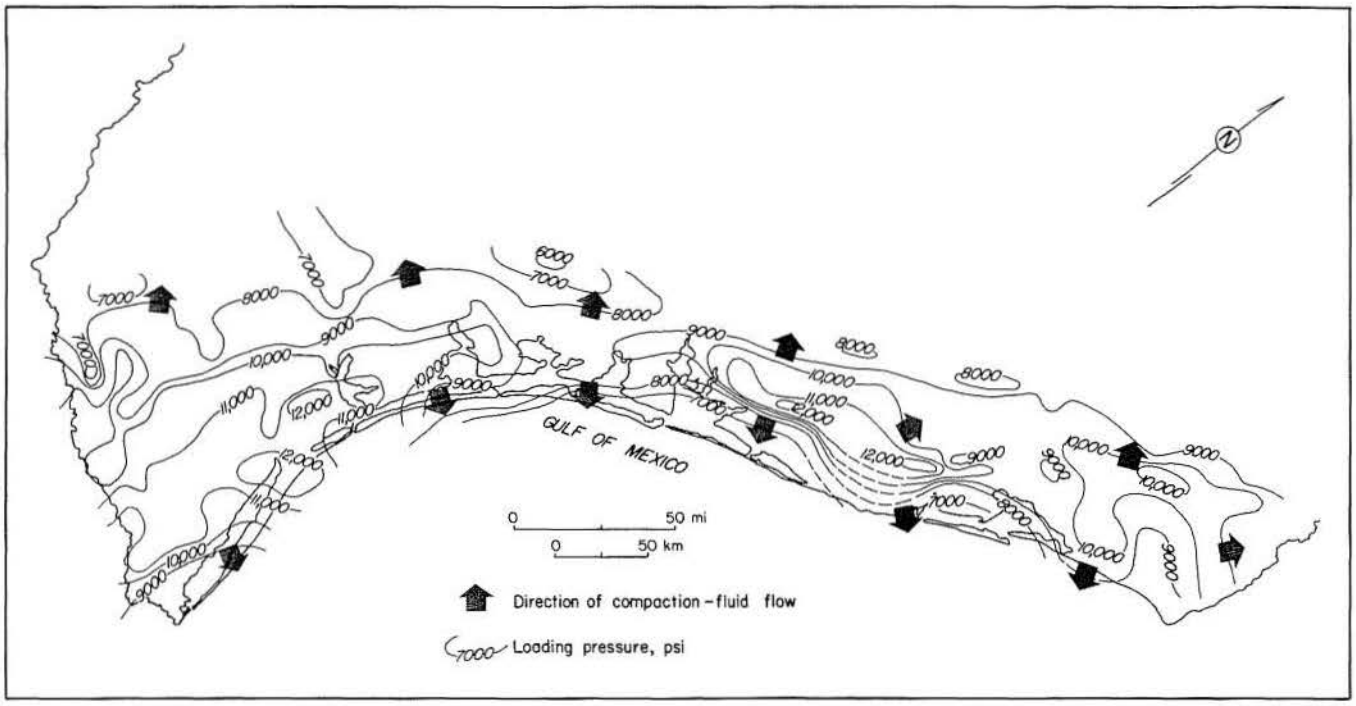

Figure 40. Overburden loading map showing total weight (in psi) of geologic section above top of geopressured section in which fluid-pressure gradients exceed 0.7 psi per ft (0.16 kg per cm^2 per m) in the Texas Gulf Coast. This map suggests large-scale lateral fluid flow from points of greater loading to points of lesser loading.

product value increases from shelf to fluvial deposits, but in the study area, shales in the fluvial facies are commonly immature; thus, there is a relatively small number of oil and gas fields producing from this facies. The relatively high product values for the fluvial and streamplain environments do suggest that were the interbedded shales mature, or had large-scale vertical migration occurred along major structural conduits, the facies, possessing good combinations of reservoirs and seals, would be excellent for hydrocarbon accumulation. In fact, one such producing trend, coincident with the Vicksburg Flexure, occurs in South Texas, and it is one of the richest plays of the Gulf Coast. Deltaic systems predictably provide excellent opportunities for primary migration and entrapment; barrier/strandplain systems are comparably favorable. Basinward margins of both systems would be less productive on a whole-rock volume basis, but production per unit volume of reservoir might be prolific.

HYDROCARBON PRODUCTION

The Frio Formation has produced nearly 6 billion bbl of oil and 60 trillion ft^3 of gas, for a total of 16.3 billion boe of hydrocarbons. Included in this figure is a substantial contribution from very old fields discovered and developed during the early part of the century, as well as significant new discoveries made in the last decade. In all,

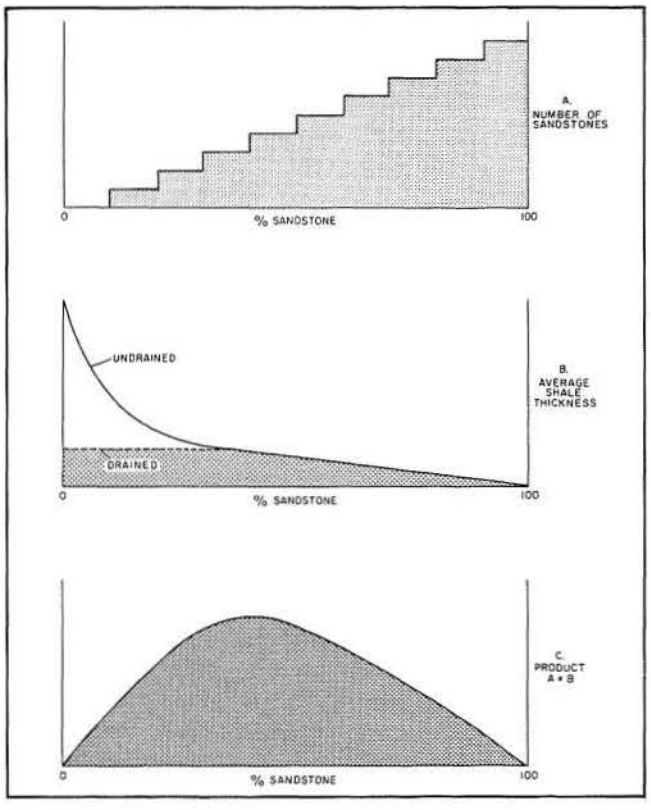

Figure 41. Diagrammatic model predicting optimum sandstone percent for hydrocarbon accumulation. Refer to text for detailed explanation.

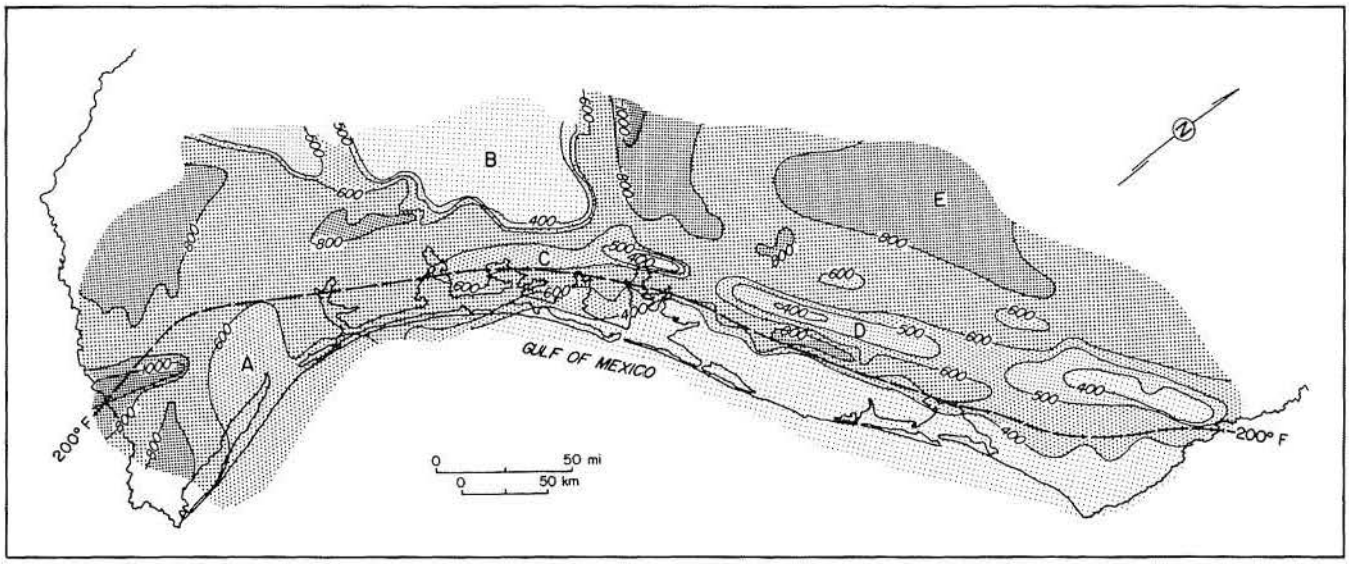

Figure 42. Contour map showing product of number of sandstones and average thickness of interbedded shales, Frio MSU. Refer to text for detailed explanation of areas A, B, C, D, and E.

Frio production covers most of 24 counties, and a few fields occur offshore in State and Federal waters. In addition, sands of the Frio contain an estimated 264 trillion ft^3 (44 billion boe) of dissolved methane (Gregory and others, 1980).

The hydrocarbon inventory produced for this study considered only those fields containing more than 1 million boe. We estimate that the resultant data base includes more than 95 percent of the known reserves of the Frio, an estimate consistent with the observation in other basins that most producible hydrocarbons occur within large pools. Errors introduced by deletion of smaller fields are likely to be less significant than the uncertainty introduced by the incomplete records of early production in many of the largest and most prolific fields.

PLAY RECOGNITION AND DESCRIPTION

Hydrocarbon production in the Frio MSU can be grouped into 10 geologically defined plays (pl. 19), 7 of which contain the majority of the fields. Principal defining parameters of plays include the depositional system or facies assemblage of the reservoirs, dominant structural trap style, and the type of hydrocarbon produced. Key attributes of each play are summarized in table 4. Although genetic stratigraphy, structural style, and production are typically interrelated, some plays are defined by the dominance of one of these variables. For example, plays V and VI are separated primarily because they occur on the marine and landward sides, respectively, of the axis of the Greta/Carancahua system. Play III is defined by a single major structural feature, the Vicksburg Flexure. Plays VIII and IX are distinguished by the relative importance of piercement salt domes to overall structural style. Play II is characterized by the fact that it produces gas almost exclusively.

Quantitative geologic attributes of each play are listed in table 5. In addition to play area, total rock volume and volume of sandstone and mudstone were determined by planimetering appropriate isopach and isolith maps. Cross sections were used to estimate the percentage of the section lying below the 200° F (93° C) isotherm and within the hydrocarbon maturation window. The approximate volume of thermally mature mudstone was then calculated using this estimate. Structural features, including number of miles of faulting, number of salt piercement diapirs, and number of closures, were determined from commercial and published structural maps. These data provide at best a qualitative comparison, however, because mapping horizons and their position within the Frio differ from play to play. Average sandstone porosity was estimated from regional Frio consolidation profiles (Loucks and others, 1979). Average drilling density, expressed as the number of well penetrations of middle Frio per square mile, was estimated from county well depth audits tabulated from the Petroleum Information Corp. well data file. Interpreted source-rock quality, likely source facies, and the average of available total-organic-carbon values provided by company and public sources completed the geologic description.

A hydrocarbon inventory of each play (table 6) shows cumulative production of oil, associated gas, and

nonassociated gas. Cumulative production statistics were used as the primary data base for most further calculations because they are historical production figures and are subject to minimal interpretation or extrapolation. Total of produced hydrocarbons for each play was calculated by using the conversion factor based on energy equivalency of 6,000 Mcf of gas per bbl of oil. Other conversions might be used, but energy equivalency establishes a yardstick for comparison of the produced and potential *total energy content* of each play volume. The total can be readily disaggregated following various calculations by using known or assigned proportions of gas to oil. Data on projected producible reserves of larger fields provided the basis for calculating the percentage of gas and oil already produced. Total in-place reserves could also be calculated, but recovery factors for oil are available only as generalized averages of larger fields for each of the three Railroad Commission of Texas districts that encompass the Coastal Plain. Because the validity of such figures for individual plays is subject to question, the decision was made to utilize historical production figures rather than to introduce an additional variable in further calculations.

Combination of volumetric data and hydrocarbon production statistics produced a series of yield factors (table 6) based on volumes of total rock, reservoir rock, and thermally mature shale and on relative abundance of structural features. Yield factors were calculated using figures for total produced hydrocarbons and then disaggregated to give values for total oil and gas. These figures are minima in the sense that they are based generally on the 80 to 90 percent of the producible hydrocarbon reserve that has actually been extracted. However, casual examination of table 6 shows that calculations based on interpreted total producible or total in-place hydrocarbons would have little effect on the relative play ranking. Comparison of the relative productivity of Frio plays is illustrated graphically in figures 44 and 45. Both whole-rock and reservoir yield factors display an order-of-magnitude range. For comparison, White and others (1975) calculated a reservoir yield factor of approximately 3.1×10^6 boe per mi^3 for the gas-prone Oligocene-Miocene section of Louisiana. We agree with their conclusion that production per unit volume of reservoir is the best index of hydrocarbon productivity.

PLAY STRATIGRAPHY, STRUCTURAL RELATIONSHIPS, AND HYDROCARBON PRODUCTION

Each of the 10 Frio plays (pl. 19) is characterized by a distinct association of structural features, sedimentary facies, and hydrocarbon production; but the relative importance of specific criteria varies from one play to

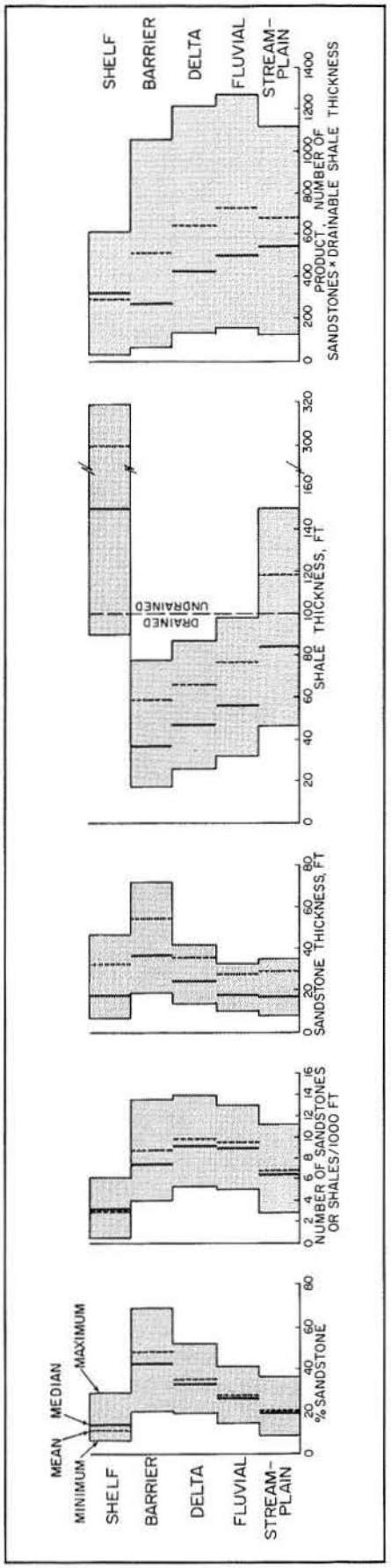

Figure 43. Statistical summary of the five Frio genetic facies assemblages. First four diagrams are identical to those shown in figure 15. The diagram at far right shows the product of number of sandstones and average thickness of interbedded shales, using an assumed 100-ft (30-m) cutoff for drainable shale thickness. Refer to text for detailed explanation.

Table 4. Defining geologic and exploration attributes of Frio MSU plays.

Play	Productive System(s)	Structural Style	Exploration Maturity	Frontiers	Limiting Factors
I	Norias Delta System	Growth fault & shale ridge	Immature	Depth & OCS	(1) Reservoir quality (2) Migration efficiency
II	Norias Delta System	Growth fault & shale ridge	Mature	Depth	(1) Reservoir quality (2) Migration efficiency
III	Norias and Gueydan Systems	Vicksburg Flexure	Supermature	None	(1) Well density
IV	Gueydan Fluvial System	Inherited low-amplitude fault & anticline	Mature	None	(1) Well density (2) Thin, shallow section (3) Lack of indigenous mature source
V	Greta/ Carancahua Barrier/ Strandplain System	Growth fault & shale ridge	Mature	Depth & downdip (Limited)	(1) Reservoir distribution/ volume (2) Well density
VI	Greta/ Carancahua Barrier/ Strandplain System	Growth fault & shale ridge	Supermature	None	(1) Well density
VII	Moulton Streamplain & Chita/ Corrigan Fluvial Systems	Inherited low-amplitude fault & anticline	Mature	None	(1) Well density (2) Thin, shallow section (3) Lack of indigenous mature source
VIII	Houston Delta System	Salt diapirism & associated faulting	Mature	Depth	(1) Reservoir distribution/ volume?
IX	Houston Delta System	Growth fault & minor salt diapirism	Mature	Depth	(1) Reservoir distribution/ volume
X	Buna Strandplain System	Growth fault & salt diapirism	Mature	Depth?	(1) Reservoir distribution/ volume

another. The plays vary considerably in areal extent and thickness. Updip plays extend to the Catahoula outcrop; downdip plays extend gulfward to the limit of well coverage, which is largely depth imposed. This downdip limit corresponds approximately to the distal extremities of known reservoir sands, although these may persist at greater depth.

Play I (pl. 19) is a poorly explored, gas-prone division corresponding to the upper slope, prodelta, and distal delta front of the Norias delta system (table 4). Sandstone percentage is low, and most of the shale source rock is thermally mature (table 5). These mudrocks, of prodelta and slope origin, therefore constitute a potential hydrocarbon source, but source-rock quality is poor, averaging only 0.3 percent TOC (table 5). Reservoir quality is also poor because of fine grain size and advanced diagenetic destruction of porosity and permeability. Migration efficiency is low because of low permeability and limited interfingering of sandstone and mudstone.

Dominant structures are growth faults and shale ridges, with the associated anticlines acting as hydrocarbon traps. Reservoir facies include marine-modified delta-front sandstones within the upper Frio. The producing interval lies directly below the Anahuac Shale, which provides a seal. The play has been sparsely drilled; well density averages only 0.04 per mi^2 (table 5).

Play II corresponds to the main body of the Norias delta system and its transition zone with the Gueydan fluvial system (table 4). It is characterized by production of

Table 5. Quantitative geologic attributes of Frio MSU plays.

Play	Area (mi^2)	ROCK VOLUME					STRUCTURE						
		Rock volume (mi^3)	Sandstone (mi^3)	Mudstone (mi^3)	Percent that is thermally mature†	Thermally mature mudstone (mi^3)	Miles of faulting	Number of salt diapirs	Number of mapped closures	Average sand porosity (%)	Average well density (wells/mi^2)‡	Source-rock quality (avg. TOC)	Principal potential source-rock facies
I	3,120	6,360 (depth ≤ 20,000')	900+	5,460	95±	5,000	570	0	28	18	0.04	0.3	Prodelta and slope mudstone
II	4,420	6,800	1,900	4,900	80	3,900	1,010	0	64	18	0.11	0.3	Prodelta and slope mudstone
III	2,534	1,760	370	1,390	6	80	270	1	24	26	1.53	0.3	Delta-plain mudstone
IV	4,310	1,625	200	1,425	0	0	minimal	2	not mapped	27	1.02	0.4	Floodplain mudstone
V	5,300	8,090	640	7,450	95±	7,000	970	2	41	25	1.13	0.2	Shelf and upper slope mudstone
VI	4,088	3,195	1,120	2,075	31	650	690	1	35	30	1.85	0.3	Shelf and lagoonal mudstone
VII	21,868	6,378	1,286	5,092	0	0	minimal	11	not mapped	30	1.12	0.4	Floodplain mudstone
VIII	3,740	2,731	793	1,938	60	1,170	125	58	58	31	1.20	0.3	Prodelta, shelf, and upper slope mudstone
IX	2,630	2,980	189	2,791	87	2,435	111	35	35	29	2.2	0.3	Prodelta, shelf, and upper slope mudstone
X	1,750	1,400	252	1,148	44	500	16	12	12	33	0.9	0.3	Shelf and upper slope mudstone
TOTALS	53,760	41,319	7,650	33,669		20,735	3,762+	122	297+				

† Present temperature ≥ 200° F (93°C)

‡ Average penetration of upper half of total Frio interval

Table 6. Hydrocarbon inventory for Frio MSU plays (numbers subject to minor rounding).

	Cumulative Production					Percent Already Produced		Remaining Proved Reserve				
Play	Oil (10^6bbl)	Associated gas (10^3MMcf)	Nonassociated gas (10^3MMcf)	Total gas (10^3MMcf and liquid equivalent* in 10^6boe)	Total hydrocarbons (10^6boe)	Oil	Gas	Average oil recovery (%) †	Oil (10^6bbl)	Associated gas (10^3MMcf)	Nonassociated gas (10^3MMcf)	Average $\frac{\text{boe gas}}{\text{bbl oil}}$
I	29	281	185	$\frac{466}{80}$	107	~60	~60	34	3.6	9.6	303	2.7
II	50	1	6,530	$\frac{6,531}{1,090}$	1,140	—	81	34	0	0	1,600	22
III	917	7,690	7,110	$\frac{14,800}{2,470}$	3,390	96	91	34	28	322	1,500	2.7
IV	52	2	77	$\frac{79}{15}$	65	100	95	34	1	0.04	6	0.2
V	519	4,200	7,700	$\frac{11,900}{1,980}$	2,500	98	83	44	11	89	2,400	3.8
VI	2,500	4,750	5,850	$\frac{10,600}{1,765}$	4,230	85	90	44	440	836	1,200	0.7
VII	41	45	886	$\frac{931}{155}$	191	82	83	46	8	8.2	199	4.8
VIII	1,620	1,110	2,440	$\frac{3,550}{590}$	2,210	77	85	48	490	336	630	0.4
IX	857	2,120	4,150	$\frac{6,270}{1,045}$	1,900	89	88	48	110	272	870	1.2
X	236	465	1,530	$\frac{1,995}{330}$	567	96	83	48	9	17.7	420	1.4
TOTAL	6,821	20,664	36,458	$\frac{57,122}{9,520}$	16,300				1,100	1,890	9,130	1.4

nonassociated gas but little oil (table 6). Play II suffers from the same diagenetically reservoir-imposed limitations as play I, and source-rock quality and migration efficiency are likewise poor. Mudstone makes up three-quarters of the total play volume, and 80 percent is thermally mature (table 5). The major structural features are growth faults and shale ridges. Shale-cored rollover anticlines and faulted anticlines are the most important traps. Some hydrocarbons are trapped within upthrown blocks by closure against faults on the upthrown side; there are also subordinate stratigraphic traps. Reservoir facies vary with stratigraphic position. Thick, upward-coarsening, wave-reworked delta-front sandstone reservoirs are most prevalent in the lower Frio; fluvial sandstones are predominant in the middle and upper Frio operational units. Drilling density is low, averaging 0.11 wells per mi^2 (table 5).

Play III, a gas-prone play located over the Vicksburg Flexure, has reached the supermature stage of exploration (tables 4, 5, and 6). It includes part of the Gueydan fluvial system extending into the farthest updip positions of the Norias delta system and into coastal lake and streamplain systems along strike. Eighty percent of the total rock volume is mudstone, of which only 6 percent is thermally mature. Average TOC content is only 0.3 percent. Reservoir porosity averages 26 percent and is thus greatly improved over downdip plays. Migration efficiency is likewise enhanced.

Dip-oriented fluvial channel-fill sands are the dominant reservoir facies, along with some reworked deltaic sands in the lower Frio. Anticlines, faulted anticlines, and fault closure along the Vicksburg Flexure are the most important traps. Stratigraphic features contribute to trapping in approximately one-half of the

Table 6 (cont.)

Yield Factors (f)														
Production/Total Volume - 10^6boe/mi^3						Production/Reservoir Volume - 10^6boe/mi^3								
Entire Play			Best Area			Entire Play			Best Area					
Oil	Gas	Total	Oil	Gas	Total	Oil	Gas	Total	Oil	Gas	Total	Production/mile of faulting (10^6 boe/mi)	Production/structural closure (10^6 boe/trap)	Production/volume of thermally mature mudstone (10^6 boe/mi^3)
0.005	0.012	0.017	0.016	0.042	0.06	<0.033	<0.086	<0.12	<0.08	< 0.22	< 0.3	0.2	4	0.02
0.007	0.16	0.17	0.009	0.198	0.21	0.026	0.57	0.60	0.039	0.86	0.9	1.1	18	0.3
0.52	1.40	1.93	0.92	2.47	3.40	2.48	6.68	9.16	5.06	13.64	18.7	12.5	140	42
0.032	0.008	0.04	0.088	0.023	0.11	0.26	0.067	0.33	0.95	0.24	1.2	NA	NA	NA
0.064	0.25	0.31	0.076	0.30	0.37	0.81	3.09	3.90 (2.2)‡	0.41	1.58	2.0	2.5	60	0.3
0.78	0.55	1.32	0.56	0.40	0.95	2.23	1.55	3.78 (3.1)‡	1.71	1.19	2.9	6.1	121	6.5
0.006	0.025	0.03	0.017	0.067	0.08	0.032	0.12	0.15	0.064	0.24	0.3	NA	NA	NA
0.59	0.22	0.81	0.56	0.21	0.77	2.04	0.74	2.78	2.64	0.96	3.6	17.7	41	1.9
0.29	0.35	0.64	0.60	0.73	1.33	4.53	5.50	10.03	4.13	5.01	9.2	17.1	58	0.8
0.17	0.24	0.41	0.33	0.46	0.79	0.94	1.31	2.25	1.46	2.04	3.5	35.4	52	1.1
0.17	0.23	0.40				0.89	1.24	2.13						0.8

• Calculated energy equivalent in bbl of oil (6 Mcf = 1 boe)

† Figures apply to entire production within the RRC district in which the play lies

‡ Exclusive of a giant field lying within the play

fields; this results from the abrupt facies changes along the Vicksburg Flexure. The play is densely drilled, averaging 1.53 wells per mi^2. The nonproductive gap in the middle of the strike-elongate play corresponds to the sand-rich axis of the Gueydan fluvial system and probably reflects the near absence of continuous shales necessary for trap sealing.

Play IV is characterized by minor oil-dominant production in the updip Gueydan fluvial system (tables 4 and 6). This thin, shallow interval contains a low proportion of sandstone. The mudstones average 0.4 percent TOC, but have undergone inadequate thermal maturation for oil generation (table 5). The play is therefore entirely lacking in indigenous hydrocarbon liquids. Inherited low-amplitude faults and anticlines are the major structures. Reservoir facies are mainly fluvial sandstones, and faulted anticlines and stratigraphic traps are most prevalent. Drilling density is moderately high.

Play V comprises a gas-prone trend lying mainly within the Greta/Carancahua barrier/strandplain system and adjacent shelf (tables 4 and 6). It has reached a mature stage of exploration, with 1.13 wells per mi^2 (table 5). Shelf and upper slope mudstones contain only 0.2 percent TOC, but more than 95 percent of their volume is thermally mature. Sandstones downdip of the barrier/strandplain axis constitute the major reservoirs. These have an average porosity of 25 percent and are interbedded with mudrocks, which provide maximum efficiency of hydrocarbon migration. Traps are simple to faulted, shale-cored anticlines and growth faults with closure on the

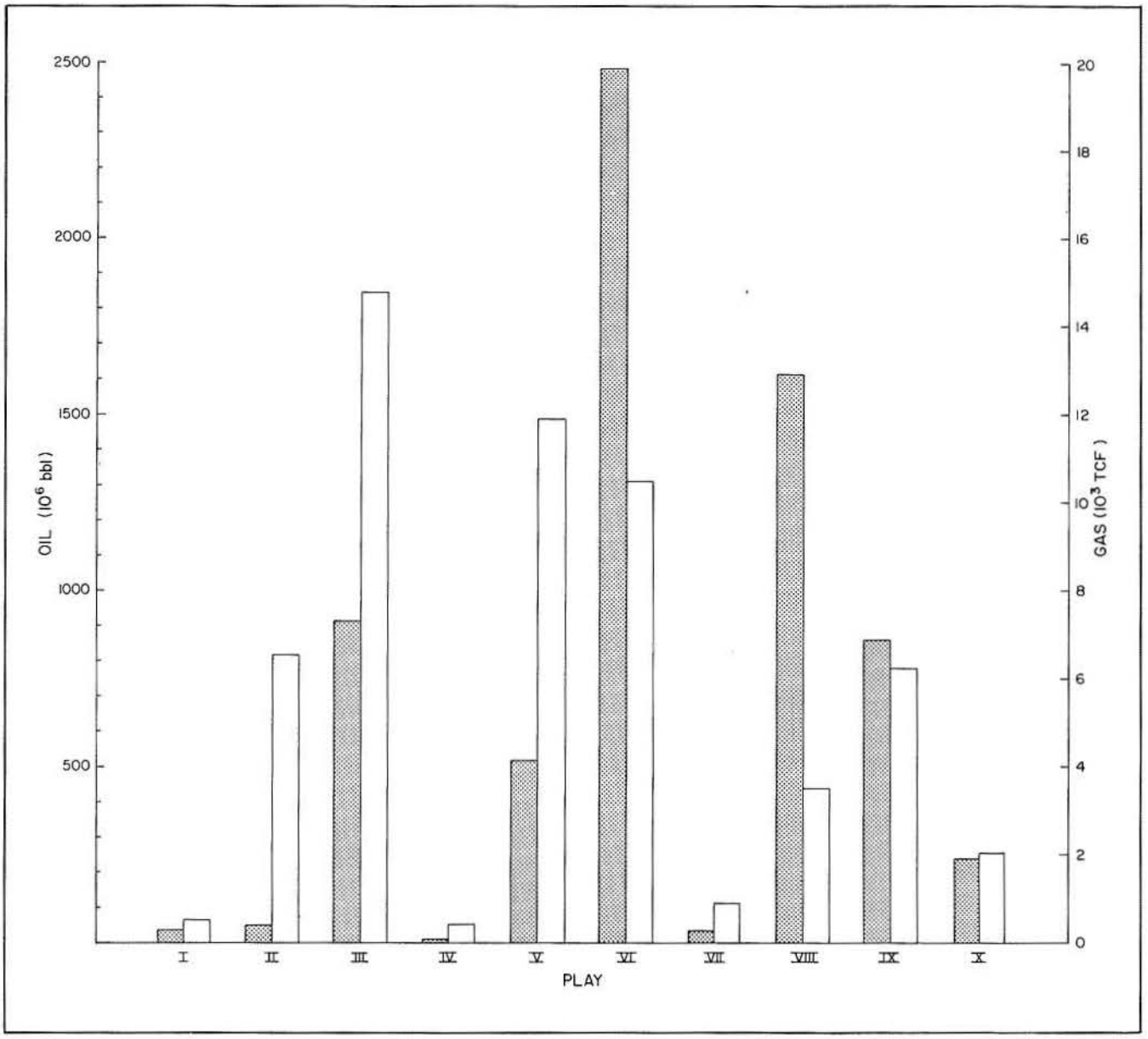

Figure 44. Cumulative production of oil and gas for each of the 10 Frio plays.

upthrown block. The produced hydrocarbons show a well-defined thermal zonation (pl. 9), with gas dominating at greater depth.

Play VI, the most prolific in terms of oil and total hydrocarbon production, is another intensively explored area, with 1.85 wells per mi^2 (tables 4, 5, and 6). It lies updip of the main barrier/strandplain axis and, like play V, shows favorable alternation of source and reservoir rocks. However, the source mudstones of shelf and lagoonal origin have a low organic carbon content (table 5), and only one-third of the total mudstone volume is thermally mature.

Reservoir sandstones are highly porous, averaging 30 percent. The main producing facies are mixed progradational-aggradational units and stacked, blocky sandstone units of barrier and strandplain origin, along with thick successions of irregularly alternating sandstone and shale, which probably represent back-barrier deposits. Many of the thickest continuous sandstones are unproductive because they lack adequate

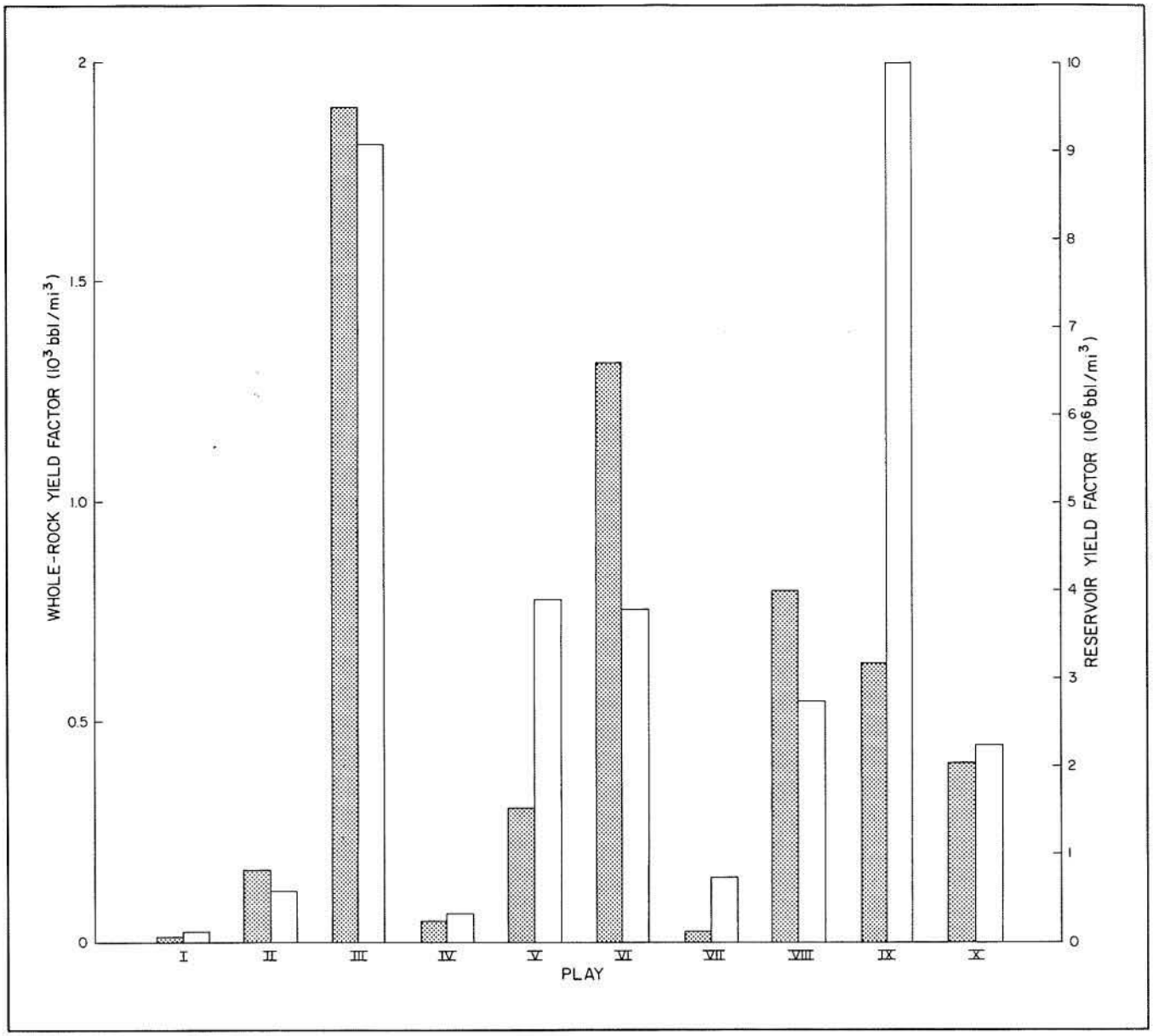

Figure 45. Total hydrocarbon yield factors calculated on the basis of volume of total rock and total sandstone (reservoir rock) contained within each of the 10 Frio plays. Yield factor referenced to reservoir volume provides the best index of play productivity for volumetric calculation of undiscovered hydrocarbon potential.

seals. Growth faults and shale diapirs are well developed. Simple and faulted anticlines are the dominant traps, with some stratigraphic and combination traps.

Play VII constitutes a large but relatively unimportant hydrocarbon-producing area extending across the Choke Canyon/Flatonia coastal lake/streamplain and Chita/Corrigan fluvial systems and incorporating the updip limits of the Greta/Carancahua and Buna barrier and strandplain systems (tables 4, 5, and 6). Floodplain mudstone contains higher-than-average organic carbon, but none is thermally mature. Low-amplitude faults and anticlines inherited from the underlying Wilcox Group are the principal traps. The area has been drilled to a density of 1.12 wells per mi^2, primarily as a result of exploration for deeper targets.

Play VIII extends from the downdip edge of the Chita/Corrigan fluvial system through the Houston delta system. It is distinguished by having as many as 58 salt diapirs (table 5), many of which are large and have profoundly influenced structure, sedimentation, and hydro-

carbon production patterns. It is an oil-prone area that has produced a large volume of hydrocarbons (table 6). A substantial proportion of sandstone has high porosity (table 5). Approximately 60 percent of the prodelta, shelf, and upper slope mudstones are thermally mature, but they have a low organic carbon content. Dominant structures are salt diapirs and associated fault patterns, large salt-withdrawal basins, and growth faults.

Hydrocarbons are present in faulted anticlines adjacent to salt diapirs and in fault traps sealed against the upthrown block. Reservoir facies range from basinward, mudstone-dominated successions with upward-coarsening or randomly interbedded sandstones in the lower and middle Frio to reworked delta-front and channel-fill deposits in the middle and upper Frio.

Play IX differs from play VIII in having fewer large salt diapirs and salt-withdrawal basins. It consists of a part of the Houston delta system together with equivalent shelf and slope facies. The proportion of sandstone is exceptionally low, amounting to only 6 percent (table 5), but what occurs has good porosity. About 87 percent of the shales and mudstones are thermally mature, but again are characterized by low levels of organic carbon.

Reservoir facies include mudstone-rich progradational sequences and slope channel fills in the lower Frio, with fluvial channel-fill and reworked delta-front sandstones in the middle and upper Frio. Traps include faulted anticlines above deep salt ridges, simple anticlines, and growth faults. Play IX is the most intensively drilled of any play, averaging 2.2 wells per mi^2.

Play X is a gas-prone area of limited production (table 6). Sandstone reservoirs, which constitute 18 percent of the total volume, have exceptionally high porosity (table 5). Forty-four percent of the shelf and upper slope mudstone volume is thermally mature. Repetitive interfingering of source and reservoir rocks provides an ideal avenue for hydrocarbon migration and collection. Both growth faults and salt diapirs influenced patterns of sedimentation and hydrocarbon trapping.

Reservoir facies are extremely diverse and include turbidite sandstones in the middle Frio (Hackberry facies), the seaward margins of the Buna strandplain/barrier system, and updip channel complexes. Hydrocarbon traps range from salt domes to simple rollover anticlines and faulted anticlines. Stratigraphic traps are present in the Hackberry wedge, where deep-water sandstones pinch out updip against a scoured basal unconformity. The area has an average of 0.9 wells per mi^2 (table 5).

EVALUATIONS OF REMAINING RESOURCE POTENTIAL

To evaluate the ultimate hydrocarbon potentials of the discovered and the undiscovered reservoirs, three different approaches may be applied: (1) historical, (2) volumetric, and (3) source and migration potential.

HISTORICAL APPROACH

Three graphical methods were applied: (1) Amounts of discovered oil and gas per number of exploratory wells drilled each year were plotted against the cumulative number of the exploratory wells. (2) Amounts of discovered oil and gas per footage drilled by exploratory wells each year were plotted against the cumulative footage of exploratory wells (Zapp, 1961 and 1962). (3) Amounts of oil and gas discovered each year were plotted against time (Hubbert, 1967).

Each of these methods has both advantages and disadvantages. One advantage of the first method is that it defines the limit of the number of exploratory wells to be drilled in an area. For example, one well per square mile or per half square mile may be considered the ultimate limit of exploratory drilling. On the basis of such a limit of well density, it is possible to estimate the ultimate number of exploratory wells to be drilled in an area. However, a disadvantage of this method is that changing economic conditions are not considered.

The second method, which plots discovery rate against cumulative footage, is advantageous both in limiting drilling density and in considering possible economic limits. However, because of improving technology and changing prices of oil and gas, historical economic limits may not apply in the future. In a relatively mature basin (in the sense of exploration activities), it is natural to expect that the discovery rate based on the footage drilled declines continuously as the average drill depth increases. Therefore, a prediction based on cumulative footage would provide a pessimistic view of future oil and gas discoveries. However, relatively deep drilling may still be economically feasible given increasing prices of oil and gas.

The third method, analyzing discovery volumes versus time, is probably the least reliable of the three, but also requires the least information. Therefore, a prediction can be made on the basis of the existing data spanning a longer time. Political, economic, and technologic factors, which would have influenced the fluctuations of the oil and gas discoveries in the past, are ignored in this method. Using the method, developed by Hubbert (1967), it is also essential to determine the time when peak discovery was attained; however, because of the large variations in oil and gas discovery each year, it is usually difficult to find this peak.

Historical data for the total hydrocarbon discovery and numbers and footages of exploratory wells have been reported by the American Petroleum Institute and the American Association of Petroleum Geologists for each Railroad Commission of Texas district. No such statistical data base exists specifically for the Frio MSU; thus, future

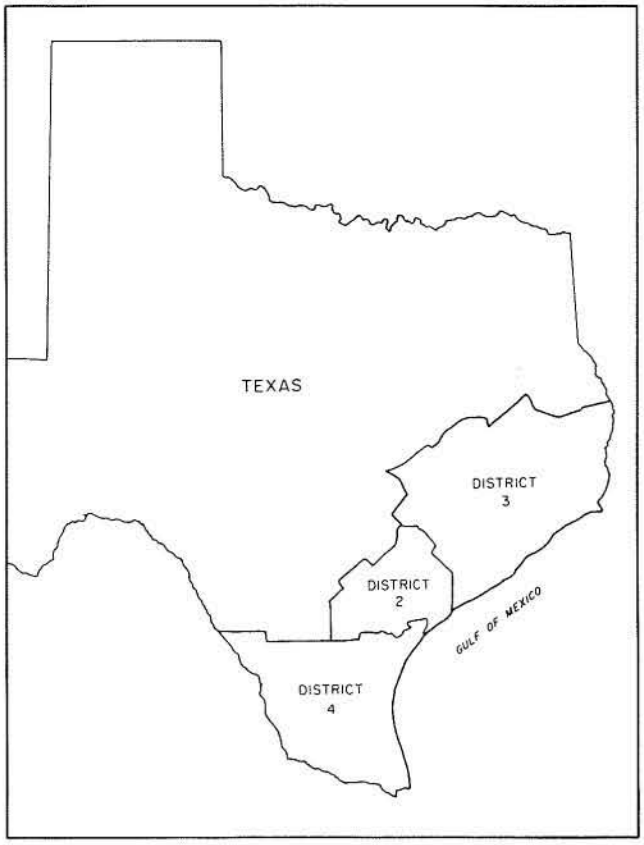

Figure 46. Location and boundaries of Railroad Commission of Texas (RRC) Districts 2, 3, and 4.

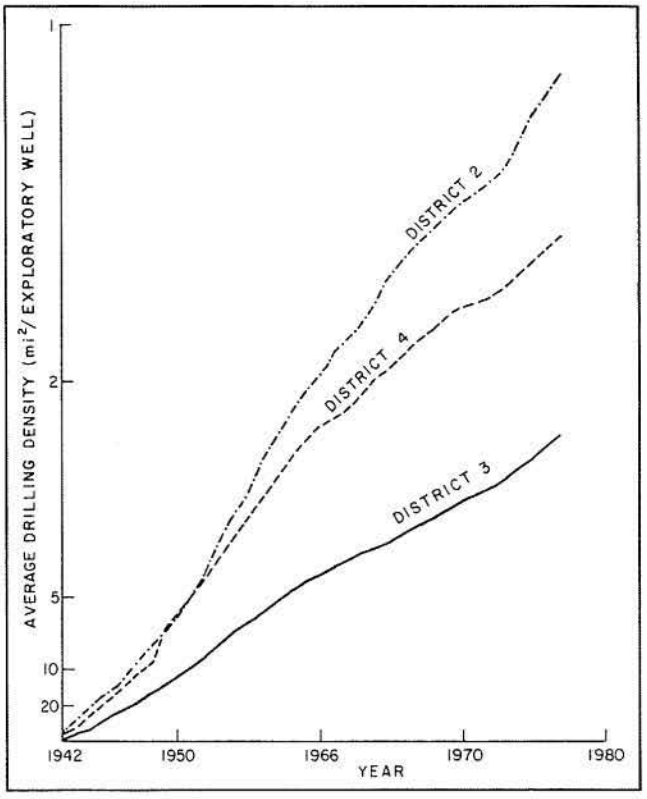

Figure 47. Historical changes of drill density (mi^2 per exploratory well) for RRC Districts 2, 3, and 4. Data were derived from bulletins of the American Association of Petroleum Geologists giving annual summaries of developments in North America for the years 1942 to 1977.

discoveries for the Frio can only be estimated from the general district data by assuming that undiscovered petroleum occurs in the same proportion as known reserves and by modifying the total discovery predicted for Railroad Commission Districts 2, 3, and 4 (fig. 46) accordingly.

Cumulative Number of Exploratory Wells

Change from 1942 to 1977 in the average drilling density (expressed in square miles per exploratory well) for each district is shown in figure 47. District 2 (Middle Texas Gulf Coast) had a drilling density of nearly 1 mi^2 (2.6 km^2) per exploratory well as of 1977, whereas District 3 (Upper Texas Gulf Coast) had a level of only approximately 3 mi^2 (7.7 km^2) per exploratory well. This suggests that District 3 retains more room for future exploration than District 2. Drilling density of District 4 (Lower Texas Gulf Coast) is intermediate.

Figure 48 is a plot of oil discovery (in 1,000 bbl or 160 m^3 per exploratory well) versus cumulative number of wells from 1942 to 1977 in District 2. The amount of the recoverable oil discovered before 1942 is about 1,884 million bbl (300 million m^3) (American Petroleum Institute, 1978), but there are no drilling statistics available for this period. The cumulative discovery of oil from 1942 to 1977 is about 662 million bbl (105 million m^3). The average discovery rate for each 1,000 wells declined from about 192,000 bbl (30,500 m^3) per well from approximately 1942 to 1946 to only about 4,300 bbl (680 m^3) per well from 1974 to 1977 (table 7). Using this final discovery rate, it is estimated that only about 50 million bbl (7.9 million m^3) remain to be discovered before a drilling density of 0.5 mi^2 (1.3 km^2) per exploratory well is reached (table 7). Although this drilling density sounds very high, much of the earlier drilling explored the shallow intervals only.

Similar plots for Districts 3 and 4 are shown in figures 49 and 50, respectively; the statistical summary for oil is shown in table 7, which suggests that significant amounts of oil remain to be discovered in these districts.

Plots for gas discoveries (figs. 51, 52, and 53) show that Districts 2 and 4 suffered significant declines in gas discovery rates, whereas the District 3 gas discovery rate improved even beyond a total of 10,000 exploratory wells. District 3 is the least drilled among the three (fig. 47); therefore, it has the highest potential for future gas discoveries. Statistics of past and future gas discoveries are summarized in table 8.

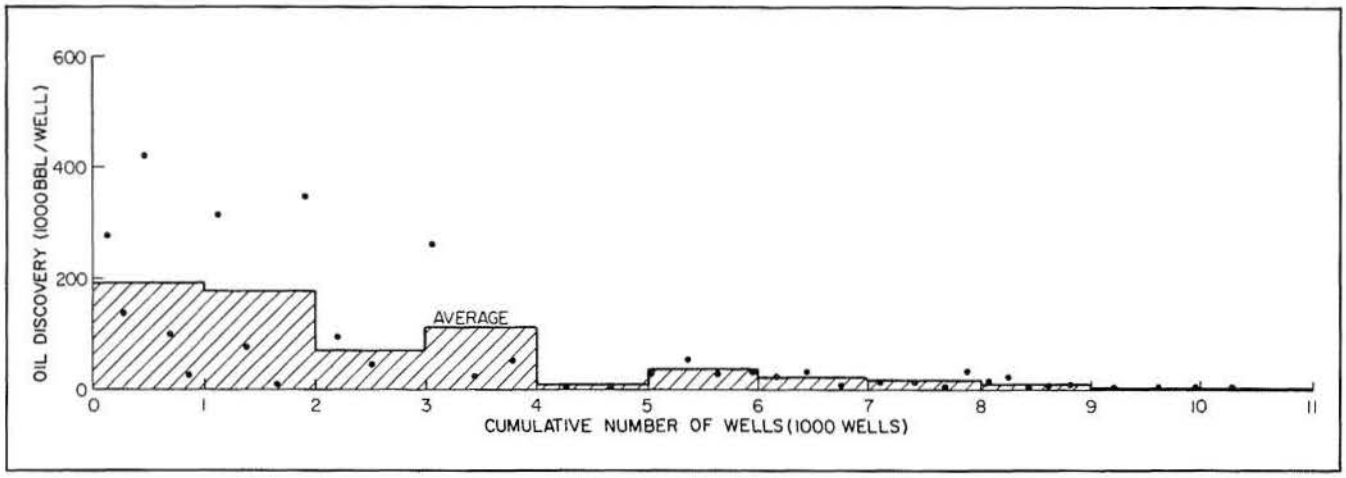

Figure 48. Plot of recoverable oil discovery (1,000 bbl or 160 m^3 per exploratory well) versus cumulative number of wells drilled from 1942 to 1977 in RRC District 2. Data derived from American Petroleum Institute (1978) and bulletins of the American Association of Petroleum Geologists (1942-1977).

Table 7. Statistical summary of recoverable oil, million bbl (cumulative-well-number method).

Location		Oil discovery before 1942	Oil discovery 1942-1977	Total oil discovery by 1977	Oil to be discovered up to a drill density of 0.5 mi^2/well	Total recoverable
Dist. 2 (11,000 mi^2)	All formations	1,884	662	2,546	50	2,596
	Frio (% of above)			2,080 (81.7)	41 (81.7)	2,121 (81.7)
Dist. 3 (30,000 mi^2)	All formations	6,663	907	7,570	410	7,980
	Frio (% of above)			3,890 (51.4)	211 (51.4)	4,101 (51.4)
Dist. 4 (21,000 mi^2)	All formations	2,078	979	3,057	169	3,226
	Frio (% of above)			1,890 (61.8)	104 (61.8)	1,994 (61.8)
Dist. 2, 3, 4 Total	All formations	10,625	2,548	13,173	629	13,802
	Frio (% of above)			7,860 (59.7)	356 (56.6)	8,216 (59.5)

To demonstrate the depth ranges of oil and gas accumulations and the significance of numbers of wells drilled in each district, figure 54 was constructed using the Petroleum Information Corp. well data file. Plot A shows the number of wells (both exploratory and developmental) drilled into each successive 2,000-ft (600-m) depth increment. The central plots (B and C) show the numbers of gas and oil tests, respectively, in each depth slice. Below 12,000 ft (3,600 m), the total number of gas and oil tests declines significantly because the number of wells drilled through the deepest intervals is also reduced. To normalize the effect of the decreasing number of wells in the deeper sections, the percentages of gas and oil tests per number of wells drilled, expressed as

$$\frac{B \times 100}{A} \text{ and } \frac{C \times 100}{A}, \text{ respectively,}$$

were calculated. In all the districts, the depth limit for oil accumulation seems to be about 12,000 ft (3,600 m). There appears to be a bimodal distribution of gas occurrence in Districts 2 and 3. The upper distribution ranges from about 2,000 to 16,000 ft (600 to 4,800 m). Most of this gas may be related to the generation and subsequent thermal destruction of oil. Below about 16,000 to 18,000 ft (4,800 to 5,400 m) in Districts 2 and 3, another gas discovery peak appears in each of the normalized plots. This may reflect a pulse of direct generation of gas from gas-prone Type III kerogen (Tissot, 1978), which requires higher temperatures for maturation. Fortunately, in Districts 2 and 3, the reservoir porosity and permeability seem high enough to sustain commercial gas production even at great depth, leading us to believe that more gas reservoirs will be discovered in the future.

District 4, in contrast, displays a single distribution pattern for gas. This is probably because of the combination of higher geothermal gradient, dominance of gas-prone source rocks, and poorer reservoir quality.

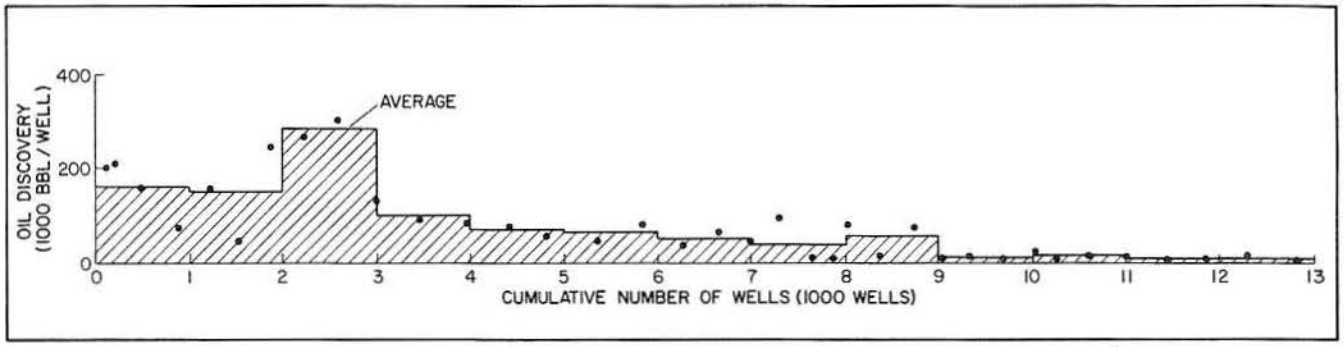

Figure 49. Plot of recoverable oil discovery (1,000 bbl or 160 m^3 per exploratory well) versus cumulative number of wells drilled from 1942 to 1977 in RRC District 3. Data derived from American Petroleum Institute (1978) and bulletins of the American Association of Petroleum Geologists (1942-1977).

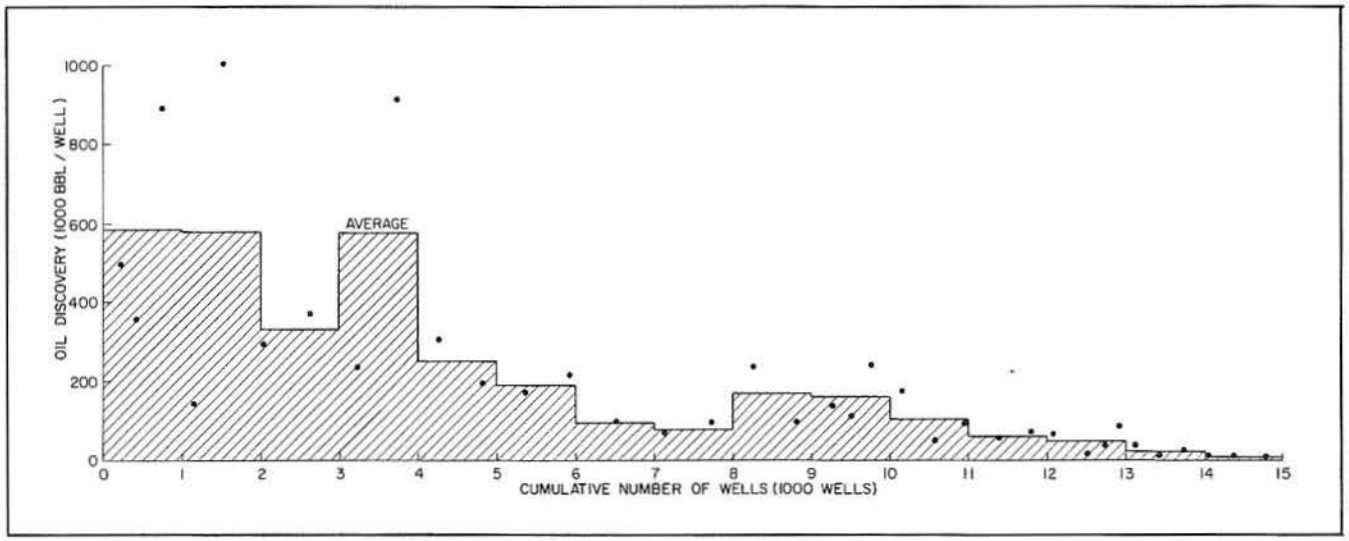

Figure 50. Plot of recoverable oil discovery (1,000 bbl or 160 m^3 per exploratory well) versus cumulative number of wells drilled from 1942 to 1977 in RRC District 4. Data derived from American Petroleum Institute (1978) and bulletins of the American Association of Petroleum Geologists (1942-1977).

A cross plot of the number of production tests (oil and gas) against the number of wells for each county within the three districts (fig. 55) shows that although points are scattered, more wells mean more production tests and more discoveries. Significantly, the proportion of production tests shows little evidence of decline, even in the most densely drilled counties.

Figures 56, 57, and 58 show the areal distribution of the total numbers of wells and of oil and gas production tests in the study area.

Cumulative Footage of Exploratory Drilling

A method of predicting future discoveries of oil and gas based on the historical change of the discovery rate per drilled footage was proposed by Zapp (1961 and 1962). As mentioned above, this method has an advantage over previous methods because the economic factors related to the footage of exploratory drilling can be incorporated in the prediction. This is important when one considers that the average depth of the exploratory wells drilled between 1942 and 1977 was only 6,530 ft (1,960 m) (table 9), whereas future discoveries must be made in much deeper sections.

Plots of oil discovery rates (barrel per foot of exploratory drilling) versus cumulative footage for Districts 2, 3, and 4 (figs. 59, 60, and 61) show drastic declines in the discovery rate for each district. Future oil discoveries at a cumulative drilling footage of 15,000 ft per mi^2 (1,760 m per km^2) have been estimated and are shown in table 10.

Similar plots of gas discovery rates, shown as 1,000 ft^3 per ft (90 m^3 per m) of drilling, are shown in figures 62, 63, and 64 (Districts 2, 3, and 4). The discovery rates for Districts 2 and 4 (figs. 62 and 64) have continuously

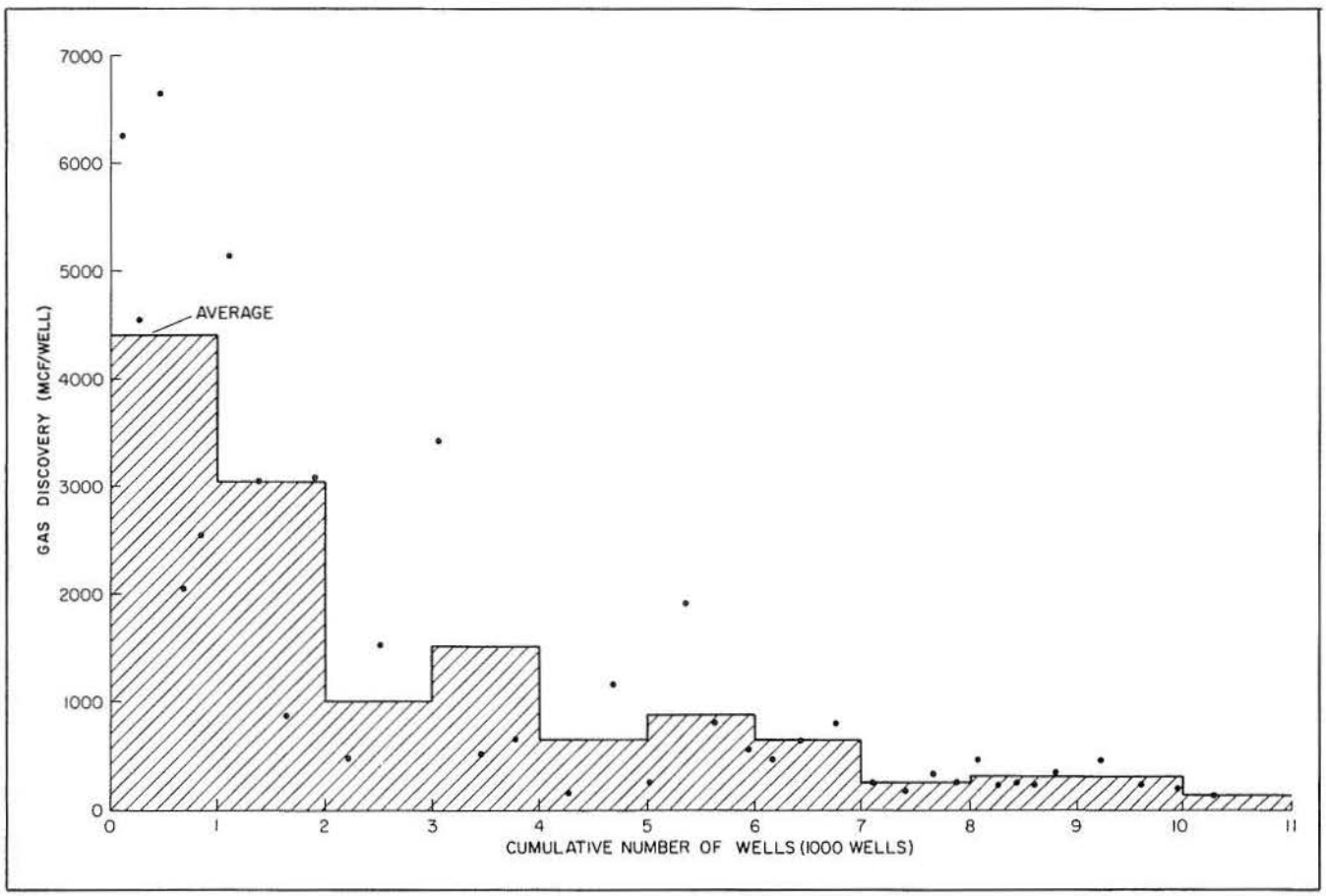

Figure 51. Plot of recoverable gas discovery (Mcf per exploratory well) versus cumulative number of wells drilled from 1942 to 1977 in RRC District 2. Data derived from American Petroleum Institute (1978) and bulletins of the American Association of Petroleum Geologists (1942-1977).

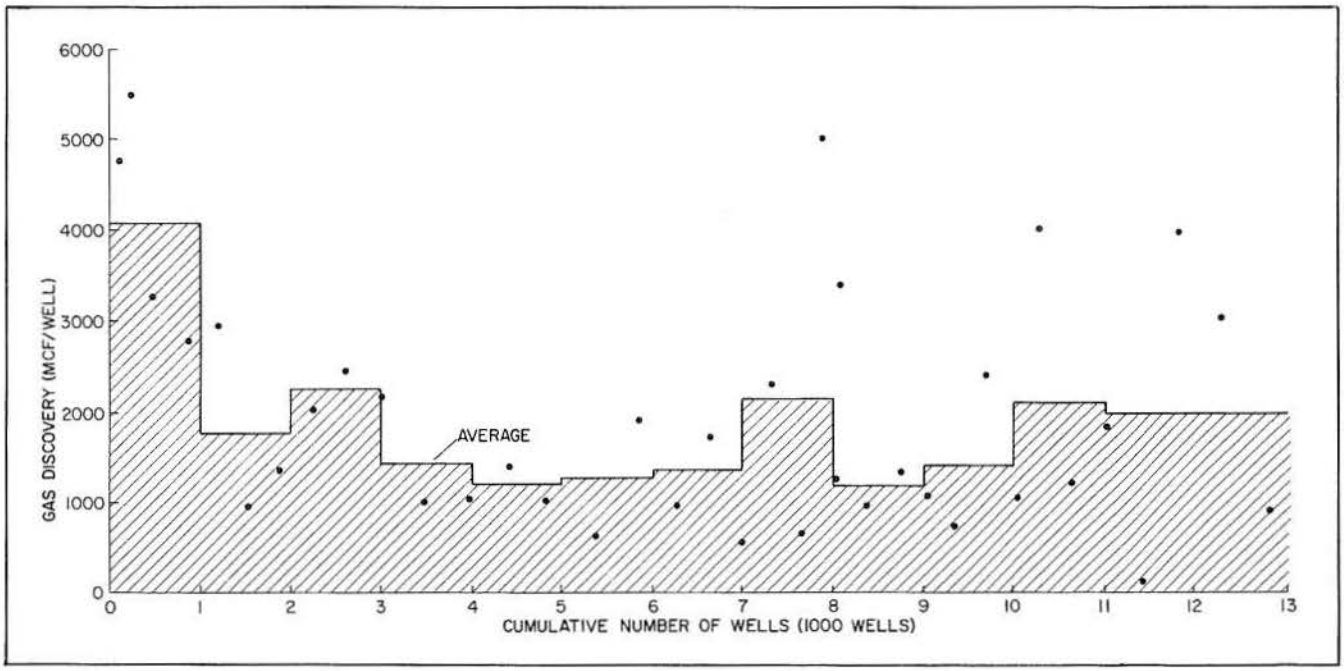

Figure 52. Plot of recoverable gas discovery (Mcf per exploratory well) versus cumulative number of wells drilled from 1942 to 1977 in RRC District 3. Data derived from American Petroleum Institute (1978) and bulletins of the American Association of Petroleum Geologists (1942-1977).

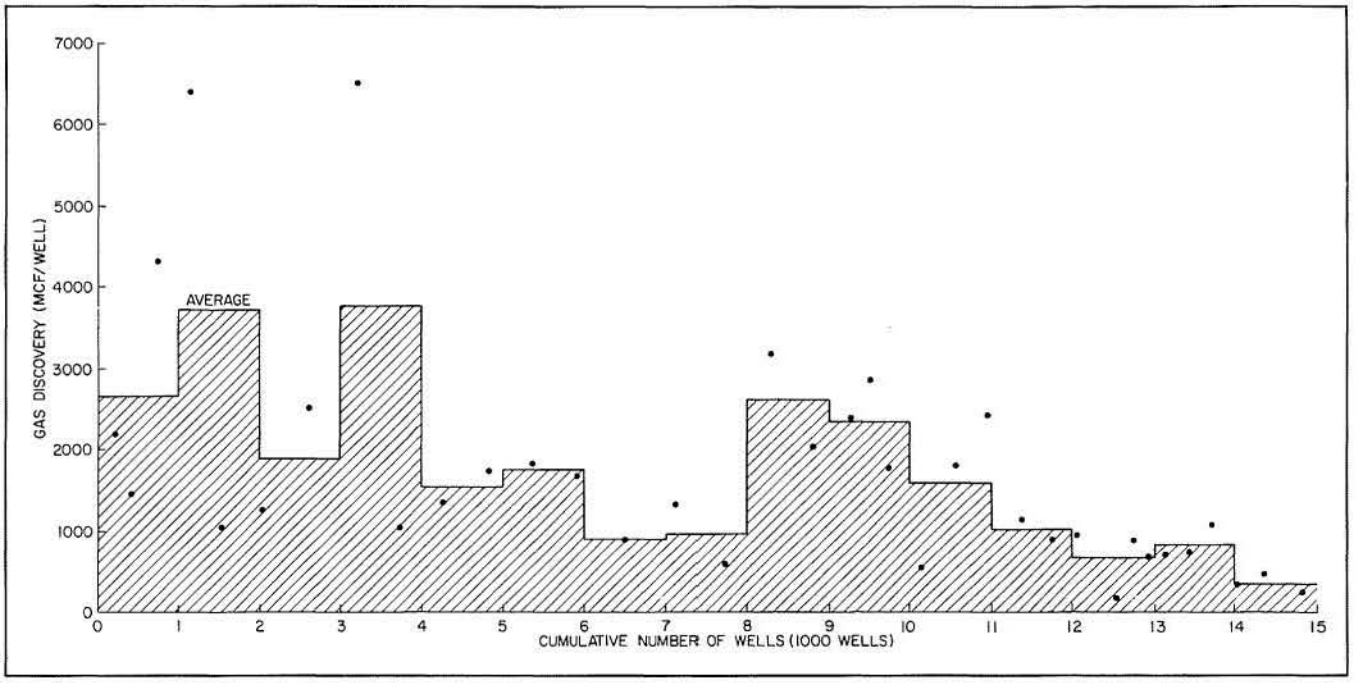

Figure 53. Plot of recoverable gas discovery (Mcf per exploratory well) versus cumulative number of wells drilled from 1942 to 1977 in RRC District 4. Data derived from American Petroleum Institute (1978) and bulletins of the American Association of Petroleum Geologists (1942-1977).

Table 8. Statistical summary of recoverable gas, bcf (cumulative-well-number method).

Location		Gas discovery before 1942	Gas discovery 1942-1977	Total gas discovery by 1977	Gas to be discovered up to a drill density of 0.5 mi^2/well	Total recoverable
Dist. 2 ($11,000\ mi^2$)	All formations	12,206	12,857	25,063	3,159	28,222
	Frio (% of above)			8,070 (32.2)	1,107 (32.2)	9,087 (32.2)
Dist. 3 ($30,000\ mi^2$)	All formations	30,564	22,640	53,204	93,750	146,954
	Frio (% of above)			25,000 (47.0)	44,063 (47.0)	69,063 (47.0)
Dist. 4 ($21,000\ mi^2$)	All formations	22,839	26,543	49,382	9,051	58,433
	Frio (% of above)			32,400 (65.6)	5,937 (65.6)	38,337 (65.6)
Dist. 2, 3, 4 Total	All formations	65,609	62,040	127,649	105,960	233,609
	Frio (% of above)			65,470 (51.3)	51,017 (48.2)	116,487 (49.9)
	Frio liquid equivalent			10,912 million bbl	8,502 million bbl	19,415 million bbl

declined, while the one for District 3 (fig. 63) has recently improved. Using the final average discovery rate, the future gas discoveries up to the drilling of 15,000 ft per mi^2 (1,760 m per km^2) were estimated and are shown in table 11. Volume of the future Frio discoveries was also estimated on the basis of the known ratio of Frio gas reserves to total gas reserves for each district.

Discovery Versus Time

This method was described in detail by Hubbert (1967), who proposed a simultaneous analysis of the time variation of the following three curves: cumulative production (Q_p), proved reserves (Q_r), and cumulative proved discoveries (Q_d), defined as the sum of cumulative production and proved reserves. The discovery curve

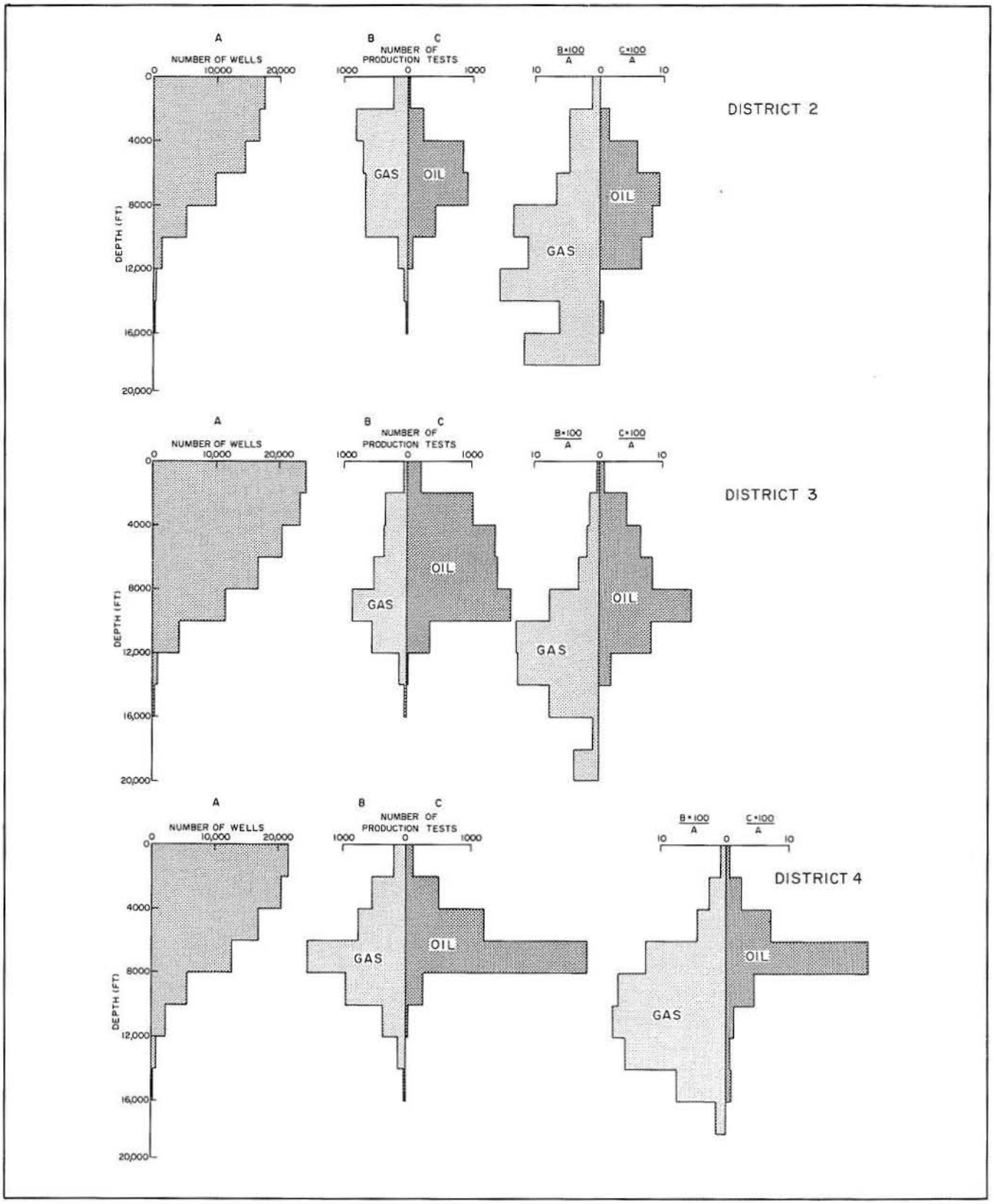

Figure 54. Depth distribution of number of (A) all exploratory and developmental wells drilled, (B and C) numbers of gas and oil tests, and (B x 100/A and C x 100/A) number of gas and oil tests normalized for number of wells drilled. Data are grouped in 2,000-ft increments. Based on Petroleum Information Corp. well data file. Refer to text for explanation.

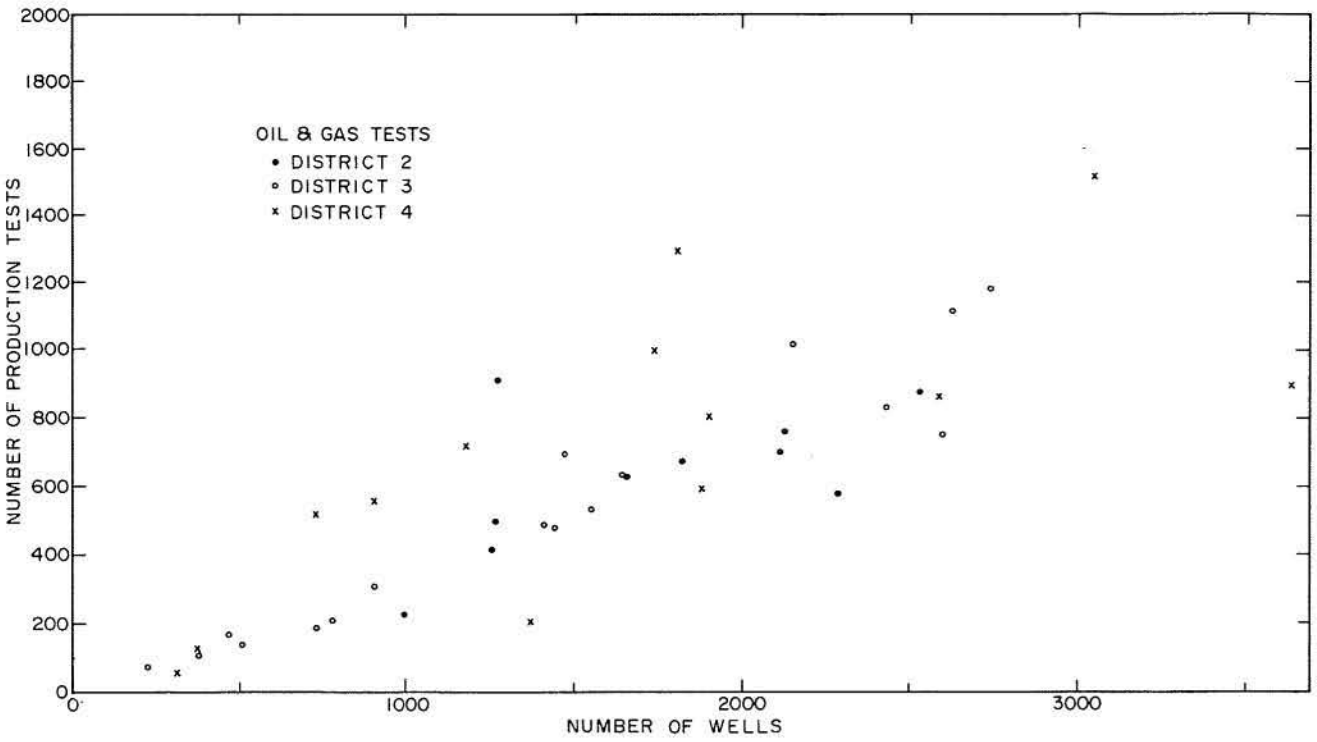

Figure 55. Number of hydrocarbon production tests versus number of wells (both exploratory and developmental) for each county in RRC Districts 2, 3, and 4. Data from Petroleum Information Corp. well data file.

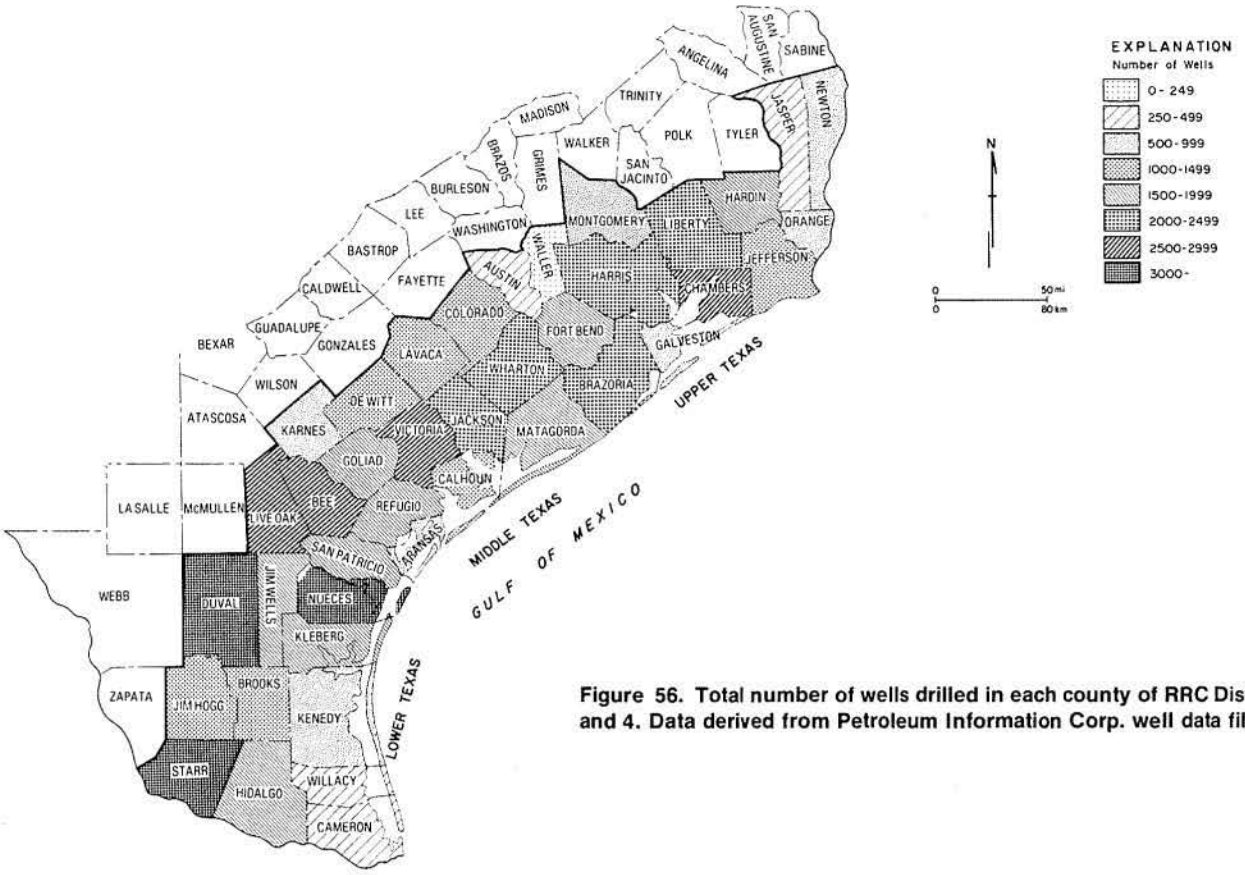

Figure 56. Total number of wells drilled in each county of RRC Districts 2, 3, and 4. Data derived from Petroleum Information Corp. well data file.

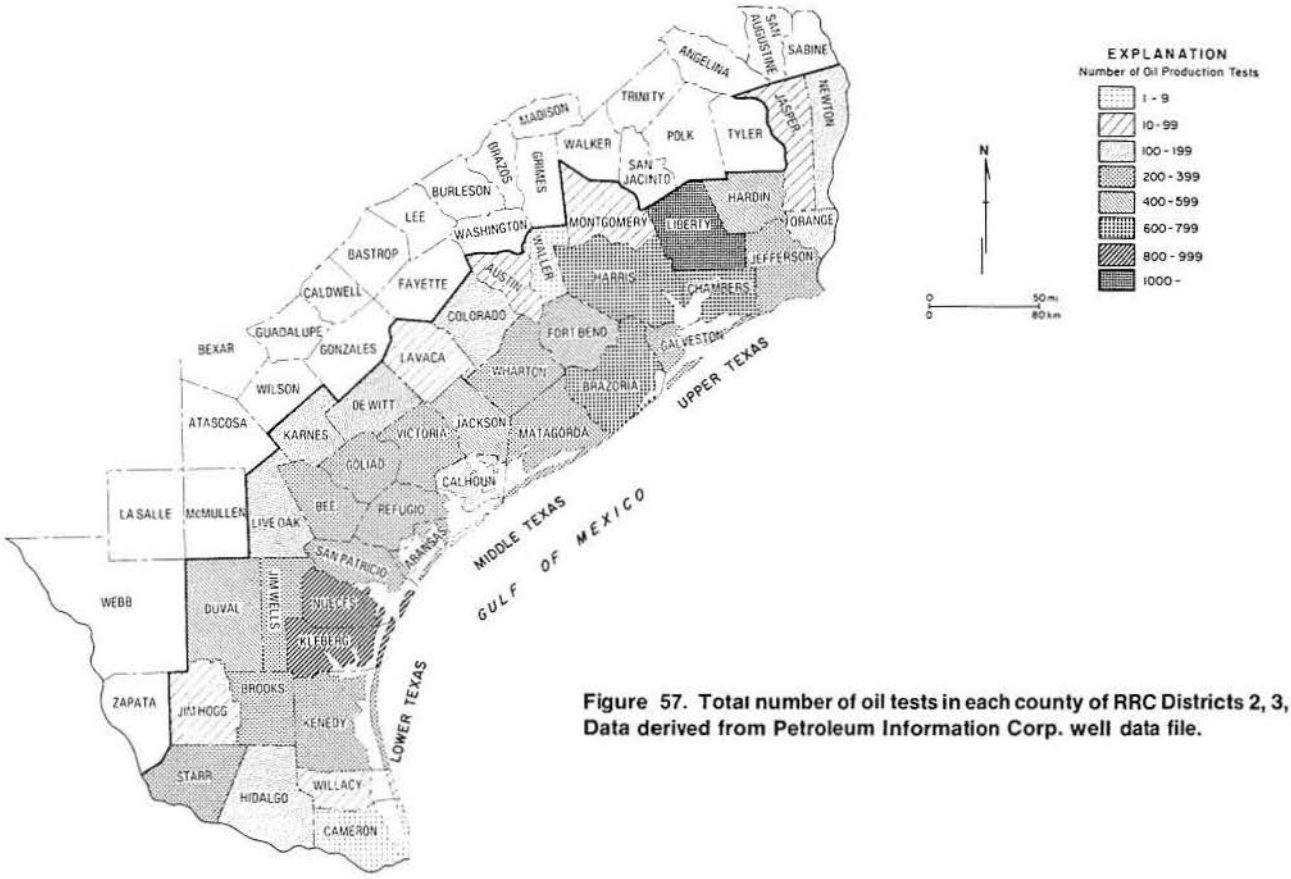

Figure 57. Total number of oil tests in each county of RRC Districts 2, 3, and 4. Data derived from Petroleum Information Corp. well data file.

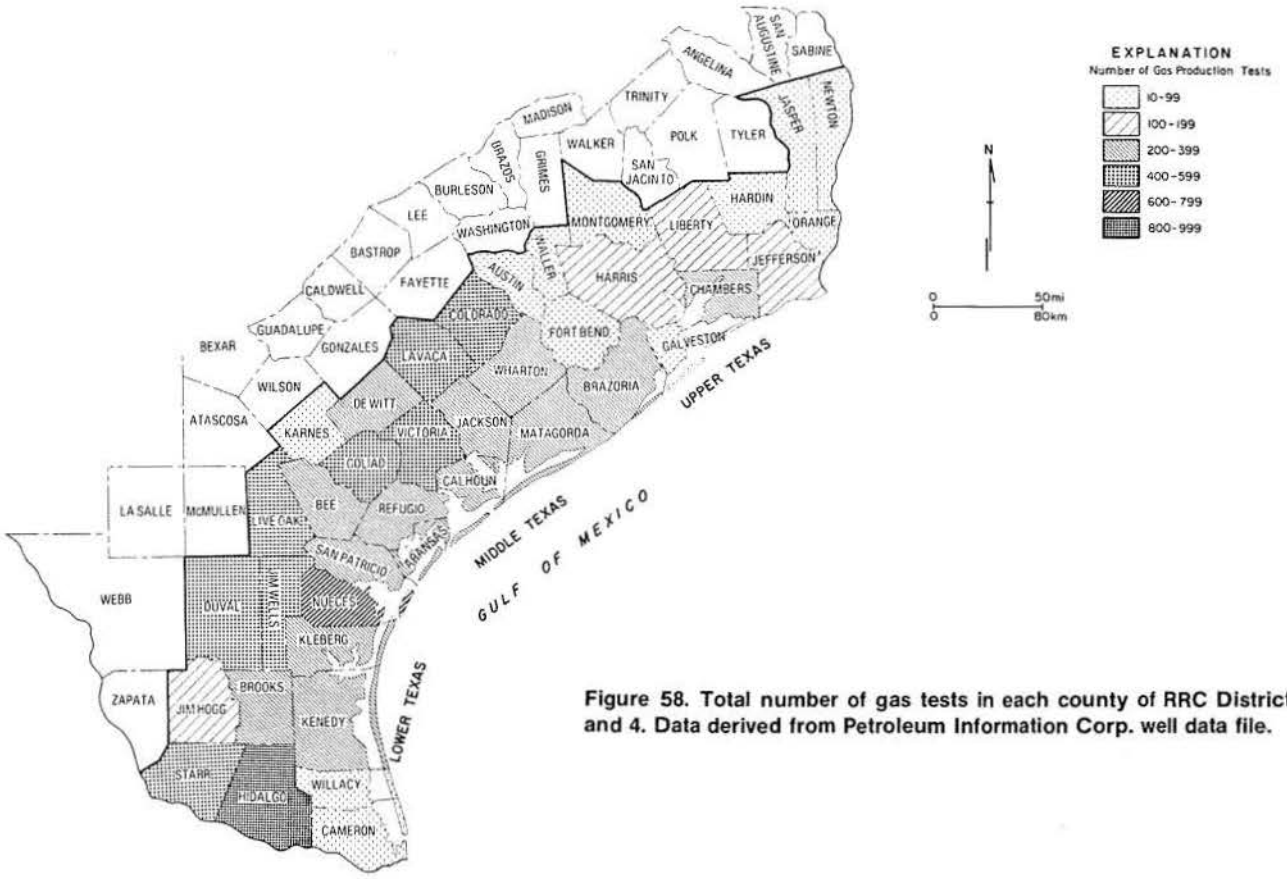

Figure 58. Total number of gas tests in each county of RRC Districts 2, 3, and 4. Data derived from Petroleum Information Corp. well data file.

Table 9. Statistical summary of total number, footage, and average depth of exploratory wells, 1942-1977.

	Number	Footage, 1,000 ft	Average depth, ft
Dist. 2	10,299	62,739	6,090
Dist. 3	12,842	100,229	7,810
Dist. 4	14,819	84,845	5,730
Dist. 2, 3, 4 Total	37,960	247,913	6,530

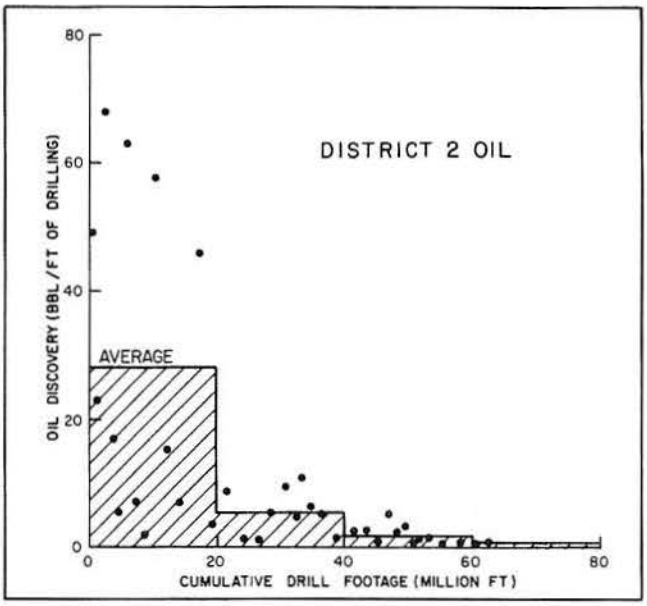

Figure 59. Plot of recoverable oil discovery rate (bbl per ft of exploratory drilling) versus cumulative footage for RRC District 2. Data derived from American Petroleum Institute (1978) and bulletins of the American Association of Petroleum Geologists (1942-1977).

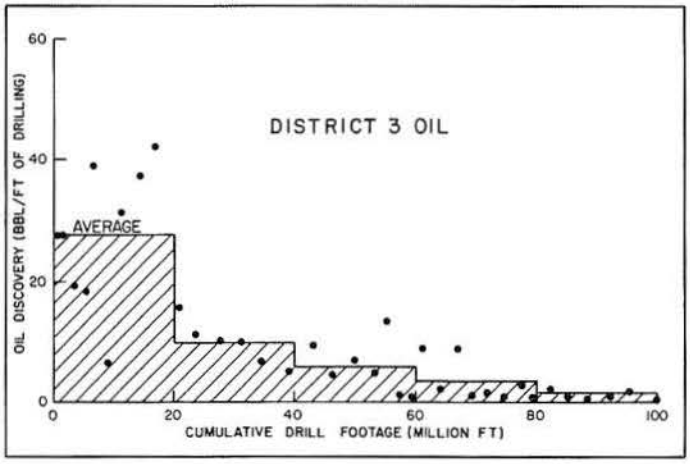

Figure 60. Plot of recoverable oil discovery rate (bbl per ft of exploratory drilling) versus cumulative footage for RRC District 3. Data derived from American Petroleum Institute (1978) and bulletins of the American Association of Petroleum Geologists (1942-1977).

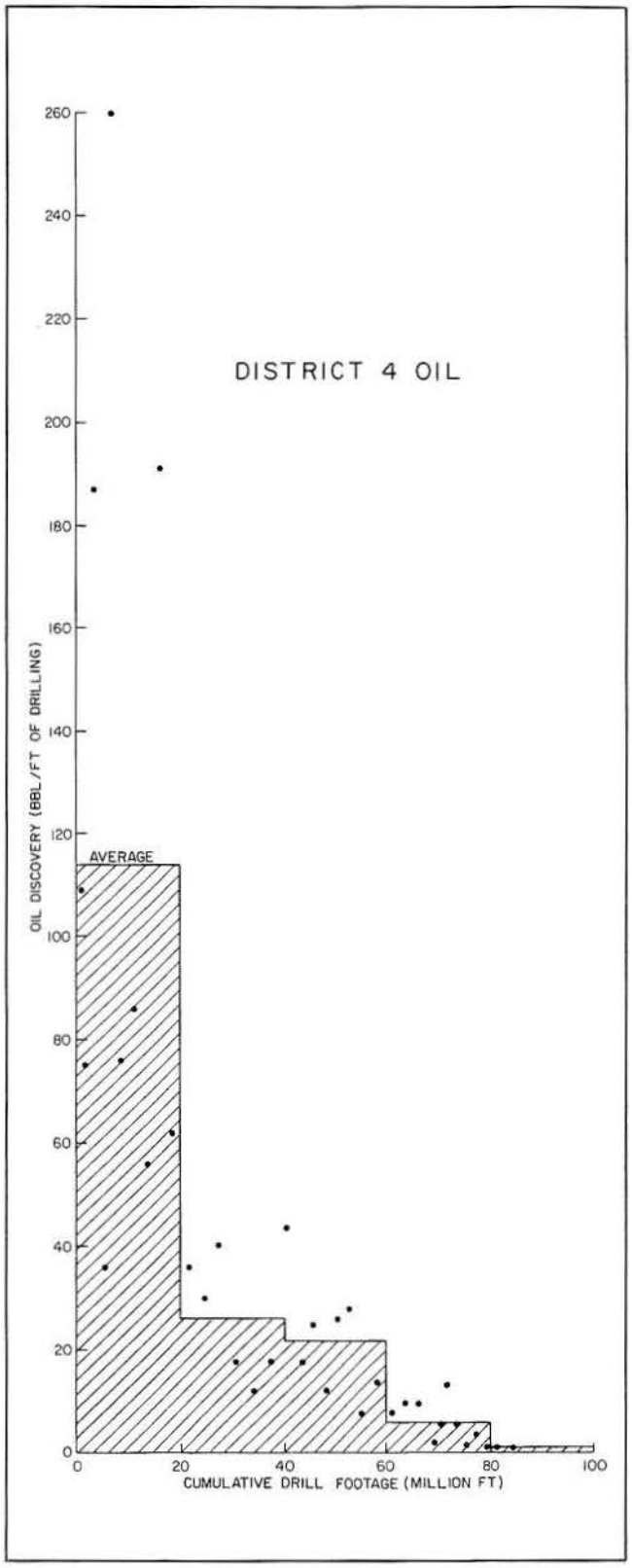

Figure 61. Plot of recoverable oil discovery rate (bbl per ft of exploratory drilling) versus cumulative footage for RRC District 4. Data derived from American Petroleum Institute (1978) and bulletins of the American Association of Petroleum Geologists (1942-1977).

Table 10. Statistical summary of recoverable oil, million bbl (cumulative-footage method).

Location		Oil discovery before 1942	Oil discovery 1942-1977	Total oil discovery by 1977	Oil to be discovered up to exploratory footage of 15,000 ft/mi^2	Total recoverable
Dist. 2 (11,000 mi^2)	All formations	1,884	662	2,546	83	2,629
	Frio (% of above)			2,080 (81.7)	68 (81.7)	2,148 (81.7)
Dist. 3 (30,000 mi^2)	All formations	6,663	907	7,570	553	8,123
	Frio (% of above)			3,890 (51.4)	284 (51.4)	4,174 (51.4)
Dist. 4 (21,000 mi^2)	All formations	2,078	979	3,057	265	3,322
	Frio (% of above)			1,890 (61.8)	164 (61.8)	2,054 (61.8)
Dist. 2, 3, 4 Total	All formations	10,625	2,548	13,173	901	14,074
	Frio (% of above)			7,860 (59.7)	516 (57.3)	8,376 (59.5)

Table 11. Statistical summary of recoverable gas, bcf (cumulative-footage method).

Location		Gas discovery before 1942	Gas discovery 1942-1977	Total gas discovery by 1977	Gas to be discovered up to exploratory footage of 15,000 ft/mi^2	Total recoverable
Dist. 2 (11,000 mi^2)	All formations	12,206	12,857	25,063	4,618	29,681
	Frio (% of above)			8,070 (32.2)	1,487 (32.2)	9,557 (32.2)
Dist. 3 (30,000 mi^2)	All formations	30,564	22,640	53,204	103,927	157,131
	Frio (% of above)			25,000 (47.0)	48,846 (47.0)	73,846 (47.0)
Dist. 4 (21,000 mi^2)	All formations	22,839	26,543	49,382	15,116	64,498
	Frio (% of above)			32,400 (65.6)	9,916 (65.6)	42,316 (65.6)
Dist. 2, 3, 4 Total	All formations	65,609	62,040	127,649	123,661	251,310
	Frio (% of above)			65,470 (51.3)	60,249 (48.8)	125,719 (50.0)
	Frio liquid equivalent			10,912 million bbl	10,042 million bbl	20,953 million bbl

precedes the production curve in the midrange region by some time interval (Δt as given by Hubbert).

The equation relating the three curves (Hubbert, 1967) is as follows:

$$Q_d = Q_p + Q_r$$

The rates of discovery, of production, and of increase in proved reserves are given as

$$\frac{dQ_d}{dt} = \frac{dQ_p}{dt} + \frac{dQ_r}{dt}$$

when proved reserves are at their maximum

$$\frac{dQ_r}{dt} = 0$$

and hence

$$\frac{dQ_d}{dt} = \frac{dQ_p}{dt}$$

This means that at the time of the peak proved reserves, the curves of discovery and production rates must cross. The production rate is thereafter increasing, whereas the discovery rate is decreasing. An example of these three curves based on U.S. oil statistics is shown in figure 65.

Because of the significant variation of oil discovery with time, it is impossible to draw a smooth curve through a similar plot of the recoverable oil discovery versus production for District 2 (fig. 66). An obvious peak for oil discovery occurs in 1934, and two major production peaks occur in 1948 and 1972. The time that elapsed between the discovery peak and the first production peak is 14 years, which is longer than the 10 to 12 years of the corresponding period for the entire United States (Hubbert, 1967). If it is assumed that the cumulative discovery up to 1934 (the peak discovery) amounts to about 50 percent of the ultimate oil discovery, the latter amount is estimated to be about 3,028 million bbl (480 million m^3) for all the formations in District 2, or about

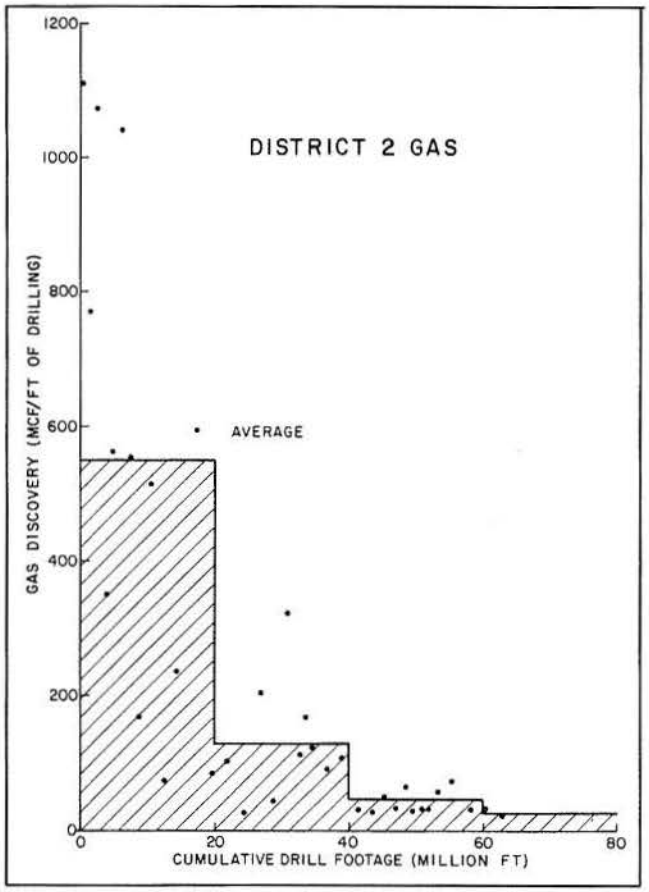

Figure 62. Plot of recoverable gas discovery rate (Mcf per ft or 90 m^3 per m of exploratory drilling) versus cumulative footage for RRC District 2. Data derived from American Petroleum Institute (1978) and bulletins of the American Association of Petroleum Geologists (1942-1977).

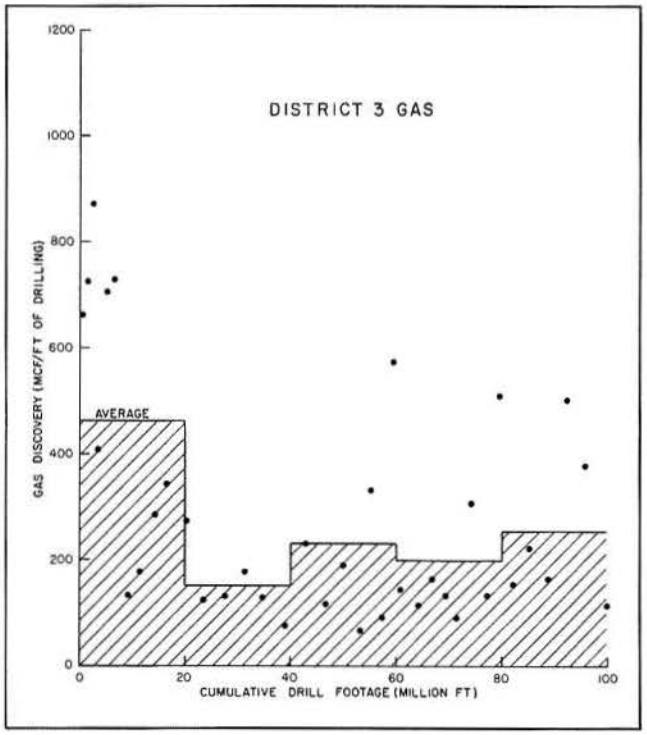

Figure 63. Plot of recoverable gas discovery rate (Mcf per ft or 90 m^3 per m of exploratory drilling) versus cumulative footage for RRC District 3. Data derived from American Petroleum Institute (1978) and bulletins of the American Association of Petroleum Geologists (1942-1977).

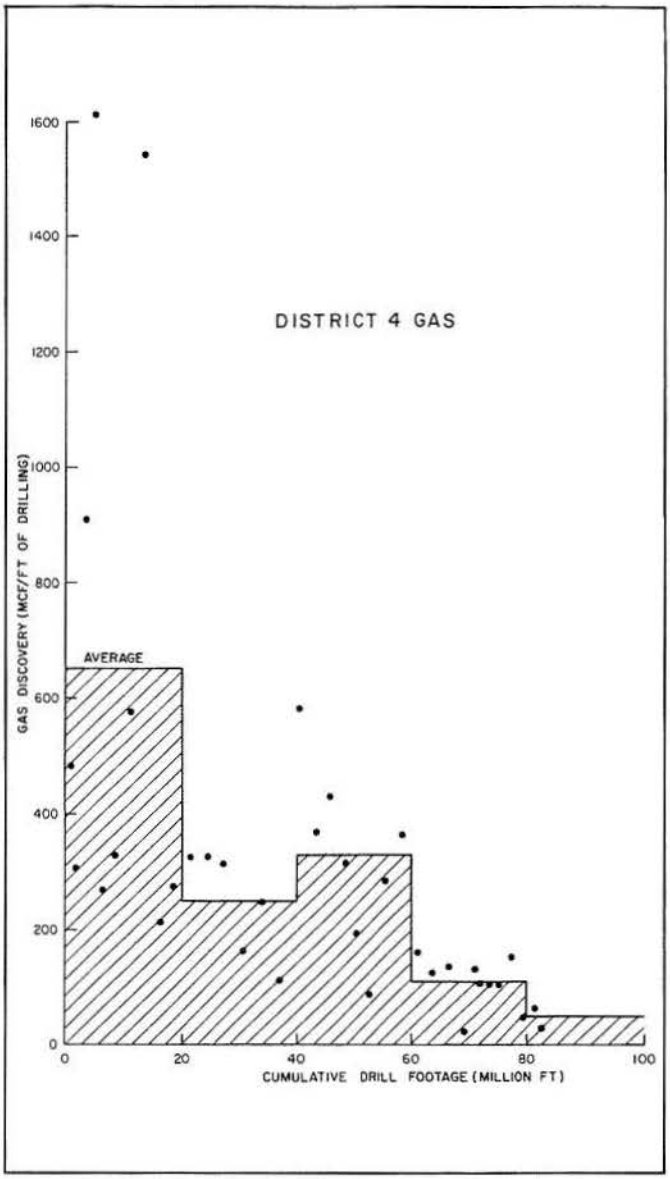

Figure 64. Plot of recoverable gas discovery rate (Mcf per ft or 90 m^3 per m of exploratory drilling) versus cumulative footage for RRC District 4. Data derived from American Petroleum Institute (1978) and bulletins of American Association of Petroleum Geologists (1942-1977).

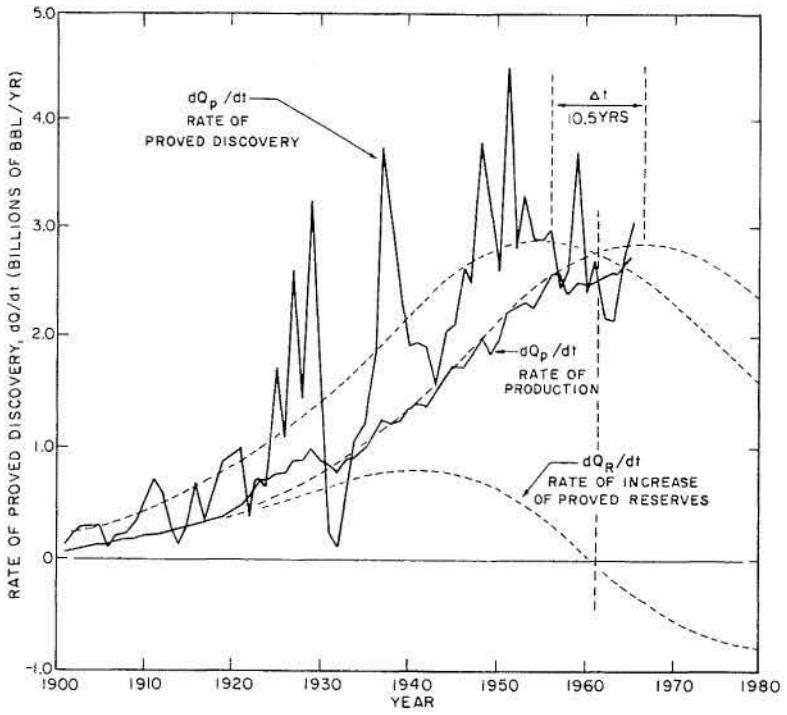

Figure 65. Recoverable oil discovery, oil production, and increase (or decrease) in proved U.S. oil reserves versus time (after Hubbert, 1967).

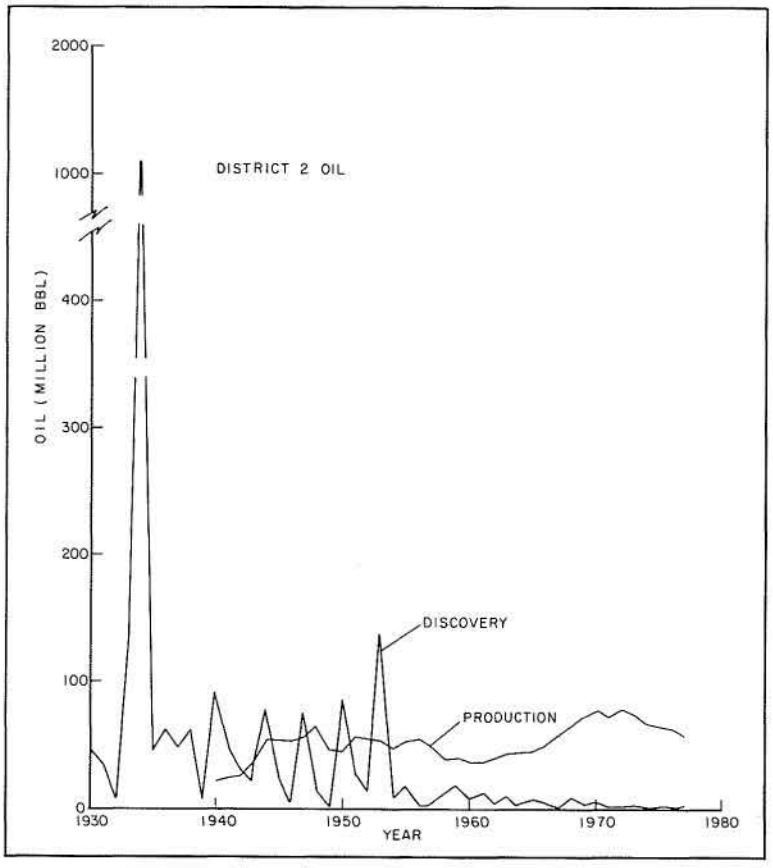

Figure 66. Recoverable oil discovery and production versus time for RRC District 2. Data derived from American Petroleum Institute (1978).

2,474 million bbl (390 million m^3) for the Frio in District 2. Since the total discovery as of 1977 is about 2,546 million bbl (405 million m^3), with 2,080 million bbl (330 million m^3) for the Frio, about 482 million bbl (77 million m^3) remains to be discovered in all formations and about 394 million bbl (62 million m^3) in the Frio (table 12). Percentage of the historical oil discovery in proportion to the estimated ultimate discovery can also be plotted on probability paper (fig. 67). For District 2, 50 percent of ultimate discovery was surpassed in 1934, after which the discovery rate dropped significantly. By extrapolating the latest decline trend into the future, it appears almost impossible to reach the ultimate discovery estimated above. This suggests that the amount of the future discovery of 482 million bbl (77 million m^3) for all formations (394 million bbl or 62 million m^3 for the Frio) is too optimistic. In fact, these figures are six to nine times more than those predicted by the other two methods (tables 7 and 10).

Figure 68 shows plots of recoverable oil discovery and of production for District 3. There are three discovery peaks, the middle one occurring in 1934 and two major peaks occurring in 1948 and 1972. The time that elapsed between the peak discovery and the first peak production is 14 years, which is also the same as that of District 2. The estimated future oil discovery is about 1,172 million bbl (187 million m^3) (table 12), which is probably too optimistic on the basis of the other estimates (tables 7 and 9). The cumulative-percent discovery plot (fig. 67) shows a significant drop in the discovery rate for District 3 after 1937.

Historical oil discovery and production for District 4 are shown in figure 69. Peak oil discovery occurs in 1937 and 1938, and the first peak in oil production is between 1951 and 1953, again a difference of about 14 years. The cumulative-percent discovery for District 4 is shown in figure 67, and the estimated future and total discoveries are shown in table 12.

For a similar historical analysis of gas discovery, the estimated discoveries of associated and nonassociated gas were plotted against time (figs. 70, 71, and 72). Historical data of gas production are not included in American Petroleum Institute statistics.

It is rather difficult to define the peak discovery of gas in District 2 (fig. 70).

Assuming that the peak is in 1944, the total recoverable gas for District 2 is estimated to be about 29,790 billion ft^3 (800 billion m^3) for all formations and 9,592 billion ft^3 (260 billion m^3) for the Frio (table 13). The estimated future discovery is about 4,727 billion ft^3 (127 billion m^3) for all formations and about 1,522 billion ft^3 (41 billion m^3) for the Frio (table 13). The above estimates are slightly higher than those predicted by the other two methods (tables 8 and 11).

Assuming the peak discovery for District 3 is in 1940 (fig. 71), and for District 4 in 1949 (fig. 72), the total and future discoveries were similarly estimated and are shown in table 13. The values estimated for District 3 are significantly less than those estimated by other methods (tables 8 and 10) and suggest that the estimates by the other methods could be optimistic. Our overall judgment on the amounts estimated by the different methods will be discussed in the final section of this report.

The cumulative percentages of gas discovery for Districts 2, 3, and 4 are shown in figure 73; all indicate significant declines in gas discovery rates in the years since peak discovery occurred. District 3, however, has maintained relatively high discovery rates in recent years.

Table 12. Statistical summary of recoverable oil, million bbl (discovery-versus-time method).

Location		Total oil discovery by 1977	Oil to be discovered	Total recoverable
Dist. 2	All formations	2,546	482	3,028
	Frio (% of above)	2,080 (81.7)	394 (81.7)	2,474 (81.7)
Dist. 3	All formations	7,570	1,172	8,742
	Frio (% of above)	3,890 (51.4)	602 (51.4)	4,492 (51.4)
Dist. 4	All formations	3,057	573	3,630
	Frio (% of above)	1,890 (61.8)	354 (61.8)	2,244 (61.8)
Dist. 2, 3, 4 Total	All formations	13,173	2,227	15,400
	Frio (% of above)	7,860 (59.7)	1,350 (60.6)	9,210 (59.8)

Table 13. Statistical summary of recoverable gas, bcf (discovery-versus-time method).

Location		Total gas discovery	Gas to be discovered	Total recoverable
Dist. 2	All formations	25,063	4,727	29,790
	Frio (% of above)	8,070 (32.2)	1,522 (32.2)	9,592 (32.2)
Dist. 3	All formations	53,204	6,550	59,754
	Frio (% of above)	25,000 (47.0)	3,079 (47.0)	28,079 (47.0)
Dist. 4	All formations	49,382	18,720	68,102
	Frio (% of above)	32,400 (65.6)	12,280 (65.6)	44,680 (65.6)
Dist. 2, 3, 4 Total	All formations	127,649	29,997	157,646
	Frio (% of above)	65,470 (51.3)	16,881 (56.3)	82,351 (52.2)
	Frio liquid equivalent	10,912 million bbl	2,814 million bbl	13,725 million bbl

Comparative Results

Table 14 summarizes the estimated future discoveries of recoverable oil and gas from the Frio by the three different methods. The estimate normally is highest with the cumulative-well method, next highest with the discovery-versus-time method, and lowest with the cumulative-footage method. The amount estimated by the first method is a possible minimum, that by the second a most likely amount, and that by the third a possible maximum. The gas estimate of District 3 is a significant exception: The estimated amounts of gas discovery calculated by the cumulative-well and cumulative-footage methods are significantly more than that calculated by the discovery-time method. This is due to improved gas discovery rates in recent years for that district. Extrapolating a similar high discovery rate into the future is questionable and results in unrealistically high totals for future gas discoveries.

VOLUMETRIC APPROACH

Volumetric predictions of the total recoverable hydrocarbons remaining within the Frio Formation were made on the basis of oil and gas production data, oil field distribution, and rock volumes. All calculations involved

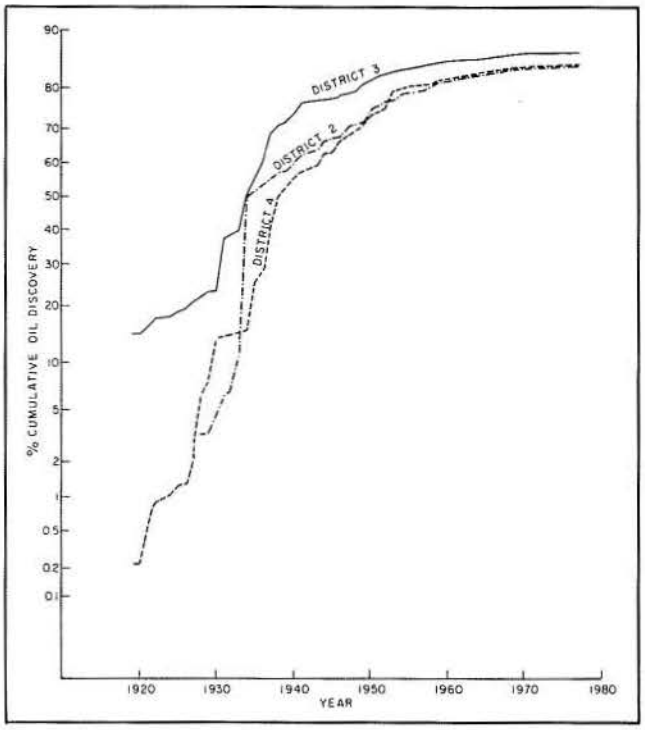

Figure 67. Cumulative percentage of oil discovery versus time for RRC Districts 2, 3, and 4. Refer to text for explanation.

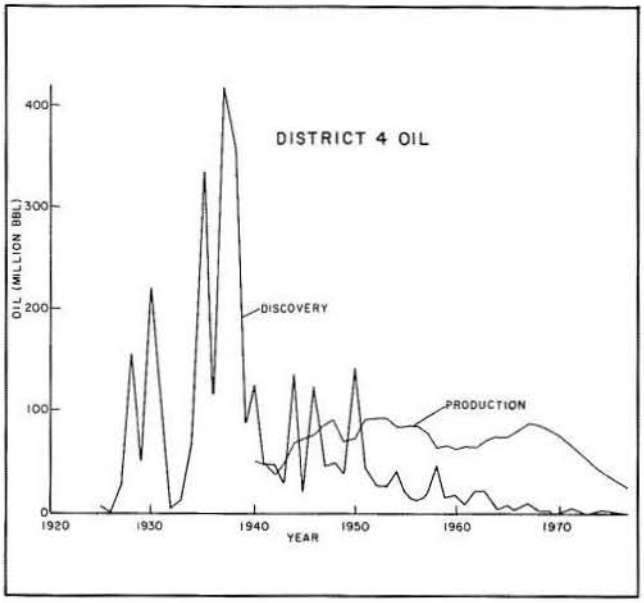

Figure 69. Recoverable oil discovery and production versus time for RRC District 4. Data derived from American Petroleum Institute (1978).

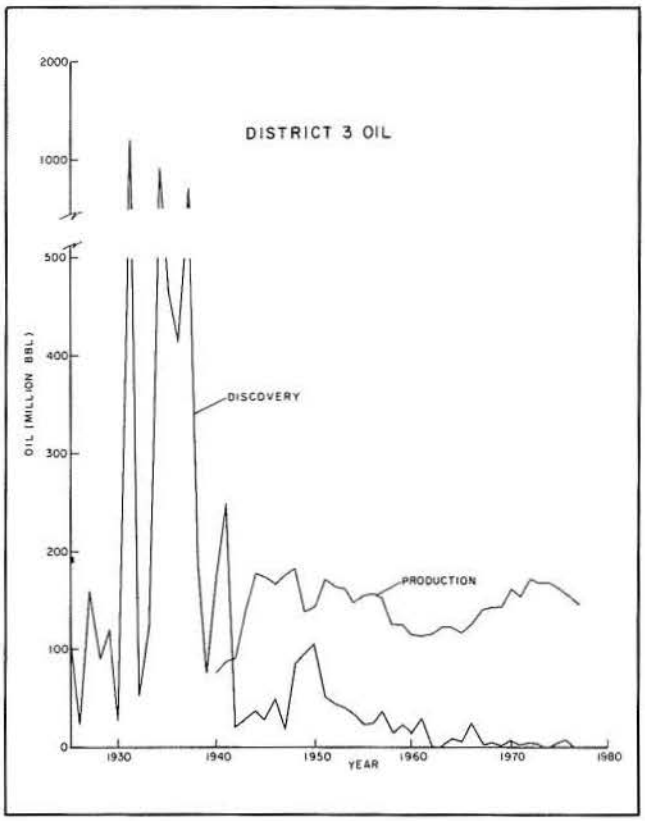

Figure 68. Recoverable oil discovery and production versus time for RRC District 3. Data derived from American Petroleum Institute (1978).

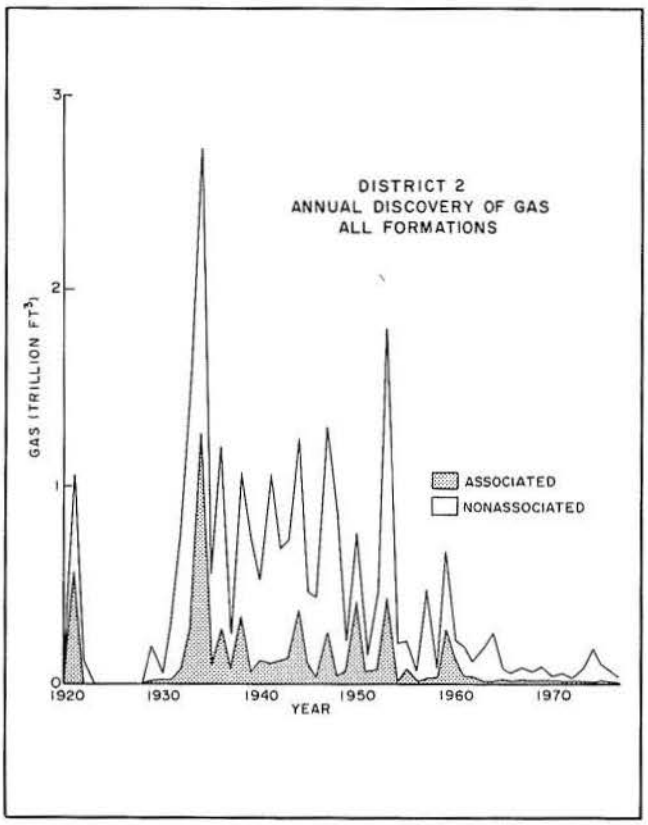

Figure 70. Recoverable gas discovery and production versus time for RRC District 2. Data derived from American Petroleum Institute (1978).

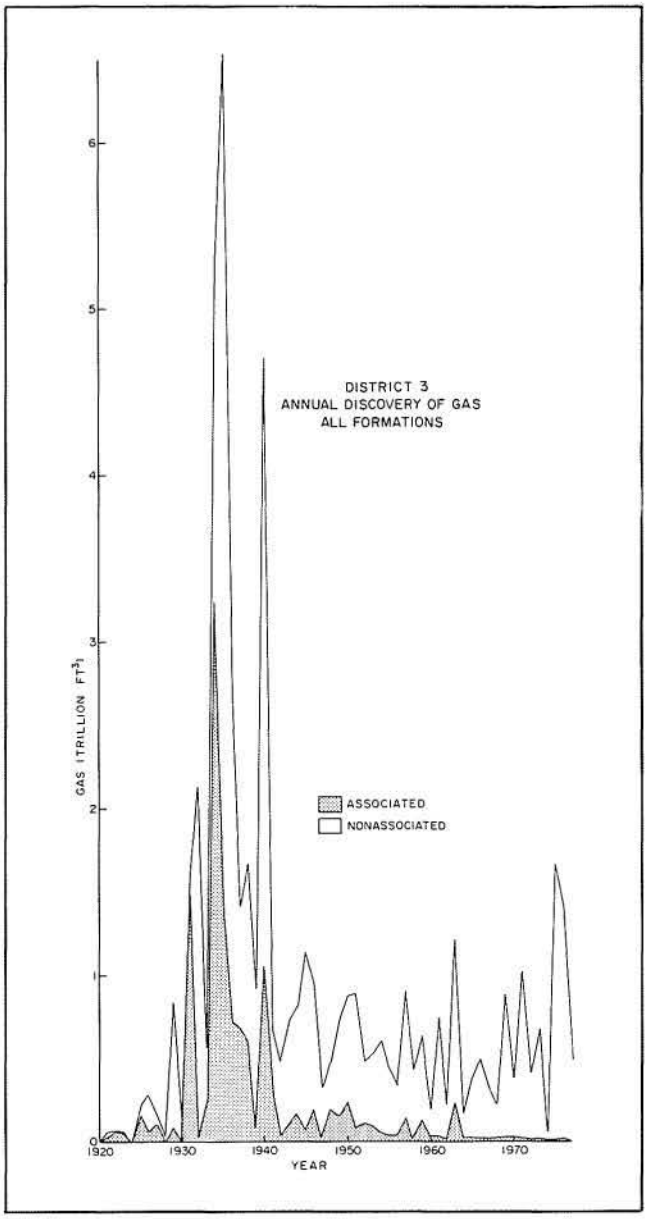

Figure 71. Recoverable gas discovery and production versus time for RRC District 3. Data derived from American Petroleum Institute (1978).

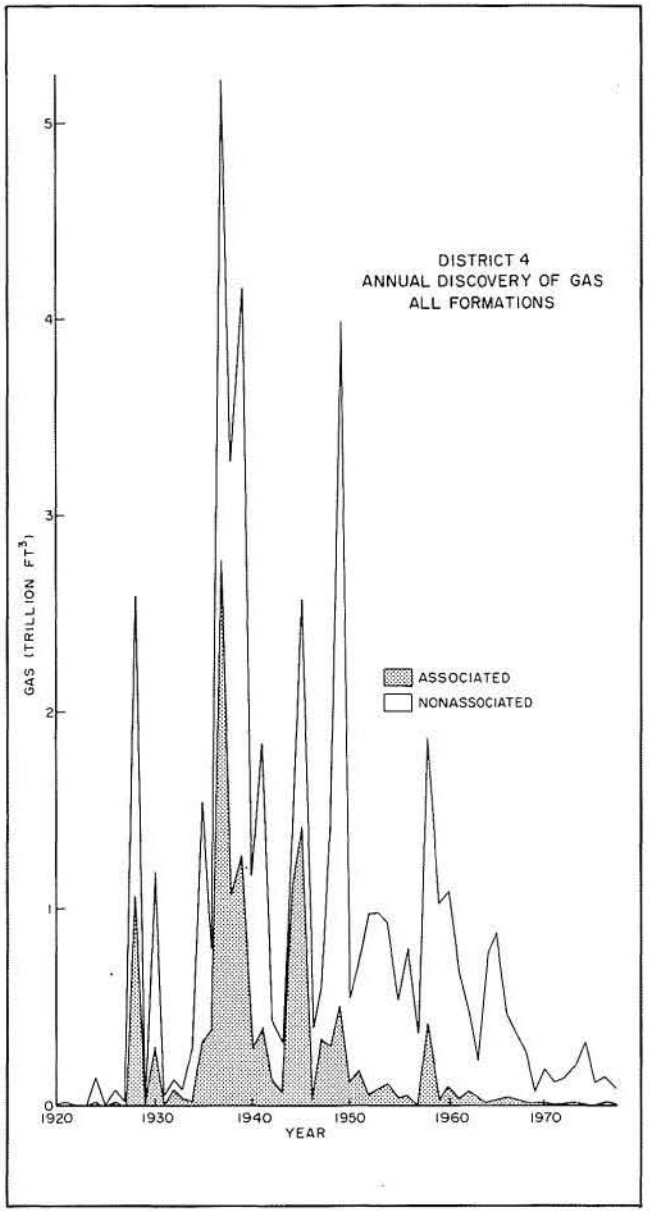

Figure 72. Recoverable gas discovery and production versus time for RRC District 4. Data derived from American Petroleum Institute (1978).

relatively homogeneous subdivisions (plays) of the Frio MSU.

The basic approach followed Mallory's (1975) method, in which undiscovered recoverable resources are estimated by multiplying a volume of undrilled rock in a particular play by a numerical richness or yield factor. The volume of undrilled favorable rock in Mallory's equation is the volume of favorable rock minus the volume of rock represented by the strata containing the oil pool and its possible extensions and minus the strata proved barren by drilling. Because of the overwhelming amount of data available for the Frio MSU (more than 100,000 wells have penetrated at least part of the Frio), we utilized a system of calculating volumes of undiscovered hydrocarbons that involved selection of "best areas," characterized by maximum drilling density and high productivity within each play. Best areas (pl. 19) were arbitrarily chosen to include an 835 mi^2 (2,150 km^2) area (or two subareas) in each play; they vary from rectangular to irregular in plan. Hydrocarbon production figures were obtained for each of these optimum areas.

Total volume of the Frio Formation within each play and each best area was determined by planimetry of the regional isopach map (pl. 3). Volume of reservoir sand in the upper, middle, and lower Frio operational units was similarly derived for each play and best area by using the

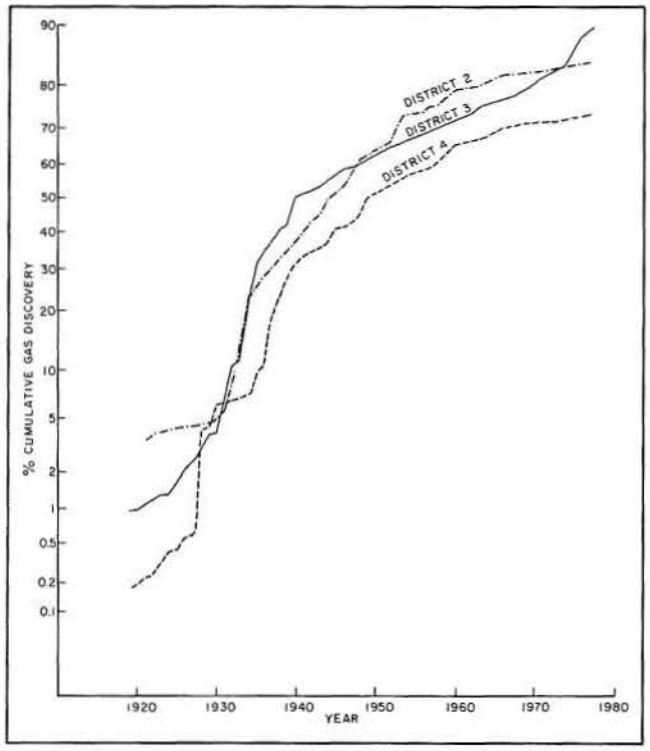

Figure 73. Cumulative percentage of gas discovery versus time for RRC Districts 2, 3, and 4. Refer to text for explanation.

net-sand isolith maps (pls. 4, 5, and 6). Source-rock volume was obtained by subtracting reservoir volume from total volume.

A yield factor (table 6) was derived for each play by dividing the total volume of produced hydrocarbons by the volume of the Frio Formation within each play and best area. Total hydrocarbons within each area divided by the volume of sand gave a reservoir yield factor.

In most plays, estimates based on total Frio rock volume as opposed to those based on reservoir volume are different (table 15), but only in plays V, VIII, and IX is there a major difference involving large positive versus negative values. Since the objective of hydrocarbon assessment should be to obtain a range of possible values rather than a single number with no specified probability (White and others, 1975), these estimates provide numerical values within the probability range. In some instances, play III, for example, the extremely large values derived by using total volume and reservoir volume were broadly in agreement, but were regarded as geologically unrealistic and were eliminated from consideration. Play III was delineated to coincide with a narrow belt of particularly favorable stratigraphic and structural features that have been intensively tested by the drill. It is therefore unlikely that such large volumes of undiscovered hydrocarbons remain within this play. Negative values arise where intensely drilled best areas are not obvious because dense drill penetration and extensive production typify the entire play.

Table 14. Summary of estimates of future discoveries, Frio MSU, derived from historical projections.

	Cumulative well number	Cumulative footage	Discovery time
Oil (million bbl)			
Dist. 2	41	68	394
Dist. 3	211	284	602
Dist. 4	104	164	354
Total	356	516	1,350
Gas (bcf)			
Dist. 2	1,017	1,487	1,522
Dist. 3	44,063	48,846	3,079
Dist. 4	5,937	9,916	12,280
Total	51,017	60,249	16,881
Liquid equivalent	8,502 million boe	10,042 million boe	2,814 million boe

Giant fields introduce major complications. If placed within a best area, they generate unduly optimistic projections; for example, in play V, Old Ocean field accounts for about 1,100 million bbl and nearly doubles the play yield factor. However, if excluded from the best area, production from the giants overwhelms any other choice.

A negative value in the volumetric estimate utilizing the best-area approach means that exploration is sufficiently dense so that inhomogeneities within the play increasingly dominate patterns of production. Reserve additions will depend more on further accentuation of such inhomogeneities in petroleum distribution patterns, and utilization of average yield factors is ineffective for projection. Volumetric projections are thus most appropriate to plays such as I, II, V, VII, IX, and X, which contain large volumes of sparsely drilled sediment at depth or offshore.

The most promising plays, according to interpreted volumetric calculations, are II, VIII, IX, and X (table 15). Greater reliance probably should be put on estimates based on reservoir volume (White and others, 1975). Negative values, such as for plays V, VI, and IX, indicate mature plays with substantial distortion of petroleum distribution introduced by the presence of a few giant fields. Modified judgmental volumetric estimates that attempt to incorporate the best elements of this approach, tempered by other considerations, are included in the final column of table 15.

SOURCE AND MIGRATION POTENTIAL APPROACH

This approach was thoroughly discussed in the section entitled "Hydrocarbon Source, Maturation, Migration, and Entrapment." The main conclusion derived from analysis of this approach is that the

Table 15. Volumetric estimations of undiscovered hydrocarbons (UH) in plays of the Frio MSU.

	Total rock volume (TV) $UH_{TV} = (f_{best} - f_{play}) \times (Vol_{play} - Vol_{best})$ ($\times 10^6$ bbl)					Reservoir volume (RV) $UH_{RV} = (f_{R\ best} - f_{R\ play}) \times (R\ Vol_{play} - R\ Vol_{best})$ ($\times 10^6$ bbl)					
Play	Oil	Associated gas	Nonassociated gas	Total gas	Total hydrocarbons	Oil	Associated gas	Nonassociated gas	Total gas	Total hydrocarbons	Modified (low, best, and high) volumetric estimates ($\times 10^6$ bbl)
I	56	96	58	154	210	15	23	16	39	55	45 90 350
II	9	0.1	217	217	226	21	0.3	467	468	489	290 615 1,000
III	516	714	666	1,380	1,896	733	1,027	950	1,977	2,709	N.R.
IV	73	0.5	18	18	91	117	0.8	30	31	148	75 90 150
V	85	126	216	342	427	−184	−245	−449	−695	−879	45 100 495
VI	−558	−168	−212	−380	−938	−471	−144	−182	−326	−796	N.R.
VII	64	16	226	242	306	39	9	137	146	183	40 120 310
VIII	−64	−7	−15	−21	−86	400	46	101	147	547	150 300 610
IX	737	306	598	904	1,641	−41	−17	−33	−50	−92	200 500 820
X	154	49	163	212	366	80	26	86	112	191	100 225 370
TOTAL*	1,694			3,468	5,163	1,405			2,920	4,330	945 2,040 4,105

*Negative values counted as zero
N.R. = not reliable

estimated amount of expelled hydrocarbons can be as much as 900 billion bbl, which is significantly larger than estimates by all other methods.

This difference may result partly because significant amounts of hydrocarbons are lost to the surface, scattered in relatively poor-quality reservoirs and traps, and contained in nonreservoir rocks. The estimate given by the source and migration approach indicates a possible ultimate limit on hydrocarbons expelled from source rocks, but cannot be used as a value relating either to total in-place hydrocarbons in reservoirs or to hydrocarbons recoverable by conventional methods. In addition, this amount may be an overestimation, as it was based on the assumption that source potential is relatively uniform. If the quality of source rock in certain sections is not as good as was assumed, the calculation would produce an overestimation. The data base for this assessment is also extremely limited at the present time.

In summary, this approach remains an ineffective method for evaluating potential Frio hydrocarbon reserves. In the future, however, increased data and quantification of the efficiency of hydrocarbon expulsion may make this approach a practical method for hydrocarbon resource assessment.

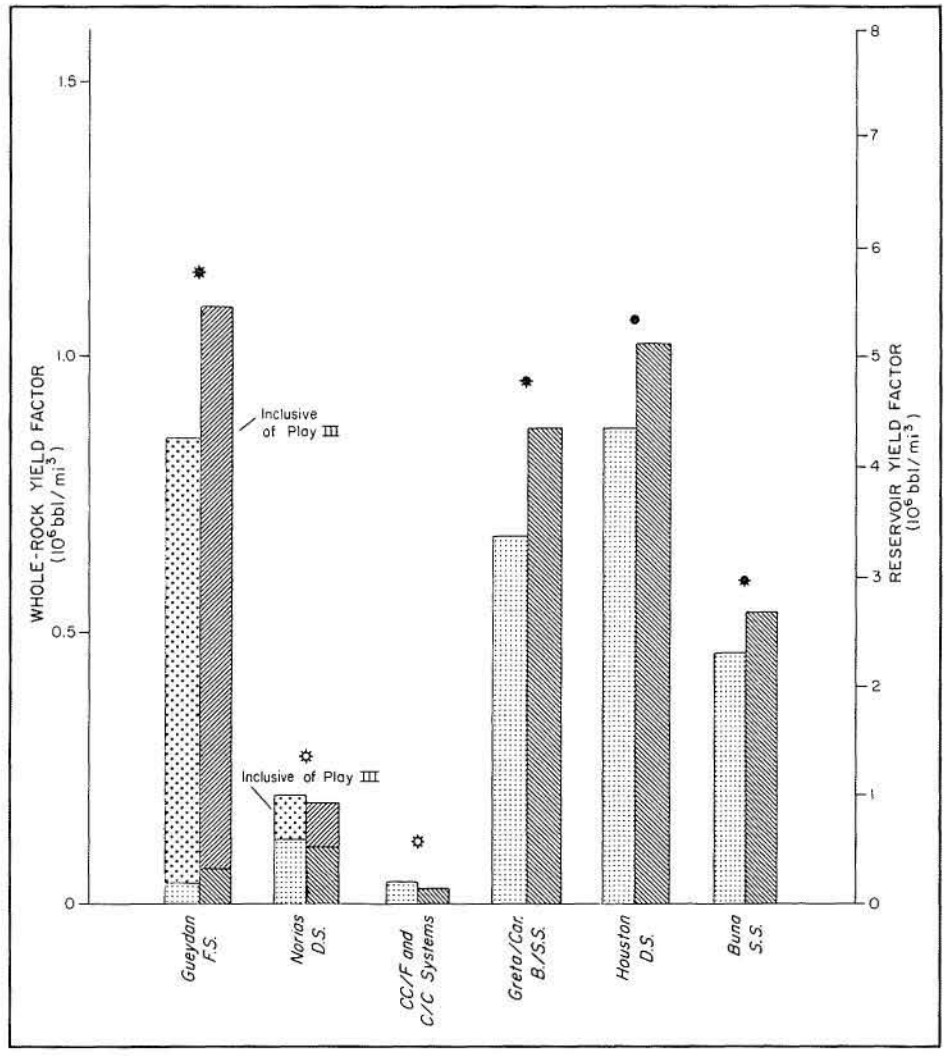

Figure 74. Correlation between whole-rock and reservoir yield factors and Frio depositional systems. Play III bridges the Gueydan and Norias systems; however, several lines of evidence suggest that play III hydrocarbons are not indigenous to the Frio MSU, but were derived from underlying units.

CONCLUSIONS

Delineation of the regional genetic stratigraphic framework, structural style, and compactional history of the Frio Major Stratigraphic Unit, combined with a thorough inventory of contained hydrocarbons, allows definition of 10 geologically homogeneous hydrocarbon-producing plays. Seven of the plays are important producing entities. Each play is characterized by some combination of differing reservoir geometries (determined by the depositional system), trap style (determined largely by the nature and timing of associated growth faulting or diapirism), and hydrocarbon type (determined by burial history and kerogen types within interbedded or underlying source facies). Facies, structure, and burial history, operating in various combinations, have produced greatly differing hydrocarbon yield factors for the individual plays. The geologic and economic significance of each play is further indicated by consistent differences in exploration history, nature and characteristics of contained hydrocarbons, and fundamental reservoir properties, such as permeability.

The Frio MSU contained more than 8 billion bbl of recoverable oil and 68 trillion ft^3 of gas in known fields of 1 million boe or larger. On an energy-equivalency basis, the Frio has produced more gas than oil, and this ratio is likely to increase with continued exploration and development. Average yield factor for the entire formation is about 3×10^6 bbl per mi^3 of sandstone; however, yield factors range from more than 9×10^6 to less than 0.3×10^6 bbl per mi^3 in mature exploration plays. Hydrocarbon yield appears to be particularly sensitive to the depositional system. If shallow, externally derived hydrocarbons of play III are excluded, the fluvial systems are extremely poor producers (fig. 74), primarily because of low source-rock quality and thermal immaturity. Where the Gueydan fluvial system taps deeper, functional source rocks, however, its per-volume productivity is the greatest of any system, as predicted by the sandstone-shale product model (fig. 41). The thick, highly progradational

Norias delta system of the Rio Grande Embayment has an average reservoir yield factor of about 0.5×10^6 bbl per mi^3 of sandstone. In contrast, the Houston delta system has efficiently produced hydrocarbons, as predicted by the model (fig. 41), at a ratio of more than 5×10^6 bbl per mi^3. Interdeltaic barrier and strandplain systems also comprise highly efficient hydrocarbon-producing systems.

Although data on the organic geochemistry of Frio shales and mudstones are sparse, evidence consistently indicates that a large proportion of the contained producible hydrocarbons was derived from low-quality source facies that contain gas-prone or mixed organic-matter types. Maximum maturation and expulsion of liquid hydrocarbons occurred within a relatively restricted interval of normally to moderately undercompacted, interbedded shale and sandstone. Large-scale upward and landward migration of hydrocarbons accompanied or closely followed primary expulsion. Shallow, displaced hydrocarbons of play III document local but efficient entry of matured hydrocarbons from underlying stratigraphic units. The apparent and highly significant lesson of the Frio is that a stratigraphic unit that would be discounted by commonly accepted screening criteria for source quality and maturity can internally generate, collect, and produce world-class petroleum reserves. Characteristics that distinguish such a system are worthy of more careful scrutiny and quantification.

In addition to establishing geologically defined units of production, the plays provide the basic unit for analyzing and predicting remaining undiscovered hydrocarbon potential of the entire Frio MSU. Of greater importance, examination of volumetric, historical (table 14), and geologic (table 15) attributes of each play allows comparative ranking of the exploration potential of specific parts of the Frio. On the basis of these data, we rank the potential of each play as follows:

Play IX is among the most promising for reserve additions, despite the facts that sandstone content is low and decreases gulfward and that the area has been very densely drilled. There are, nevertheless, two potential sites of future hydrocarbon discoveries (mainly gas). Deep, distal delta-front sandstones have not been fully penetrated and are associated with excellent structural traps. The deep-water Hackberry facies of the middle Frio may extend into play IX and so would provide the possibility of stratigraphic entrapment within an onlapping slope wedge. Important discoveries in play IX are likely to be restricted to deep wildcats and offshore wells.

Play VIII is viewed optimistically on the basis of past production volumes and steady rates of discovery in recent years. Salt diapirism has disrupted the continuity of reservoirs, and hydrocarbons are concentrated vertically around the areally limited domes. Future discoveries of gas will occur in deep wildcat wells drilled in downdip areas. There is the problem of gulfward decrease in overall sand content, but some significant, presently untested, intraslope sand bodies may exist at depth. Both oil and gas will continue to be discovered in relatively small volumes by infill wells drilled in updip areas.

Most remaining hydrocarbons in *play V* likely are dry gas or gas plus distillate. Greatest potential for major new fields lies at depth and in possible offshore extensions of distal shoreface and shelf reservoirs along the southern margin of the play. In addition, infill exploration in and around known fields should yield significant accumulated new reserves in isolated reservoirs and small traps. The seaward and landward areas of the play are limited by a deficit or surplus of sandstone, respectively. In the former situation, migration and accumulation of producible amounts of hydrocarbons are severely limited. In contrast, updip stacking of barrier sands produces large areal gaps in known and potential production because of the lack of adequate seals.

Prospects for additional discoveries of oil and gas in *play VI* are viewed with moderate optimism despite several negative factors. The area has been densely drilled, so future discoveries are unlikely to be in large pools. There is, nevertheless, continued production from a large number of wells, and infill wells and small satellite traps may add significant additional reserves. The downdip belt of exceptionally thick, uniform sandstone development is downgraded because of the paucity of seals. Seals are better developed in the updip, productive area, which has been intensively explored. Patterns of historical finding rates suggest limited numbers of small new discoveries, probably dominated by oil.

Remaining hydrocarbons in *play II* likely consist almost entirely of gas and distillate. Although this play exhibits the greatest volume of sand and minimal well density within much of the deeper sand-rich section, potential of the play is severely limited by the diagenetically induced poor reservoir quality of the sandstones and by an apparent decrease in size of complex anticlinal and fault traps with depth. Extensive development of overpressure further indicates limited expulsion and migration efficiency for generated hydrocarbons. Thus, this play has, and likely will retain, one of the lowest yield factors within the Frio.

Although highly mature from the exploration perspective, *play III* is projected to yield additional hydrocarbons, including gas and oil. Infill and satellite exploration should continue to add reserves from small stratigraphic and combination traps passed over in early exploration and field development. Density of drilling in and around the areally extensive major fields is the principal limiting factor in assigning additional reserves to the play, which has by far the richest yield factor of any within the Frio.

Play X is an area of limited to moderate potential for deep wildcat gas discoveries. Sandstone content decreases abruptly seaward, but the best prospects for

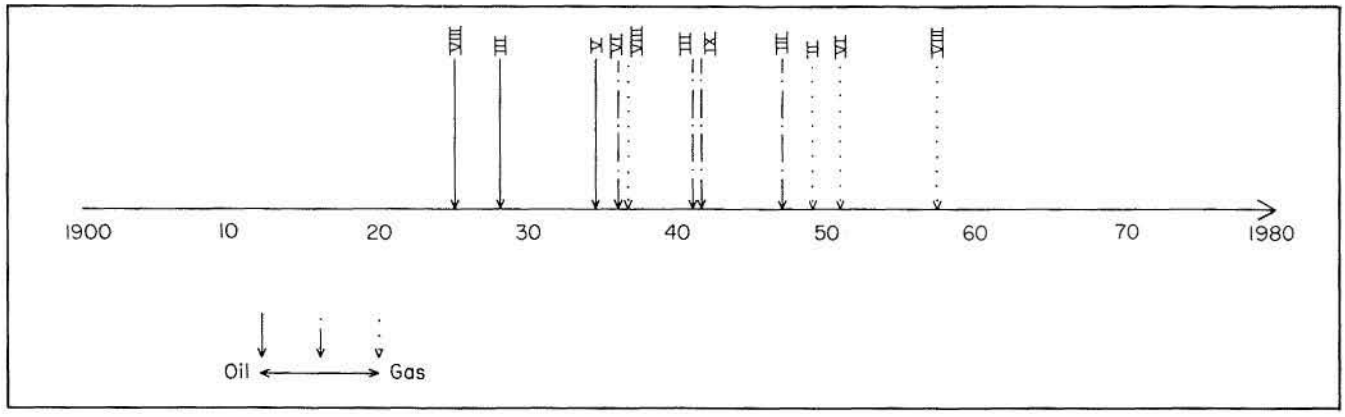

Figure 75. Historical distribution of major peaks in reserve additions, indicating discovery and rapid development of fairways within all Frio plays. Each fairway contained more than one-half billion bbl of oil or gas equivalent and thus represents a major incremental addition to the ultimate Frio reserve base.

large accumulations are in upper slope reservoirs comparable to the currently exploited Hackberry facies. A decrease in the historical finding rates has not been encouraging, but many wells have been drilled in updip areas; deeper wells may prove to be more successful, but only if isolated sandstone reservoirs are encountered.

Although oil is an important proportion of existing production, future discoveries in *play I* likely will be dominantly gas found in deep upper and middle Frio sections that lie below the oil window in gas-prone facies similar to those of play II. Although proportionally large volumes of Frio sandstone occur at depth and extend offshore within this play, potential appears severely limited by the pervasive burial diagenetic destruction of Norias delta sandstones. By analogy with play II, the ultimate yield factor will remain low. Further limits are imposed by the decrease in trap size with depth and the increase in reserve volumes necessary to economically produce deep, overpressured, and, possibly, offshore accumulations.

Play VII has extremely limited potential; however, because of its vast area, a few small, isolated traps may remain to be discovered by shallow drilling. Indigenous mature source facies are absent, but hydrocarbons have been introduced locally from deeper stratigraphic units. Minor undiscovered gas resources may be present in traps related to deep-seated structures.

Play IV retains minimal potential. The shallow, immature, relatively structureless, densely drilled section may contain modest volumes of hydrocarbons, including both oil and shallow, low-pressure gas. Inexpensive drilling should uncover multiple small, producible accumulations.

We conclude that together, the component plays of the Frio MSU likely contain from 1 to 4 billion boe of undiscovered, conventionally producible hydrocarbons, dominantly as natural gas. This figure presumes that more than 80 percent of the petroleum endowment of the Frio has been discovered and that about 80 percent of the discovered hydrocarbons have been produced.

It should be noted that these figures represent an extrapolation of current trends. As such, they may be considered rather conservative. As pointed out by Ryan (1973), prediction of the major new plays or significant subplays that account for major increases in province reserves is impossible on a statistical basis. Our estimate presumes a continuation of trends that have dominated the past 20 years of Frio discovery and development. The geologic potential for major new plays or new trends within the defined plays should be examined, though of necessity such examination is a highly speculative venture.

To increase extrapolated productivity figures significantly, a totally new trend would need to contain reserve additions of at least 500 million boe. As shown in figure 75, the last discovery of such a trend within the Frio occurred more than 20 years ago. Prior to that discovery, new plays or trends appeared at the average rate of 1 every 3 years, with no more than 7 years between major discovery peaks (fig. 75). Historical trends suggest that few if any trends or new plays remain to be discovered within the Frio.

Our analysis of the Frio indicates three possible but speculative geologic features that might produce one or more new trends of such magnitude:

1. *Upper Frio sandstones of the Norias delta system.* Along the South Texas coast and offshore in State and Federal waters, upper Frio delta-margin and delta-flank sandstones interfinger with regionally transgressive marine shelf mudstones of the Anahuac facies. This interfingering of favorable reservoir and oil-prone source facies in an expanded section at the downdip limits of the Norias delta system may produce a much improved exploration fairway in play I (fig. 76A). Although depth and

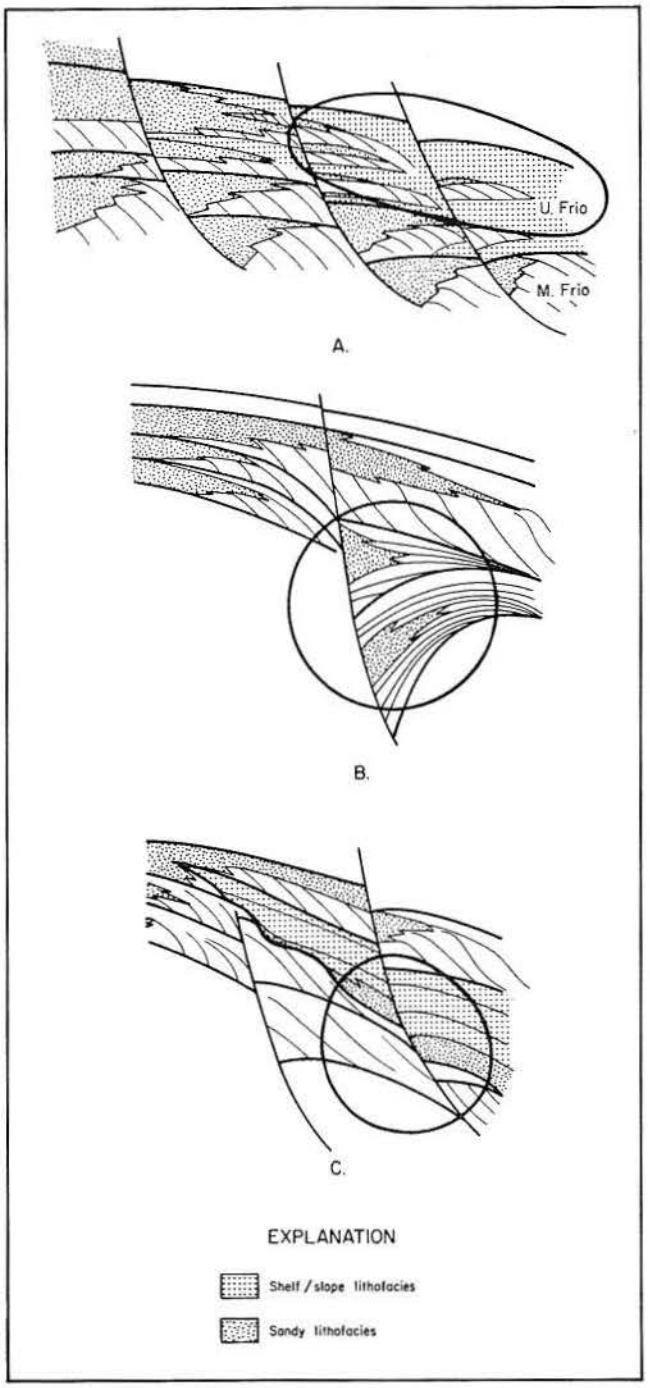

Figure 76. Speculative, unpredictable, undiscovered Frio hydrocarbon fairways that might provide major incremental reserve additions. A. Upper Frio delta-margin sandstones interbedded with shelf facies of the equivalent Anahuac wedge. B. Sandstone-filled shelf edge and upper slope growth-fault subbasin. C. Sandstone-bearing, onlapping slope wedge.

temperature of the prospective interval would probably generate gas, one may speculate that the associated oil-prone marine facies analogous to those of the Houston delta system may partially mitigate the pervasive carbonate cementation that severely limits deeper production in plays I and II. If reservoir quality persists at depth within a normally to moderately overpressured upper Frio section, the potential for major discoveries within play I increases substantially. Deep offshore drilling is limited, particularly in Federal waters.

2. *Deep, structurally defined lower to middle Frio intraslope basins.* Expanded sections within the downdropped blocks of major Frio growth faults consist predominantly of progradational distal deltaic facies. However, a few major fault subbasins may be interpreted alternatively as silled, bathymetric troughs along the offlapping shelf edge and upper slope. Although the mechanics of shale tectonics necessitate continual loading to initiate and sustain active structural deformation (Bishop, 1978), development of persistent depressions adjacent to principal depocenters within or marginal to the Norias delta system is conceivable. Such basins might fill in part by gravitationally resedimented shoreface or channel-mouth-bar sand and silt. The product would be thick, isolated, strike-elongate, fault-bounded pods of interbedded and mixed sand, silt, and mudstone (fig. 76B), occurring at great depth within sparsely drilled prodeltaic and slope mudstone sequences of the lower and middle Frio of the Norias delta system (play II) and along its northern margin in play V. If they do exist, however, such sandstone bodies would likely be characterized by extremely poor reservoir quality, a product of depth-related diagenesis and the poor sorting typical of resedimented slope sands, and they would occur deep within the geopressured zone. Production would be gas with some condensate.

3. *Unrecognized onlap (Hackberry-type) slope wedges.* Thick, erosionally based, onlapping slope wedges or gorges may occur in other interdeltaic areas within the downdip Frio section (fig. 76C). Development of major additional reserves within extensions of the Hackberry or undiscovered analogs will depend on the inclusion of significant volumes of sand within the wedge, which, in turn, requires reworking of coastal sands along the updip margin of the onlap sequence (Brown and Fisher, 1977). Such sandstones would lie sufficiently downslope within the wedge to be stratigraphically and geographically isolated from associated deltaic or coastal systems. Further, as in the Hackberry wedge, reservoirs would tend to lie offstructure. Thus, although data used in this study suggest no apparent examples of additional onlap wedges, limited drill penetration of distal play V, and possibly VIII and IX, leaves some room for their development. Careful seismic stratigraphic analysis and paleontologic synthesis might locate such wedges. Production would likely be gas-dominated and lie deep within the geopressured section.

Each of these possibilities for untested fairways is totally speculative and is presented only to illustrate that

some unpredictable potential may remain even within mature exploration plays. Although the majority of the extractable hydrocarbons and the great majority of the oil that occur within the Frio MSU have been found and extracted, remaining undiscovered reserves are substantial and will continue to justify expenditure of time, effort, and money. Synthesis of the vast amount of data generated by the exploration effort can improve the economics of that expenditure and provide a natural laboratory for generating and testing generic concepts of petroleum origin, migration, and entrapment that may aid exploration of the remaining frontier basins of the world.

ACKNOWLEDGMENTS

This research was partially funded by the U.S. Geological Survey, Department of the Interior, under USGS Grant No. 14-08-0001-G-640. Both technical and data-base assistance by USGS personnel of the Oil and Gas Branch were particularly helpful.

Organic geochemical data used in this report were supplied by J. L. Clayton and L. C. Price of the Energy Resources Branch of Oil and Gas Resources, USGS (Denver, Colorado), and by M. Smith of the Conservation Department, USGS (Metairie, Louisiana). Additional data were supplied by J. A. Momper and R. L. Ames of Amoco Production Co. (Tulsa, Oklahoma). Source-rock samples for geochemical analysis were provided by L. C. Bonham and R. W. Jones of Chevron Oil Field Research Co. (La Habra, California).

Statistical data on oil and gas production and drilling were provided by the Petroleum Information Corp. through the aid of R. F. Mast and T. Dyman of the USGS (Denver, Colorado). Engineering data on oil and gas discoveries of the Frio MSU were supplied by the Energy Information Administration Office, U.S. Department of Energy (Dallas, Texas). Discussions with T. Garland, J. Hicks, M. Carrales, Jr., and H. Rahman of the same office are deeply appreciated.

M. M. Dodge and J. S. Posey contributed freely to the assembly of the data base and in locating and providing additional useful information. W. L. Fisher, R. A. Morton, L. F. Brown, Jr., and Noel Tyler (Bureau of Economic Geology) and A. Peterson and T. Anderson (CONOCO, Inc.) reviewed the manuscript and added to the clarity of the presentation and conclusions. This publication was edited by Michelle C. Gilson and Jean Trimble. Typesetting was done by Phyllis J. Hopkins under the direction of Lucille C. Harrell. Figures were drafted under the direction of Dan F. Scranton by John T. Ames, Robert S. Baum, Thomas M. Byrd, Richard P. Flores, Jeffrey Horowitz, Jamie McClelland, and Charles Rogers. Text illustration camerawork was by James A. Morgan. Jamie S. Haynes designed and assembled the publication. The efforts of all these individuals are acknowledged.

Finally, Research Assistants Diana Morton, Mark Helper, Victor Gavenda, and Nathan Smith worked diligently and ably in many aspects of data compilation and synthesis. Their contribution was critical to completion of the study.

REFERENCES

Agagu, O. K., 1975, Depositional characteristics of the Frio Formation, subsurface South Texas: The University of Texas at Austin, Master's thesis, 100 p.

American Petroleum Institute, 1978, Reserves of crude oil, natural gas liquids, and natural gas in the United States and Canada as of December 31, 1977: Washington, D. C., v. 32, 265 p.

Baker, E. T., Jr., 1978, Stratigraphic and hydrogeologic framework of part of the Coastal Plain of Texas: U.S. Geological Survey Open-File Report 77-712, 32 p.

Barker, C., 1977, Aqueous solubility of petroleum as applied to its origin and primary migration: discussion: American Association of Petroleum Geologists Bulletin, v. 61, p. 2146-2149.

Bebout, D. G., Loucks, R. G., and Gregory, A. R., 1978, Frio sandstone reservoirs in the deep subsurface along the Texas Gulf Coast: The University of Texas at Austin, Bureau of Economic Geology Report of Investigations No. 91, 92 p.

Berg, R. R., and Powers, B. K., 1980, Morphology of turbidite-channel reservoirs, lower Hackberry (Oligocene), southeast Texas: Gulf Coast Association of Geological Societies Transactions, v. 30, p. 41-48.

Bishop, R. S., 1977, Shale diaper emplacement in South Texas: Laward and Sheriff examples: Gulf Coast Association of Geological Societies Transactions, v. 27, p. 20-31.

——— 1978, Mechanism for emplacement of piercement diapirs: American Association of Petroleum Geologists Bulletin, v. 62, p. 1561-1583.

Boyd, D. R., and Dyer, B. F., 1964, Frio barrier bar system of South Texas: Gulf Coast Association of Geological Societies Transactions, v. 14, p. 309-322.

Brown, L. F., Jr., Brewton, J. L., McGowen, J. H., Evans, T. J., Fisher, W. L., and Groat, C. G., 1976, Environmental geologic atlas of the Texas Coastal Zone—Corpus Christi area: The University of Texas at Austin, Bureau of Economic Geology Special Publication, 123 p.

Brown, L. F., Jr., and Fisher, W. L., 1977, Seismic-stratigraphic interpretation of depositional systems: examples from Brazilian rift and pull-apart basins, *in* Payton, C. E., ed., Seismic stratigraphy—applications to hydrocarbon exploration: American Association of Petroleum Geologists Memoir 26, p. 213-248.

Brown, S. W., 1979, Hydrocarbon source facies analysis, Department of Energy and General Crude Oil Company, Pleasant Bayou No. 1 and 2 wells, Brazoria County, Texas, *in* Dorfman, M. H., and Fisher, W. L., eds., Proceedings, fourth U.S. Gulf Coast geopressured-geothermal energy conference: research and development, v. 1, p. 132-152.

Bruce, D. H., 1973, Pressured shale and sediment deformation: mechanism for development of regional contemporaneous faults: American Association of Petroleum Geologists Bulletin, v. 57, p. 878-886.

Closs, H., Narain, H., and Garde, S. C., 1974, Continental margins of India, *in* The geology of continental margins: New York, Springer-Verlag, p. 629-639.

Coleman, J. M., and Prior, D. B., 1980, Deltaic sand bodies: American Association of Petroleum Geologists, Continuing Education Course Note Series No. 15, 171 p.

Connan, J., 1974, Time-temperature relations in oil genesis: American Association of Petroleum Geologists Bulletin, v. 58, p. 2516-2521.

Conybeare, C. E. B., 1976, Geomorphology of oil and gas fields in sandstone bodies, *in* Developments in Petroleum Science No. 4: New York, Elsevier, 431 p.

Crans, W., Mandl, G., and Haremboure, J., 1980, On the theory of growth faulting: a geomechanical delta model based on gravity sliding: Journal of Petroleum Geology, v. 2, p. 265-307.

Curtis, D. M., 1970, Miocene deltaic sedimentation, Louisiana Gulf Coast, *in* Deltaic sedimentation, modern and ancient: Society of Economic Paleontologists and Mineralogists Special Publication No. 15, p. 293-308.

Dailly, G. C., 1976, A possible mechanism relating progradation, growth faulting, clay diapirism and overthrusting in a regressive sequence of sediments: Bulletin of Canadian Petroleum Geology, v. 24, p. 92-116.

Dodge, M. M., and Posey, J. S., 1981, Structural cross sections, Tertiary formations, Texas Gulf Coast: The University of Texas at Austin, Bureau of Economic Geology Cross Sections.

Domenico, S. N., 1980, Velocity and lithology: Notes, American Association of Petroleum Geologists - Society of Exploration Geophysicists Stratigraphic Interpretation of Seismic Data School, September 23-27, American Association of Petroleum Geologists, Tulsa, Oklahoma, 62 p.

Dow, W. G., 1978, Petroleum source beds on continental slopes and rises: American Association of Petroleum Geologists Bulletin, v. 62, p. 1584-1606.

Dow, W. G., and Pearson, D. B., 1974, Organic matter in Gulf Coast sediments: Seventh Offshore Technology Conference Preprints, paper OTC 2343.

Dutton, S. P., 1980, Petroleum source rock potential and thermal maturity, Palo Duro Basin, Texas: The University of Texas at Austin, Bureau of Economic Geology Geological Circular 80-10, 48 p.

Fisher, W. L., Brown, L. F., Jr., McGowen, J. H., and Groat, C. G., 1973, Environmental geologic atlas of the Texas Coastal Zone—Beaumont-Port Arthur area: The University of Texas at Austin, Bureau of Economic Geology Special Publication, 93 p.

Fisher, W. L., Brown, L. F., Jr., Scott, A. J., and McGowen, J. H., 1969, Delta systems in the exploration for oil and gas: The University of Texas at Austin, Bureau of Economic Geology Special Publication, 212 p.

Fisher, W. L., and McGowen, J. H., 1967, Depositional systems in the Wilcox Group of Texas and their relationship to occurrence of oil and gas: Gulf Coast Association of Geological Societies Transactions, v. 17, p. 105-125.

Frazier, D. E., 1974, Depositional episodes: their relationship to the Quaternary stratigraphic framework in the northwestern portion of the Gulf Basin: The University of Texas at Austin, Bureau of Economic Geology Geological Circular 74-1, 28 p.

Galloway, W. E., 1975, Process framework for describing the morphologic and stratigraphic evolution of deltaic depositional systems, *in* Broussard, M. L., ed., Deltas: models for exploration: Houston Geological Society, p. 87-98.

____ 1977, Catahoula Formation of the Texas Coastal Plain: depositional systems, composition, structural development, ground-water flow history, and uranium distribution: The University of Texas at Austin, Bureau of Economic Geology Report of Investigations No. 87, 59 p.

Galloway, W. E., and Kaiser, W. R., 1980, Catahoula Formation of the Texas Coastal Plain: origin, geochemical evolution, and characteristics of uranium deposits: The University of Texas at Austin, Bureau of Economic Geology Report of Investigations No. 100, 81 p.

Garrett, J. B., 1938, The Hackberry assemblage, an interesting foraminiferal fauna of post-Vicksburg age from deep wells of the Gulf Coast: Journal of Paleontology, v. 12, p. 309-317.

Gregory, A. R., Dodge, M. M., Posey, J. R., and Morton, R. A., 1980, Volume and accessibility of entrained (solution) methane in deep geopressured reservoirs — Tertiary formations of the Texas Gulf Coast: The University of Texas at Austin, Bureau of Economic Geology Contract Report prepared for Gas Research Institute, 390 p.

Gulf Coast Association of Geological Societies, 1972, Tectonic map of the Gulf Coast region U.S.A.: Tulsa, Oklahoma, American Association of Petroleum Geologists, scale 1:1,000,000.

Halbouty, M. T., and Barber, T. D., 1961, Port Acres and Port Arthur fields, Jefferson County, Texas: Gulf Coast Association of Geological Societies Transactions, v. 11, p. 225-234.

Hubbert, M. K., 1967, Degree of advancement of petroleum exploration in United States: American Association of Petroleum Geologists Bulletin, v. 67, p. 2207-2227.

International Oil Scouts Association, 1978, Texas oil and gas development, Texas yearbook, 1978: Austin, Texas, v. 6, 360 p.

Japanese Association of Petroleum Technologists, 1973 (Nihon no Sekiyu Kogyo to Gijutsu) Petroleum Mining and Technology of Japan: 430 p.

Kraft, J. C., and John, C. J., 1979, Lateral and vertical facies relations of transgressive barrier: American Association of Petroleum Geologists Bulletin, v. 63, p. 2145-2163.

Loucks, R. G., 1978, Sandstone distribution and potential for geopressured geothermal energy production in the Vicksburg Formation along the Texas Gulf Coast: Gulf Coast Association of Geological Societies Transactions, v. 28, p. 239-271.

Loucks, R. G., Dodge, M. M., and Galloway, W. E., 1979, Sandstone consolidation analysis to delineate areas of high-quality reservoirs suitable for production of geopressured geothermal energy along the Texas Gulf Coast: The University of Texas at Austin, Bureau of Economic Geology Contract Report No. EG-77-5-05-5554, 98 p.

Magara, K., 1978a, Compaction and fluid migration — practical petroleum geology: Amsterdam, The Netherlands, Elsevier, 319 p.

——— 1978b, Time of oil generation and migration and oil window: Canadian Petroleum Geology Bulletin, v. 26, p. 152-155.

Mallory, W. W., 1975, Accelerated national oil and gas resource appraisal (ANOGRE): American Association of Petroleum Geologists Studies in Geology No. 1, p. 23-30.

Martin, G. B., 1969, The subsurface Frio of South Texas: stratigraphy and depositional environments as related to the occurrence of hydrocarbons: Gulf Coast Association of Geological Societies Transactions, v. 19, p. 489-501.

McAuliffe, C. D., 1978, Chemical and physical constraints on petroleum migration with emphasis on hydrocarbon solubilities in water: American Association of Petroleum Geologists short course "Physical and Chemical Constraints on Petroleum Migration," Oklahoma City, 39 p.

McDowell, A. N., 1975, What are the problems in estimating the oil potential of a basin?: Oil and Gas Journal, v. 73, p. 85-90.

McGookey, D. P., 1975, Gulf Coast Cenozoic sediments and structure: an excellent example of extra-continental sedimentation: Gulf Coast Association of Geological Societies Transactions, v. 25, p. 104-120.

McGowen, J. H., Brown, L. F., Jr., Evans, T. J., Fisher, W. L., and Groat, C. G., 1976, Environmental geologic atlas of the Texas Coastal Zone—Bay City-Freeport area: The University of Texas at Austin, Bureau of Economic Geology Special Publication, 98 p.

McGowen, J. H., Garner, L. E., and Wilkinson, B. H., 1977, The Gulf shoreline of Texas: processes, characteristics, and factors in use: The University of Texas at Austin, Bureau of Economic Geology Geological Circular 77-3, 27 p.

McIvor, R. D., 1975, Hydrocarbon occurrences from JOIDES Deep Sea Drilling Project: Ninth World Petroleum Congress Proceedings, v. 2, p. 269-280.

Momper, J. A., 1978, Oil migration limitations suggested by geological and geochemical considerations, *in* Physical and chemical constraints on petroleum migration: American Association of Petroleum Geologists Continuing Education Course Note Series No. 8, p. B-1 - B-60.

Morton, R. A., 1977, Historical shoreline changes and their causes, Texas Gulf Coast: Gulf Coast Association of Geological Societies Transactions, v. 27, p. 352-364.

Morton, R. A., and McGowen, J. H., 1980, Modern depositional environments of the Texas coast: The University of Texas at Austin, Bureau of Economic Geology Guidebook 20, 167 p.

Nanz, R. H., Jr., 1954, Genesis of Oligocene sandstone reservoir, Seeligson field, Jim Wells and Kleberg Counties, Texas: American Association of Petroleum Geologists Bulletin, v. 38, p. 96-117.

Paine, W. R., 1971, Petrology and sedimentation of the Hackberry sequence of southwest Louisiana: Gulf Coast Association of Geological Societies Transactions, v. 21, p. 37-55.

Powell, T. G., 1978, An assessment of the hydrocarbon source rock potential of the Canadian Arctic Islands: Geological Survey of Canada, paper 78-12, 82 p.

Price, L. C., 1976, Aqueous solubility of petroleum as applied to its origin and primary migration: American Association of Petroleum Geologists Bulletin, v. 60, p. 213-244.

Railroad Commission of Texas, 1978, Annual report of the Oil and Gas Division: Austin, Texas, 613 p.

Roberts, H. H., 1980, Sediment characteristics of Mississippi River delta-front mudflow deposits: Gulf Coast Association of Geological Societies Transactions, v. 30, p. 485-496.

Ronov, A. B., 1958, Organic carbon in sedimentary rocks (in relation to the presence of petroleum): Geochemistry, v. 5, p. 510-536.

Ryan, J. T., 1973, An analysis of crude-oil discovery rate in Alberta: Bulletin of Canadian Petroleum Geology, v. 21, p. 219-235.

Scholle, P. A., and Arthur, M. A., 1980, Carbon isotope fluctuations in Cretaceous pelagic limestones: potential stratigraphic and petroleum exploration tool: American Association of Petroleum Geologists Bulletin, v. 64, p. 67-87.

Stuckey, C. W., 1964, The stratigraphic relationship of the Hackberry, Abbeville, and Harang faunal assemblages: Gulf Coast Association of Geological Societies Transactions, v. 14, p. 209-216.

Tissot, B., 1978, The application of the results of organic geochemical studies in oil and gas exploration, chapter 2, *in* Hobson, G. D., ed., Developments in petroleum geology: London, Applied Science Publishers, p. 53-82.

Vail, P. R., Mitchum, R. M., Jr., and Thompson, S., III, 1977, Seismic stratigraphy and global changes of sea level, part 4: global cycles of relative changes of sea level, *in* Payton, C. E., ed., Seismic stratigraphy—applications to hydrocarbon exploration: American Association of Petroleum Geologists Memoir 26, p. 83-97.

Waples, D. W., 1980, Time and temperature in petroleum formation: application of Lopatin's method to petroleum exploration: American Association of Petroleum Geologists Bulletin, v. 64, p. 916-926.

Weise, B. R., Edwards, M. B., Gregory, A. R., Hamlin, H. S., Jirik, L. A., and Morton, R. A., 1981, Geologic studies of geopressured and hydropressured zones in Texas: test well site selection: The University of Texas at Austin, Bureau of Economic Geology Contract Report prepared for Gas Research Institute, 308 p.

White, D. A., 1980, Assessing oil and gas plays in facies-cycle wedges: American Association of Petroleum Geologists Bulletin, v. 64, p. 1158-1178.

White, D. A., Garrett, R. W., Jr., Marsh, G. R., Baker, R. A., and Gehman, H. M., 1975, Assessing regional oil and gas potential: American Association of Petroleum Geologists Studies in Geology No. 1, p. 143-159.

White, D. A., and Gehman, H. M., 1979, Methods of estimating oil and gas resources: American Association of Petroleum Geologists Bulletin, v. 63, p. 2183-2192.

Winker, C. D., 1979, Late Pleistocene fluvial-deltaic deposition, Texas coastal plain and shelf: The University of Texas at Austin, Master's thesis, 187 p.

——— 1980, Depositional phases in late Pleistocene cyclic sedimentation, Texas coastal plain and shelf, with some Eocene analogs, *in* Perkins, B. F., and Hobday, D. K., eds., Middle Eocene coastal plain and nearshore deposits of East Texas: a fieldguide to the Queen City Formation and related papers: Gulf Coast Section, Society of Economic Paleontologists and Mineralogists, p. 46-66.

Zapp, A. D., 1961, World petroleum resources, *in* Domestic and world resources of fossil fuels, radioactive minerals, and geothermal energy: Preliminary reports prepared by members of the U.S. Geological Survey for the Natural Resources Subcommittee of the Federal Science Council, November 28, 1961 (unpublished).

——— 1962, Future petroleum producing capacity of the United States: U.S. Geological Survey Bulletin 1142-H, 36 p.